

**PATHOPHYSIOLOGICAL MODELING OF THE NORMALIZED BRAIN
TISSUE-LEVEL VOLUMETRIC EVALUATIONS OF YOUTH ATHLETES
PARTICIPATING IN COLLISION SPORTS**

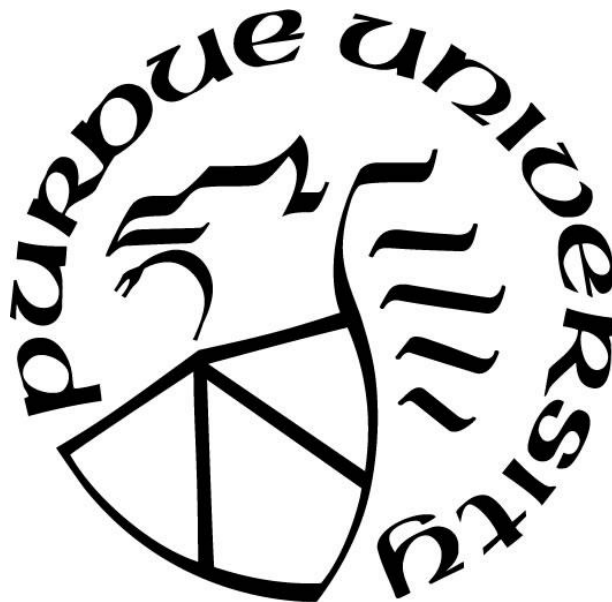
by
Pratik Kashyap

A Dissertation

Submitted to the Faculty of Purdue University

In Partial Fulfillment of the Requirements for the degree of

Doctor of Philosophy



School of Electrical and Computer Engineering
West Lafayette, Indiana
May 2022

THE PURDUE UNIVERSITY GRADUATE SCHOOL
STATEMENT OF COMMITTEE APPROVAL

Dr. Thomas Talavage, Chair

School of Electrical and Computer Engineering

Dr. Eric Nauman

School of Mechanical Engineering

Dr. Amy Reibman

School of Electrical and Computer Engineering

Dr. Maggie Zhu

School of Electrical and Computer Engineering

Approved by:

Dr. Dimitrios Peroulis

Dedicated to Madelina

ACKNOWLEDGMENTS

I am very grateful to my chair, Tom Talavage, and committee members Eric Nauman, Amy Reibman and Maggie Zhu for their guidance all these years. Taking classes like medical imaging, biomechanics, video analysis and probability with them was an added bonus. I am also thankful to all my family, especially my parents and my partner to whom I am deeply indebted for being the pillar of support.

This work would not have been possible without the aid of collaborators Sharlene Newman, Larry Leverenz, Gregory Tamer and Yunjie Tong. The research is funded from sources such as CTSI spinal cord and brain injury research fund, Brainscope Inc., Indiana CTSI collaboration in translational research grant, Indiana state department of health and committee on institutional cooperation.

I am thankful to my friends from Purdue graduate student govt., Purdue university cricket club, and sports teams: Hammering homers, Purdue peace cricket club, AeroAssault. I am also thankful to my colleagues from Purdue neurotrauma group, Nathan Kline institute and Duke university for shaping my academic journey.

I am ever grateful to my lab mates Kausar, Trey, Sumra, Ikbeom, Joe, Diana, Vincent, Nicole, Chetas, Taylor, Roy, Kevin, Shawn, Art, Brad, Antonia, Kai and MVK. Thank you for providing me with the space to discuss and channel my ideas.

My journey at Purdue would be incomplete without mentors like Mike Melloch and Milind Kulkarni who helped me shape my teaching career. The timely administrative execution of my curriculum would not have been possible without the prompt assistance and constant presence of Elisheba VanWinkle and Matt Golden. And finally, a big thank you to Ashlee and Carla from the Graduate School who helped in formatting this document.

TABLE OF CONTENTS

LIST OF TABLES	7
LIST OF FIGURES	8
ABBREVIATIONS	10
ABSTRACT.....	11
1. INTRODUCTION	12
1.1 Neurotrauma in Youth Athletes involved in Collision-based Sports	12
1.2 Detection of Structural Alterations in these Youth Athletes	13
2. BACKGROUND	15
2.1 Neurotrauma	15
2.1.1 Mild Traumatic Brain Injury	15
2.1.2 Sports-related Neurotrauma	16
2.1.3 Health Monitoring	17
2.2 MRI Morphometric Analysis	19
2.2.1 MRI Basics	19
2.2.2 Existing Techniques	20
2.2.3 Comparison of Morphometric Techniques	21
2.2.4 Proposed Model of Morphometry	22
2.3 Pathophysiological Modeling	23
2.3.1 Glymphatics	23
2.3.2 Small Animal Models.....	25
3. METHODS	27
3.1 Experimental Study Design	27
3.1.1 Participant Demographics	27
3.1.2 Participant Schedule	27
3.1.3 Data Acquisition Protocol	30
3.2 Data Pre-processing.....	31
3.2.1 MRI Pre-processing.....	31
3.2.2 HAE Pre-processing	34
3.3 MRI Measurement Reliability	34

3.3.1	Ground Truth Measurements	34
3.3.2	Data Quality Assurance	35
3.3.3	Partial Volume Estimation	37
3.4	Statistical Analysis	38
4.	RESULTS	40
4.1	Volumetric Measures Distribution Analysis	40
4.2	Ground Truth Analysis	41
4.3	Atlas Specificity	42
4.4	Statistical Analysis of Volumetric Measures	44
4.4.1	Group-level ROI Analysis	44
4.4.2	Subject-level ROI Distribution Analysis	47
4.4.3	Longitudinal Analysis	53
4.4.4	Post hoc <i>t</i> -Tests	54
4.5	HAE Regression Analysis	56
4.6	WM ROI Distribution	61
5.	DISCUSSION	63
5.1	Volumetric Changes	63
5.2	Pathophysiological Modeling	65
6.	FUTURE DIRECTIONS	75
	REFERENCES	77
	APPENDIX	106
	VITA	112

LIST OF TABLES

Table 3.1 Demographics of participants with complete set of valid imaging data as collected at <i>Pre/ Test</i> session. (All values are: Mean \pm StdDev, [Min, Max]), CSA: Collision Sport Athletes, NCA: Non-collision Sport Athletes	28
Table 4.1 50 th and 95 th percentile values of percentage of CSA subjects exceeding NCA 95 th percentile CI bound of rTVC at Session.	52
Table 4.2 Comparisons, by tissue type, of relative tissue volumetric changes (rTVC) as a function of group and session. For each tissue of gray matter (GM), cerebrospinal fluid (CSF), white matter (WM) and deep (ventricular), CSF (<i>dCSF</i>), results are presented for both within-group analyses of the collision sport athletes (CSA), and for an across group analysis of CSA with the non-collision sports athletes (NCA). To evaluate within-group differences for CSA, Bonferroni corrected paired <i>t</i> -tests were conducted to compare the mean difference in rTVC on a pair-wise basis between follow-up sessions (<i>In1</i> , <i>In2</i> , <i>Post1</i> , <i>Post2</i>). To evaluate CSA relative to NCA, Bonferroni corrected unpaired <i>t</i> -tests were conducted to compare the mean difference in rTVC on a pair-wise basis between CSA follow-up session and the NCA follow-up session (<i>Retest</i>).	55
Table 4.3 Longitudinal statistical analysis (<i>F</i> -test and <i>t</i> -tests) of global volumetric measures rBVC, SIENA, and BVC representing the mean percentage difference across sessions. All datasets are relative normalized volumes and hence have no units.....	55
Table 4.4 Comparisons, by tissue type, of tissue volumetric changes (TVC) as a function of group and session. For each tissue of gray matter (GM), cerebrospinal fluid (CSF), white matter (WM), and deep (ventricular) CSF (<i>dCSF</i>), results are presented for both within-group analysis of the collision sport athletes (CSA), and for an across group analysis of CSA with the non-collision sports athletes (NCA). To evaluate within-group differences for CSA, Bonferroni corrected paired <i>t</i> -tests were conducted to compare the mean difference in TVC on a pair-wise basis between follow-up sessions (<i>In1</i> , <i>In2</i> , <i>Post1</i> , <i>Post2</i>). To evaluate CSA relative to NCA, Bonferroni corrected unpaired <i>t</i> -tests were conducted to compare the mean difference in TVC on a pair-wise basis between CSA follow-up session and the NCA follow-up session (<i>Retest</i>).	56
Table 4.5 Effect sizes of Pearson's <i>r</i> ($\alpha = 0.05/\text{adjusted } p_{\text{corrected}(FWER)} = 0.0125$; N=55) for rTVC against nHAE at respective PTA threshold.	57

LIST OF FIGURES

Figure 3.1 Schedule of longitudinal assessments for participants. Median intervals to each category of assessment are shown for each participant subgroup. (*Top*) Collision sport athletes (CSA) involved in boys' American football (N=38) and girls' soccer (N=19) were imaged at least five times around their competition season (*Pre*: during off-season conditioning; *In1*: during first half of the competition season (1-10 weeks after onset); *In2*: during second half of the competition season (5-15 weeks after onset); *Post1*: 1-2 months after end of the competition season (14-25 weeks after onset); *Post2*: 4-6 months after end of the competition season (24-38 weeks after onset); *Post3*: a subset of non-senior participants were imaged again 7-9 months after end of the competition season (44-52 weeks after onset). (*Bottom*) Non-collision sport athletes (NCA; N=29, F/M=14/15) involved in non-collision sports (see Table 3.1) were imaged twice during competition and conditioning (*Test* and *Retest* separated by 1-2 months). 29

Figure 3.2 Pipelines for pre-processing, generation, and application of tissue-specific masks to T1w images for calculation of volumetric changes as a function of time. (*Top*) For each athlete (*j*) and session (*k*), the native-space T1w MRI is converted to the international consortium of brain mapping standard space template/atlas (ICBM152) for subsequent masking. (*Bottom*) Three tissue-specific masks are generated and subsequently parcellated into 300 total regions of interest (ROIs, *i*) for application to the standard space T1w images, allowing quantification of volumetric measurements in each region for each athlete and session ($Vol_{i,j,k}$). Segmented tissues include gray matter (GM), white matter (WM), cerebrospinal fluid (CSF), and ventricular (or "deep") cerebrospinal fluid (dCSF). Tools used: Analysis of functional neuroimages (AFNI) and FMRIB software library (FSL)..... 32

Figure 3.3 (Columns: Left to Right) Axial, sagittal, and coronal mask images of the FSL-FAST ICBM152 segmentations for (Rows: Top to Bottom) CSF, GM, WM, and Combined (CSF+GM+WM) (a) (Above) Without partial volume estimation (b) (Below) With partial volume estimation. 37

Figure 4.1 (Rows: Top to Bottom) Depiction of WM Johns Hopkins University (JHU) ROIs, GM Shen ROIs and GM Yeo ROIs for (Columns: Left to Right) axial, sagittal and coronal views... 42

Figure 4.2 Visualizing template-specific variance in rRVC. 43

Figure 4.3 Flowchart for group-level ROI analysis. 44

Figure 4.4 Gray matter regions of interest (ROIs) in collision sport athletes (CSA) at each given imaging session (see Figure 1) that exhibited an average relative regional volume change (rRVC), relative to *Pre*, that fell outside the 95% confidence interval defined from *Test-Retest* evaluation of non-collision athletes (NCA; N=29). (A) ROIs falling above the upper bound of the CI are depicted in cyan. (B) ROIs falling below the lower bound of the CI are depicted in red. 46

Figure 4.5 Flowchart for subject-level ROI distribution analysis..... 47

Figure 4.6 Cumulative distribution of ROIs with individual ROIs representing the percentage of CSA subjects exceeding the NCA 95th percentile CI bound of rRVC for that ROI for GM (a) Lower 95th and (b) Upper 95th. 48

Figure 4.7 Cumulative distribution of ROIs with individual ROIs representing the percentage of CSA subjects exceeding/outside the <i>NCA</i> 95 th percentile CI bound of rRVC for that ROI for WM (a) Lower 95 th and (b) Upper 95 th .	49
Figure 4.8 Cumulative distribution of ROIs with individual ROIs representing the percentage of CSA subjects exceeding the <i>NCA</i> 95 th percentile CI bound of rRVC for that ROI for tissue (a) WM and (b) GM.	51
Figure 4.9 Boxplots depicting rTVC (GM, WM, CSF, dCSF) against sessions for <i>NCA</i> , <i>CSA</i> populations. (Significant differences for pairwise <i>t</i> -tests are highlighted by brackets).	53
Figure 4.10 Linear dependence ($p_{Bonf} < 0.05$) at <i>Post1</i> (N=55) for percentage relative tissue volume change (rTVC) of ventricular cerebrospinal fluid (<i>dCSF</i>) as a function of the number of head acceleration events (nHAE) exceeding 50 G. Female soccer athletes (N=19), male football athletes (N=36) are represented by solid triangles and solid circles respectively. Red solid and blue dashed lines represent the mean regression line and corresponding 95% confidence interval.	57
Figure 4.11 Linear predictor plots for rTVC at session <i>Post1</i> of GM, dCSF against nHAE at 75G, 50G respectively.	58
Figure 4.12 Linear predictor plots for rTVC at session <i>Post1</i> of GM (Left), dCSF (Right) against nHAE at 75G, 50G respectively. Top row for N=19 soccer athletes, bottom row for N=36 football athletes.	59
Figure 4.13 Linear predictor plots for rTVC at session <i>Post1</i> of dCSF against nHAE at 50G for (a) larger (Post-hoc) cohort of athletes, (b) football only.	60
Figure 4.14 WM rRVC ROI distribution by session.	61
Figure 5.1 Hypothesis of pathophysiological mechanisms linking RHT (as associated with exposure to HAEs) to observed reversible changes in GM and dCSF volumes. Other disorders (yellow) known to effect similar changes in GM and dCSF, in addition to changes in <i>WM</i> that were not observed herein, are depicted along with key pathways (blue) hypothesized to lead to these neurological observations (green).	68
Figure 5.2 Hypothesis of metabolic regulatory pathways as associated with repeated exposure to HAEs to observations of altered. The pathophysiological metabolic regulatory mechanisms (Blue) of the conditions (yellow) anorexia nervosa, dehydration, and RHT hypothesized due to the observation of similar metabolites (Myo-Inositol, Glutamine-Glutamate) concentration imbalance (Green).	69
Figure 5.3 Hypothesis of reactive astrogliosis and glymphatic system dysfunction as an explanation for the changes observed with head trauma. <i>Green</i> depicting the observed outcomes with repetitive head trauma, <i>sky blue</i> pinpointing an adverse outcome and <i>transparent dark blue</i> representing key metabolic processes.	70

ABBREVIATIONS

RHI	Repetitive Head Impacts	WM	White Matter
RHT	Repetitive Head Trauma	CSF	Cerebrospinal Fluid
TBI	Traumatic Brain Injury	TVC	Tissue Volume Change
mTBI	Mild Traumatic Brain Injury	CSA	Collision Sport Athletes
CTE	Chronic traumatic Encephalopathy	NCA	Non-collision sport Athletes
fMRI	Functional Magnetic Resonance Imaging	AFNI	Analysis of Functional Neuroimages
HAE	Head Acceleration Events	FSL	FMRIB Software Library
CVR	Cerebrovascular Reactivity	BVC	Brain Volume Change
MR	Magnetic Resonance	PTA	Peak Translational Acceleration
MRI	Magnetic Resonance Imaging	HITS	Head Impact Telemetry System
DTI	Diffusion Tensor Imaging	PBVC	Percentage Brain Volume Change
RTP	Return to Play	KS	Kolmogorov Smirnov
ROI	Region of interest	ANOVA	Analysis of Variance
VBM	Voxel-based Morphometry	JHU	Johns Hopkins University
RVC	Regional Volume Change	CI	Confidence interval
MNI	Montreal Neurological Institute	HS	High School
GM	Gray Matter	MS	Middle School
		DMN	Default Mode Network

ABSTRACT

Recent observations of short-term changes in the neural health of youth athletes participating in collision sports such as football (boys) and soccer (girls) have incited a need to explore structural alterations in their brain tissue volumes. Studies have shown biochemical, vascular, functional connectivity, and white matter diffusivity changes in the brain physiology of these athletes that are strongly correlated with repetitive head acceleration exposure from on-field collisions. Here, research is presented that highlights regional anatomical volumetric measures that change longitudinally with accrued repetitive head impacts. A novel pipeline is introduced that provides simplified data analysis on a standard-space template to quantify group-level longitudinal volumetric changes within these populations. For both sports, results highlight incremental relative regional volumetric changes in the sub-cortical cerebrospinal fluid that are strongly correlated with head exposure events greater than a 50G threshold at the short-term post-season assessment. Moreover, longitudinal regional gray matter volumes are observed to decrease with time, only returning to baseline/pre-participation levels after sufficient (5-6 months) rest from collision-based exposure. These temporal structural volumetric alterations are significantly different from normal aging observed in gender and age-matched controls participating in non-collision sports. Future work involves modeling safe repetitive head exposure thresholds with multimodal image analysis and understanding their underlying physiological functioning. A possible pathophysiological pathway is presented highlighting the probable metabolic regulatory mechanisms. The interdisciplinary nature of this work is crucial to understand this pathology accurately and aid healthcare, sport professionals in the future. It is evident that continual participation in collision-based activities may represent a risk wherein recovery cannot occur. Even when present, the degree of the eventual recovery remains to be explored but has strong implications for the well-being of collision-sport participants.

1. INTRODUCTION

1.1 Neurotrauma in Youth Athletes involved in Collision-based Sports

The work presented here contributes to the larger study conducted by the Purdue Neurotrauma Group. The group has been investigating the effect of repetitive head impacts (RHI) on the overall cognitive health of youth athletes within the West Lafayette-Lafayette region of IN, USA. The study protocol mainly implements non-invasive imaging, computerized cognitive testing combined with on-field telemetry that record real-time biomechanical data quantifying each hit (ding, whiplash or blows to the body) experienced by the local athletes participating in collision-based sports.

The effect of blunt force trauma causing symptomatic changes in the health of athletes involved in collision sports (football, soccer, rugby, ice hockey, boxing, etc.) is widely observed and quantified (Guskiewicz et al., 2004, 2006; McCrory et al., 2013; Gavett et al., 2011; McKee et al., 2016; McKee & Daneshvar, 2015; Tagge et al., 2018). Common symptoms are loss of consciousness, post-traumatic amnesia, dizziness, nausea, balance impairment, headache, emotional instability, behavioral changes, cognitive impairment, etc. Post hoc tests such as the standardized assessment of concussion, physiological monitoring, non-invasive brain imaging and other neurocognitive testing are frequently employed to further investigate the pathology of these symptoms (Papa et al., 2015; Slobounov et al., 2010, 2017). It is a vital task to explore the effects of trauma that is clinically asymptomatic but accrues over time to present with neuroradiological changes within the brain's biochemistry (Bari et al., 2019; Poole et al., 2014, 2015), vascular regulation (Svaldi et al., 2015, 2017, 2020), structural integrity (Chun et al., 2015; Jang et al., 2019; Schneider et al., 2019), cognitive functioning, etc. (Abbas, Shenk, Poole, Breedlove, et al., 2015; Abbas, Shenk, Poole, Robinson, et al., 2015; Shenk et al., 2015).

It is these unnoticed asymptomatic or silent changes that affect the overall neural health of the athletes which interests investigators to explore, observe and quantify their pathophysiological regulatory mechanisms. Assessing biomarkers that present with this pathology can benefit athletes, trainers, and healthcare professionals in creating timely intervention strategies for the athletes involved in these collision sports (J. E. Bailes et al., 2013; Nauman et al., 2020; Nauman & Talavage, 2018; Talavage et al., 2014, 2016).

1.2 Detection of Structural Alterations in these Youth Athletes

Physicians and healthcare professionals should be concerned for the neural health of athletes participating in collision-based sports. Understanding the exact mechanisms that drive traumatic change plays a pivotal role in the fast recovery of these athletes. Since the nature of this trauma is so hidden, it is unclear as to the consequences of continued participation in collision sports without timely intervention. This pathology and the head impact events that cause it do not elicit any noticeable clinical symptoms, although non-invasive imaging has demonstrated functional changes quantifying different neuroradiological parameters such as white matter structural integrity, imbalance in brain metabolite concentrations, gray matter functional connectivity, etc. With the observation of different functional changes detected by these imaging sequences, we postulate that there would be an underlying brain tissue volume change.

Neurodegenerative disorders such as dementia (Y. K. Lee et al., 2013) and multiple sclerosis (Fisher et al., 2008), psychiatric disorders such as schizophrenia (Giuliani et al., 2005) and other sports-related trauma (Meysami et al., 2019; Tremblay et al., 2019) have been previously associated with brain tissue volume changes. Here we will be investigating the longitudinal change of these brain tissue volumes to detect subtle statistical changes across populations of collision sport athletes against non-collision-based controls. To gain insights on the overall impact of RHI we will be correlating these brain volumetric measures with the athletes' on-field telemetry that quantifies the peak translational acceleration of an individual head exposure event.

Researching domain-based mathematical manipulation of MRI data to yield meaningful tissue-level volumetric measurements is a challenge. Prior research in quantifying structural brain volume changes has produced measurements with a low degree of reproducibility (Ashburner & Friston, 2001; Good et al., 2001). The existence of multiple techniques and software packages exploring various segmentation schemes has demonstrated a low degree of overlap while quantifying regional brain tissue volumes (Akujedu et al. 2018). A novel pipeline is presented here in an effort to reconcile these findings.

Moving forward, we will be tying together the observations and results of these brain volume measurements with biomechanical correlates from on-field telemetry. Addressing these challenges and explaining the nature of this repetitive head trauma (RHT) pathology will provide a basis for professionals to address this phenomenon with the right intervention strategies. Moreover, the elucidation of the biological regulatory mechanisms and pathways will increase the

visibility of studying this asymptomatic pathology by linking it with similar and/or more gross forms of neurodegenerative trauma. Bringing together all these elements will increase the importance of neuroscience research, especially within the confines of sports medicine.

Current findings demonstrate short-term reversible changes in the brain tissue volumes of athletes participating in collision sports. These changes are strongly tied to the translational head exposure loading at certain g-force thresholds. Investigating the pathways that present with similar volumetric changes in different pathologies can shed light on the nature of RHT. Understanding these regulatory pathways and mechanisms should inform clinicians and healthcare professionals about the possible indicators of this pathology. Most recent literature directs the implications of these findings to further investigate the role of the glymphatic system, the brain's waste clearance system, with RHI (Li et al., 2020; Plog et al., 2015).

The extent of these neuroimaging changes is not only observed in high-school aged youth athletes but also middle-school football athletes who are only starting to learn the sport (Appendix 8.1). Not only does age play a key role but so does the sex and sport with changes being observed in the neuroradiological images of girls' soccer athletes (Appendix 8.2). The early onset of neurological changes and a lack of age and gender bias when it comes to RHI reiterates the need to monitor the neural health of youth athletes continuously and proactively.

2. BACKGROUND

2.1 Neurotrauma

2.1.1 Mild Traumatic Brain Injury

Traumatic brain injury (TBI) is estimated to result in approximately 1.6-3.8 million cases annually (Langlois et al., 2006). Global numbers are currently estimated to be around 69 million with 25% of the cases being recorded in North America (Dewan et al., 2019). Of these numbers, mild traumatic brain injury (mTBI) represents about 80-90% of the cases (Bigler and Maxwell et al. 2012; Bigler, 2013; Sussman et al., 2017). Long-term risks involved with mTBI are neurologic disorders such as dementia (Gardner & Yaffe, 2015; Y. K. Lee et al., 2013), mild cognitive impairment (Washington et al., 2016), psychiatric disorders such as post-traumatic stress disorder (Stein et al., 2009); and in certain cases, chronic traumatic encephalopathy (CTE) (Briggs et al., 2016; Gavett et al., 2011; Martland et al., 1928) as originally observed in dementia pugilistica (a.k.a, punch-drunk syndrome). In a few case studies involving athletes (boxers, football players), this CTE is accompanied with progressive tauopathy (neurofibrillary tangles and phosphorylated tau protein) a common neurodegenerative biomarker observed here after repetitive head injury (di Virgilio et al., 2019; L. E. Hunter et al., 2019; Siman et al., 2013)

mTBIs are clinically evaluated based on the following criterion. “mTBI is a TBI with any evidence of post-traumatic amnesia less than 24 hours, loss of consciousness less than 30 minutes and a Glasgow Coma scale score of 13-15” (Carroll et al., 2004). This *World Health Organization Taskforce* criterion has evolved over the years (Alexander, 1995; Prince & Bruhns, 2017) with the involvement of other governing bodies such as the *Center for Disease and Control* and the *American Congress of Rehabilitation Medicine*. Additionally, the TBI handbook for emergency physicians (Blyth & Bazarian, 2010) and review (Sa & Syed, 2014) highlight the need to manage TBI and its related pathologies with utmost care. Delving into the neurological aspects of sports concussion (D. King et al., 2014; Mccrory, 2004) and its thresholds for diagnosis (D. King et al., 2016a; McCrory et al., 2013) educates one about the relevance of studying this pathology.

Some believe that TBI is not a disease but an event (Rapp & Curley, 2012) that leads to neurological or psychiatric disorders. “The idea that CTE can stem from hits below the level of concussion is relatively new” (Louis et al., 2010). The first known observance of dementia

pugilistica was in boxers, especially “the less expert but courageous men who take considerable injury in the hope of wearing out their opponent” (Parker et al., 1934). Reconciling these facts and statements led us to explore the RHT pathology in the under-experienced youth athletes.

2.1.2 Sports-related Neurotrauma

Sports-related mTBI is documented in athletes playing collision sports such as football and soccer (Talavage et al., 2014, 2016). It is to be noted that about 50-90% of sports-related mTBI go undiagnosed (Baugh et al., 2012) which causes serious concerns for the well-being of these athletes. The NFL documents at least 0.7 concussions per game when averaged over a period of 4 seasons (Clark et al., 2017) with a greater rate of milder repetitive head injury and exposure (Baugh et al., 2015; Daneshvar, Nowinski, et al., 2011). It is a vital task to understand the exact on-field features of head exposure such as impact location, player position, and active game time.

Football and soccer account for most sports-related mTBI in high school collision sports (J. E. Bailes et al., 2013). To further add to the toll of RHI, the incidence of concussions reported by high-school aged students has been increasing at a steady pace, ~15% annually (Lincoln et al., 2011). The national collegiate athletic association also reports that football contributes to the greatest number of injuries of all their sports (Hootman et al., 2007).

Concerns for the neural health of these youth athletes are further highlighted in observing changes in neurological behavior coupled with and without clinically observed impairment (Talavage et al., 2014). These changes can be explained by the documentation of “subconcussive” or “silent” impacts that cause cognitive deficits and neurophysiological impairment while being asymptomatic in nature. Research relating to RHT is mainly classified into neurobiological, neuropsychological and impact exposure metrics (Mainwaring et al., 2018). Cognitive impairment has been functionally detected without a clinically diagnosed concussion in football players (Talavage et al., 2014), moreover the neurophysiological deficits assessed by immediate post-concussion assessment and cognitive testing and functional magnetic resonance imaging (fMRI) in these athletes shows a strong correlation with head acceleration exposure (HAE) (Davenport et al., 2014; Nauman et al., 2015).

Soccer players have also demonstrated abnormal neurophysiological and neuropsychological function caused by subconcussive RHT (Moore et al., 2017; Strauss et al., 2021). Heading in soccer carries an inherent risk to injury aligned with the outcomes of greater

concussion literature (Maher et al., 2014). In certain cases, CTE has been detected in players without a history of concussion further eliciting the role of RHI (Bailes et al., 2015; Bailes et al., 2013; Gavett et al., 2011; Gysland et al., 2012; Koerte et al., 2015, 2021a). There lies an increased risk of developing dementia and other neurodegenerative disorders if one is involved with high school football (Savica et al., 2012). Previous studies suggest that males pose a greater risk of concussion playing football whereas it is soccer for females (Giza & Hovda, 2014; Koerte et al., 2021), without a strong correlation for age or level of participation. However, the age of first exposure is strongly correlated with neuropsychiatric and cognitive outcomes (Alosco et al., 2017) highlighting concerns for the well-being of these athletes.

It is important to note that many players do not report when being hit for the fear of being benched or removed from the game (Dvorak et al., 2007; Meier et al., 2015; Talavage et al., 2014), this phenomenon is also observed in concussion reporting (Register-Mihalik et al., 2013). Additionally, the helmets that these athletes wear is mainly designed to absorb the high intensity impacts and provides little to no protection from low or medium intensity blows whose cumulative effect can be injurious to the brain (Benson et al., 2009; Cumiskey et al., 2019; Daneshvar, Baugh, et al., 2011). It is noticed that the head impact exposure profile for football is worse when compared to rugby for the same adolescent age group, noting the fact that the latter does not require the use of much safety equipment (D. A. King et al., 2016) for its athletes. Although the gameplay of these two sports presents with some similarities, they mainly differ in how the ball is passed, which probably affects the tackling accelerations. The gruesome and hidden nature of trauma experienced by these athletes participating in these collision-based sports provides inspiration to construct protocols for continuous monitoring and safer management.

2.1.3 Health Monitoring

There are numerous imaging tools that assist with brain injury research (J. V. Hunter et al., 2012; Sharma et al., 2010; Wintermark et al., 2015). Multi-modal image analysis exploring the effect of RHI (Talavage et al., 2021, Davenport, Apkarian, et al., 2016; Davenport, Urban, et al., 2016; Dean et al., 2015; Eierud et al., 2014; Narayana et al., 2015; Slobounov et al., 2017) and structural health monitoring measures (Talavage et al., 2016) recommend a path that must be taken when it comes to dealing with RHI. Enacting along the lines of sports concussion management

(Guskiewicz et al., 2004, 2006), frequent health monitoring to detect pathological changes non-invasively using neuroradiological imaging should be a regular practice.

Neurological changes are expressed biochemically in spectroscopic measures (Bari et al., 2019; Eisele et al., 2020; Johnson et al., 2012; Lin et al., 2015), vascular autoregulatory capacity modulation that quantify cerebrovascular reactivity (CVR) (Bari et al., 2019; Svaldi et al., 2015, 2017), functional network connectivity alteration quantified using resting-state fMRI (Abbas, Shenk, Poole, Robinson, et al., 2015; DeSimone et al., 2021; Sours et al., 2015; L. Tang et al., 2011; Zhou et al., 2012), visual working memory alteration (McDonald et al., 2012; Shenk et al., 2015; Sinopoli et al., 2014; Wylie et al., 2015), and white matter diffusivity parameters (Bahrami et al., 2016; Chun et al., 2015; Davenport et al., 2014; Jang et al., 2019b; Khong et al., 2016; Lee et al., 2008; Messé et al., 2011; Sharp & Ham, 2011; Veeramuthu et al., 2015; Zhu et al., 2014) using diffusion tensor imaging (DTI) in athletes experiencing RHI. All these measures are coupled with biomechanical correlates obtained from on-field telemetry which documents the linear and rotation acceleration for each ‘ding’, hit, head acceleration event, and whiplash to the body (Breedlove et al., 2012; Davenport et al., 2014; McCuen et al., 2015; Nauman et al., 2015; Nauman & Talavage, 2018; Poole et al., 2015). Oftentimes, all these observations are correlated with neuropsychological assessments (Dean & Sterr, 2013; Fischer, Red, et al., 2016; Gysland et al., 2012; Munce et al., 2014; Nordin et al., 2016.). Moreover, multi-modal diffuse connectivity maps constructed using resting state fMRI and DTI data demonstrate the functional impairment due to diffuse axonal injury (Tang et al., 2012; Tang et al., 2011) in these athletes.

Observing such prevalent changes in the collision sports youth athlete population, we hypothesize that there would be longitudinal structural volumetric changes that can be observed on the T1-weighted structural magnetic resonance imaging (MRI). In most cases of athletes with RHT, not only is there a considerable loss of gray matter volumes and dilated ventricles (Gong et al., 2018; Ling et al., 2013; Raji et al., 2016) but also an increase in inflammatory biomarkers such as glial fibrillary acidic protein, neurofilament light protein, tau proteins, etc. (Neselius et al., 2012) suggesting the improper functioning of glial cells in the brain. Thus, providing the necessary motivation to conduct this study and accordingly analyze their MRI images for structural abnormalities.

Using the information derived from non-invasive imaging analyses, we should be able to improve the RTP/RTL (return to play/return to learn) guidelines for these individuals and their

educators (Cancelliere et al., 2014). Currently, RTP guidelines require a minimum of 14 days after a concussive incident as opposed to a minimum of 10 days for adults (Khurana et al., 2012) without much of a prescription for RHT. Factoring in the results from the MRI and creating individualized RTP protocols that document injury profile, history, and neurodevelopmental stages would be beneficial to these athletes and avoid further damage to their neural ecosystem (Mihalik et al., 2014). Sadly, we are only monitoring the RHT. The treatment will require randomized double-blind studies to ascertain if the monitored athletes improve with different RTP protocols. Regardless, continuous health monitoring is a key step in collecting the required data to observe this pathology.

It is also recommended that amongst other prescriptions such as rest from physical activity, regular non-collision-based exercise would be beneficial to the athlete (Halsen et al, 2013). Most of these guidelines are tuned to concussions/TBIs but should be extended to mTBIs and clinically asymptomatic athletes exhibiting functionally abnormal brain neuroradiological imaging parameters. With a lot of attention to avoid a second impact/ secondary injury which would be more detrimental than the first (Mccrory et al., 2012) in the case of a concussion, there should be frequent health monitoring to prevent similar cascades when it comes to RHT.

The ongoing debate of whether head trauma leads to generalizable neurological changes is an evolving topic with political influences from different parent sport associations. In the efforts to make the sport safer and being cognizant of the athlete's health, individualized monitoring would probably be the best route to avoid misinterpreting results from various studies. There is a need for technological advancement to constantly monitor these athletes, be it better telemetry to quantify rotational accelerations of head impacts, video monitoring or coaching tackling techniques, etc. Since it has been observed that athletes with similar hit distribution profiles show divergent neurological changes, continuous and proactive health monitoring provides the best alternative to detect any existing neurological deficits.

2.2 MRI Morphometric Analysis

2.2.1 MRI Basics

Coupled with some graduate-level medical imaging courses, Bitar et al. (2006) and A. F. Mills et al. (2017) go into detail about MRI imaging basics, RF pulse sequence design which

should serve as an effective primer for novice readers entering the magnetic resonance (MR) field. In this study to help us discern the RHT pathology from a control athlete population we are utilizing the T1-weighted structural MRI. T2-weighted MRIs histograms are harder to decompose/resolve/segment when compared to the T1-weighted histogram profiles of voxel-wise intensities (Diaz-de-Grenu et al., 2014). Here, we create a novel pipeline using the intensity-based T1 (spin-lattice relaxation) MRI of each athlete and correlate it with biomechanical measures collected on the field to ultimately produce valuable group level statistics of their brain volumes. It would be useful to include contrast based T1-weighted MRI, fluid attenuated inversion recovery MRI in future protocols to help us gauge the structural tissue-level changes with greater accuracy.

2.2.2 Existing Techniques

Initially, brain morphometry research was conducted on normal subjects and phantoms to assess their errors (Filipek et al., 1989), mainly executed on a 2-dimensional or slice-by-slice basis. MRI imaging was then used to highlight 3-dimensional tissue and anatomic-based contrasts to study the nature and development of the brain (Caviness Jr et al., 1996, Kennedy et al., 2002). Morphometric descriptors were analyzed using tissue segmentation, cortical parcellation, subcortical and white matter parcellation schemes. If one were to perform group-level analyses, the key task with morphometry is accurate brain segmentation and registration. The segmentation algorithms' performance was catapulted using an automated hidden Markov random field model and expectation-maximization algorithm (Zhang et al., 2001). The field then moved to semi-automated techniques that showed better reproducibility when quantifying volumes and surfaces of these MR images (Nishida et al., 2006). The bulk of the morphometric analysis was carried out on T1-weighted images, with some neurodevelopment analysis on T2-weighted images (Peterson et al., 2003). Studies with larger sample sizes were able to quantify the trajectories of brain development, tissue volume change across sexes, and across different brain regions (Lenroot et al., 2007). After which, these morphometric techniques have started being employed to study disease, learning, and aging (Mietchen et al., 2009) with other methods of contrast such as magnetization transfer ratio for applications like tumor imaging (Garcia et al., 2015).

Brain volumetric measures have vexed research scientists since the advent of non-invasive imaging (Ashburner & Friston, 2000; Bookstein, 2001; Haug, 1986). Structural volumetric changes are traditionally quantified using global or whole-brain morphometry techniques and/or

otherwise manually delineated regional volumetry. The former employs automated algorithms whereas the latter depends on the skills of the MRI technician or radiologist. The latter approach highlights the specific region-of-interest (ROI) and is mainly practiced for lesion/tumor segmentation (Hevia-Montiel et al., 2015). The lack of a gold standard to thoroughly ascertain brain volumes has led to multiple techniques and measures with a low degree of reproducibility. The myriad of neuroimaging data collected in the past few decades creates a need to develop quick and efficient algorithms to calculate brain volumes accurately with many clinical applications (Giorgio & de Stefano, 2013). Existing methods include automated voxel-based morphometry by FSL-SIENA (Smith et al., 2002), FSL-VBM (Smith et al., 2004; Andersson et al., 2007), model-based FSL-FIRST (Patenaude et al., 2011), and technician based manually segmented regional volumetry techniques (ITK-SNAP v3.8: Hashempour et al., 2019, Bartel et al., 2017; SPM-DARTEL: Lin et al., 2013, Ashburner et al., 2010). These methods have been compared in their performance for quantifying brain subcortical volumes (Akudjedu et al., 2018; Good et al., 2001).

Here, we introduce a region-based volumetry technique and test its efficacy on a dataset of high-school collision sport athletes experiencing RHI. It is to be noted that the pathology of RHT differs greatly from TBI and other more severe lesion-specific diseases that drastically affect the structural morphology of the brain (Brett et al., 2020). Hence, the degree of error while performing automated segmentation and tissue classification is lower in the former condition, allowing for easier comparisons with a healthy/control population (Irimia et al., 2012).

2.2.3 Comparison of Morphometric Techniques

Voxel-based morphometry (VBM) tools have been used in combination with manual ROI-based measures for patients with schizophrenia (Giuliani et al., 2005), studying aging in 465 normal adult human brains (Good et al., 2001) and moderate-severe TBI (Cole et al., 2018). The methods highlighted here aim to reconcile voxel-based volumetry but normalize the analysis across ROIs. A more comprehensive study with 163 subjects validating VBM for subcortical ROIs compared to manual ROI volumetry is seen in Focke et al. (2014) justifying the analysis conducted here. In essence, automated VBM performs better in cases where subcortical structures are difficult to highlight and discern thereby guaranteeing higher anatomical specificity. We reconcile this fact as the ROIs delineated for the standard space group-level templates require anatomical specificity for the computation of regional volume changes, thereby eradicating the need for manual ROI

description in the original coordinate space the image was acquired. Ross et al. (2011) reviews similar longitudinal studies on MRI volumetry tools which use intracranial volume as a normalization measure for 230 subjects diagnosed with mild to severe TBI; and as the review points out that atrophy values are different but comparable for tools ranging from semi-automatic to completely automated tools (SPM, FSL-SIENA, etc.). This low degree of reproducibility could stem from the overly comprehensive intracranial normalization (Adduru et al., 2020) used which could be erroneous as compared to a more region-specific normalization implemented here.

Spatial patterns can also be quantified using the Jacobian determinant as demonstrated in Cole et al. (2018). The Jacobian technique (Nakamura et al., 2014) also picks up brain atrophy changes after moderate-severe traumatic brain injury and remains to be quantified as an added output in future analyses. The sensitivity of morphometric techniques varies across different pathologies with different degrees of change, making comparison across RHT and concussion data a tough task. Although the final output is a volumetric entity, the nature of its implications is tied to the underlying histopathology and image processing.

2.2.4 Proposed Model of Morphometry

While quantifying brain atrophy progression, the existence of a prior distribution of T1-weighted MRI favors the reliability of longitudinal measures when compared to cross-sectional measures (Ross et al., 2022; Ross et al., 2011). Exploiting this fact, we introduce a novel pipeline to compute relative regional volumetric changes (rRVC) that normalizes regional brain volume changes at a follow-up time point with respect to the baseline T1-weighted MRI scan. Each T1-weighted MRI undergoes the standard preprocessing steps such as brain extraction/skull-stripping, bias field correction, and warping to the MNI-152 (Montreal neurological institute) standard space template (Fonov et al., 2009).

The rRVC measure is then integrated over regions of the respective tissue classes: gray matter (GM), white matter (WM), and cerebrospinal fluid (CSF) to yield relative tissue volumetric change (rTVC); across different timepoints for collision sport athletes (CSA) and non-collision athletes/controls (NCA). rTVC is further integrated over all the tissue classes to yield relative total brain volumetric change (rBVC). These volumetric measures are analyzed to develop meaningful statistical models across the CSA, NCA, and within the CSA populations. To understand their relationship with RHI as a possible explanatory variable, these measures are further assessed with

cumulative count of head acceleration events (nHAE) exceeding a certain peak translational acceleration (PTA) threshold as a covariate.

The novel pipeline introduced here helps alleviate the inconsistencies in previous volumetric methods (Ashburner et al., 2000-Bookstein et al., 2001-Ashburner et al., 2001, Giuliana et al., 2005) and simplifies group-level comparisons on a standard space template/atlas using a normalization scheme. It accommodates for regional variation of changes coupled with sensitivity to spatially complex group differences (Ashburner, 2010; Ashburner & Friston, 2001). The quantification of longitudinal changes in relative tissue volumes of CSA with nHAE at different PTA thresholds as a covariate further elicits the applicability of this pipeline.

The volumetric measures evaluated here use whole-brain white matter (Mori et al., 2005), ventricular CSF (Vrenken et al., 2014), and a gray matter (Shen et al., 2013) parcellation for male (football) and female (soccer) for CSA, non-collision controls (NCA) of similar ages. Each tissue class has different mechanical properties (Budday et al., 2019) and vital functions associated with the overall neural health. rTVC of brain tissues for CSA exhibited significant deviations during the collision season that largely recovered to pre-participation/baseline levels by 5-6 months after the season's end. Prior work has revealed longitudinal region-specific volumetric changes in both gray matter (Bigler et al., 2004; B. D. Mills et al., 2020; Zhou et al., 2013) thickness and ventricular CSF increase (N. D. Davenport et al., 2018; T. C. Harris et al., 2019; Ledig et al., 2017) in subjects with mild traumatic brain injury. The observations here document similar findings, but for a cohort of asymptomatic youth athletes involved in collision-based sports experiencing RHI. Exploring the nature of these changes coupled with the possible metabolic regulatory mechanisms and pathways involved should inch the research closer to quantifying a reliable biomarker for this pathology.

2.3 Pathophysiological Modeling

2.3.1 Glymphatics

Introduction: Understanding the implications of the underlying pathophysiological conditions that govern these observations led us to explore the intricacies of the glymphatic system. The glymphatic system or the glial-lymphatic system is the macroscopic waste clearance system of the brain. It is a system of perivascular channels formed by astroglial cells that eliminates waste,

distributes non-waste compounds (glucose, lipids, amino acids, neurotransmitters) and is largely engaged during sleep (Cai et al., 2020; Fultz et al., 2019.; Jessen et al., 2015; Mestre et al., 2020).

We hypothesize that if there are macroscopic volumetric changes observed in the CSF of CSA then there should be a disturbance in its glymphatic counterparts causing non-ideal waste clearance. Similar hypotheses have been validated in humans for TBI and aging (Iliff et al., 2012; Jessen et al., 2015; Kou et al., 2010; Kou & Iraj, 2014; Kou & VandeVord, 2014; Plog et al., 2015; Unterberg et al., 2004). As for the repetitive mTBI, changes in glymphatic clearance have been observed in rat models (Christensen et al., 2020; Li et al., 2020).

Linking the two would require in-depth modeling schemes that explore the metabolic regulatory pathways involved with this pathology. A step further would be to profile the CSF for neurodegenerative protein markers as carried out for Alzheimer's disease (Bader et al., 2020; Dayon et al., 2018), although not an ideal route due to the invasive nature of the procedures. Other non-invasive methods to quantify the glymphatic system are through phase-contrast imaging which maps the velocities of the CSF fluxes (Howden et al., 2008; Masoumi et al., 2013; Matsumae et al., 2014; Takizawa et al., 2017; Yatsushiro et al., 2018), chemical exchange saturation transfer MRI (Chen et al., 2020), CSF motion sensitive imaging (Horie et al., 2017), glymphatic MRI (Eide & Ringstad, 2019; Taoka & Naganawa, 2020), and DTI to detect diffuse axonal injury coupled with glial activation (Kou et al., 2010; Kou & VandeVord, 2014). Quantifying the function of the glymphatic system using CSF volume as a mediator with CSF flow as an outcome should prove to be a valuable causal statistical model for RHT.

Cell-biology: Delving deeper into the biological implications at the cellular level leads us to explore the interaction of this pathology with normal homeostasis. RHT that causes tissue-level changes along of the lines of neural injury could stem from damage or imbalance caused at a cellular level (Nauman et al., 2020). Head trauma from sequelae of repetitive mTBI has been known to cause disruptions in the cerebral blood flow (Champagne et al., 2020), blood brain barrier breakdown and increased neuroinflammation (Dashnaw et al., 2012; Marchi et al., 2013).

The metabolic cascades of immunoexcitotoxicity and microglial activation interact with the brain's waste clearance system via different pathways. There are multiple endogenous neuroprotective mechanisms that come into play after acute cerebral trauma/ischemia. Studying how these mechanisms regulate neuroinflammation (Chiu et al., 2016) can shed light into the

nature of the chronic pathologies involved with accrued head exposure (Leker & Shohami, 2002). It has been documented that certain biomolecules (di Virgilio et al., 2019) such as tau proteins (L. E. Hunter et al., 2019) and microRNA (Papa et al., 2019) can serve as effective biomarkers for this pathology (Siman et al., 2013). Quantifying the concentration of specific serum biomarkers (Vike et al., 2021; Bari et al., 2021) assists with the causal statistical modeling of RHT.

The pathophysiology of severe TBI exhibits great interest to researchers previously being characterized by the neurometabolic cascade of excitotoxicity, mitochondrial dysfunction, alteration in cerebral blood flow and impaired neuroplasticity (Shrey et al., 2011; Signoretti et al., 2011). There exist multiple biomarkers in the CSF that are indicative of RHT which can serve as possible indicators in future studies (Shrey et al., 2011). But the collection of CSF is a very invasive and painful process and possesses implementation setbacks. Other approaches include non-invasive imaging and electrophysiological measurements that quantify the cognitive decline and demonstrate accelerated aging with this pathology (Broglio, et al., 2012). Evaluating the interplay of these various processes and how they play a collective role in quantifying the regulatory pathways led us to model (Brock et al., 2013) the pathophysiological nature of the volumetric changes observed here.

CSF flow modeling: Understanding the production and modulation of CSF within the brain will shed light on the functioning of the glymphatic system and its role with RHT (Johanson et al., 2011). Modeling CSF flow using phase contrast imaging (Howden et al., 2008; Masoumi et al., 2013; Matsumae et al., 2014, 2019) and other modalities will inch us closer to a complete picture of the glymphatic regulation. The vascular networks in the brain also play a role with the modulation of CSF (Das et al., 2021) coupled with low-frequency oscillations in fMRI images (Ghali & Ghali, 2020) and functional near infra-red spectroscopy (Tong & Frederick, 2010, 2012). Mapping the CSF flow from the choroid plexus through the ventricles finally to the subarachnoid spaces whilst being cognitive of the vascular architecture (Bernier et al., 2018; Viviani, 2016) of the brain can serve as an effective strategy for future experiments.

2.3.2 Small Animal Models

The lack of human studies involving the exploration of the glymphatic system and other pathophysiological models is scarce. Currently the field of neurotrauma is indebted to the vast

collection of small animal models that describe this pathology (Turner et al., 2015). The ease and control for experimental implementation and validation of repetitive mTBI in mice has led to observations of neuroinflammation, blood-brain barrier disruption and elevation of other histological biomarkers (Kane et al., 2012). Multiple models explore different mechanisms of head impact delivery (Corrigan et al., 2011) leading to similar observations of hypovolemia, hypoxia (Cernak, 2005), axonal injury (Donald et al., 2007) and impaired spatial memory (Henninger et al., 2005) in these small animals. RHT has also been characterized with apoptosis (Conti et al., 1998), astrogliosis and the accumulation of tau proteins in mice brains (Luo et al., 2014; Rubenstein et al., 2019; Z. Yang et al., 2015). All these models are crucial to understanding the underlying biological pathways and translating the findings to characterizing the neural health of youth athletes exhibiting a similar pathophysiology (Nauman et al., 2020; Semple et al., 2015; Tagge et al., 2018).

3. METHODS

3.1 Experimental Study Design

3.1.1 Participant Demographics

86 high school-aged athletes participated on a voluntary basis, comprising two pools: 57 athletes participating in collision sports (CSA); and 29 athletes participating in non-collision sports (NCA; e.g., track and field, gymnastics, cross-country). Participants were not excluded from either pool due to history of concussion. Participant demographics are provided in Table 3.1.

CSA: 38 male (ages: 15–18 years) and 19 female (ages: 14–18 years) athletes, each participating in collision-based sports (M: American football; F: soccer), were recruited from three local high schools over four seasons of play.

NCA: 15 male (ages: 15–18 years) and 14 female (ages: 14–18 years) athletes, each participating only in non-collision sports, were recruited from the same high schools as the CSA participants. This pool served as a control for the reproducibility of measurements over time.

3.1.2 Participant Schedule

All CSA underwent at least five (5) MRI sessions around their competition season: *Pre*, before collision activity onset (i.e., before season-related activity commenced); *In1*, during the first half of the competition season; *In2*, during the second half of the competition season; *Post1*, near-term follow-up session after (1-10 weeks) competition season conclusion; and *Post2*, long-term follow-up session after (11-23 weeks) competition season conclusion.

For a subset of 21 CSA athletes, a sixth MRI session was conducted: *Post3*, prolonged follow-up session after (29-37 weeks) competition season conclusion. This imaging session was acquired as the *Pre* assessment for the subsequent season for individuals who were not Seniors at the time of *Pre*, *In1*, *In2*, *Post1*, and *Post2*. This session was only incorporated in analyses intended to examine the nature of volumetric changes following a prolonged period free of participation-related collision activity.

Note that all CSA were physically active, but not engaged in collision-related activities, prior to *Pre* and *Pre2/Post3*, as they were all taking part in conditioning activities for their sports.

All NCA underwent two (2) MRI sessions, *Test* and *Retest*, separated in time by 4-13 weeks. All imaging sessions were conducted during training and competition activities to maintain comparable levels of physical activity around each session. Imaging sessions and median intervals between sessions are schematized in Figure 3.1 for both CSA and NCA.

Table 3.1 Demographics of participants with complete set of valid imaging data as collected at *Pre/Test* session. (All values are: Mean \pm StdDev, [Min, Max]), CSA: Collision Sport Athletes, NCA: Non-collision Sport Athletes

Category	Males		Females	
	CSA (N=38)	NCA (N=15)	CSA (N=19)	NCA (N=14)
Age (years)	16.6 \pm 1.2 [15, 18]	16.2 \pm 1.1 [15, 18]	15.7 \pm 1.2 [14, 18]	15.8 \pm 1.2 [14, 18]
Sport	Football (38)	Basketball (2) Track and field (4) Cross-country (1) Swimming (4) More than one (4)	Soccer (19)	Basketball (4) Track and field (3) Gymnastics (1) Swimming (2) More than one (4)
Years of high school athletics participation	2.1 \pm 0.9 [0, 3]	1.77 \pm 1.1 [0, 4]	1.9 \pm 1.0 [0, 3]	1.49 \pm 1.1 [0, 3]
Number of previously diagnosed concussions	0.61 \pm 1.0 [0, 5]	0.48 \pm 0.9 [0, 2]	0.67 \pm 1.1 [0, 3]	0.51 \pm 1.0 [0, 3]
Height (inches)	71.2 \pm 2.7 [65, 77]	70.6 \pm 2.3 [66, 75]	64.5 \pm 2.2 [61, 69]	66.4 \pm 2.1 [62, 71]
Weight (lbs)	186.2 \pm 34.6 [125, 245]	152.6 \pm 24.8 [120, 190]	136.3 \pm 18.4 [106, 170]	127.1 \pm 15.9 [110, 195]
Racial and ethnic categories				
White	30	13	19	11
Black or African American	5	0	0	1
Hispanic or Latino	2	0	0	0
Asian	1	2	0	2

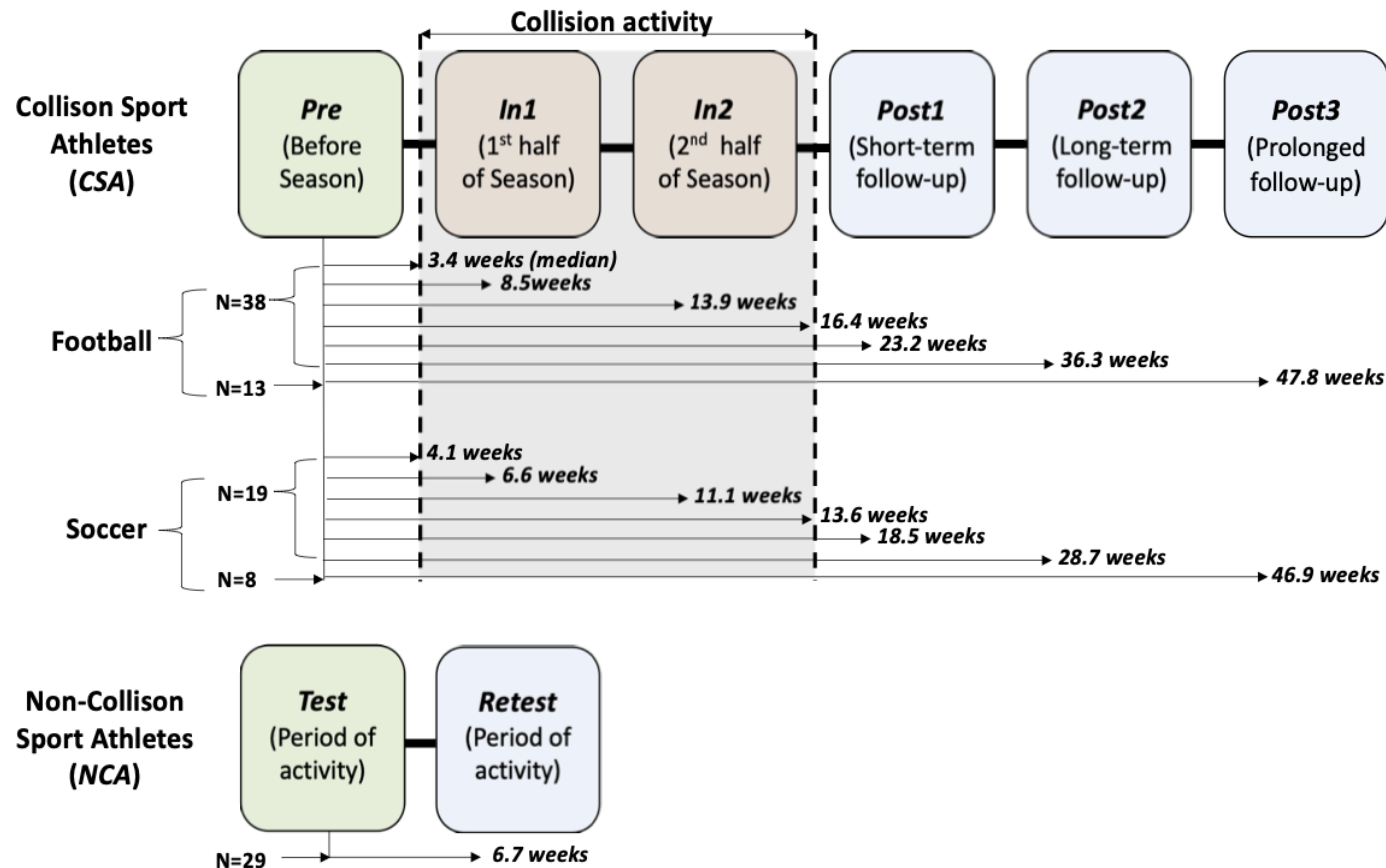


Figure 3.1 Schedule of longitudinal assessments for participants. Median intervals to each category of assessment are shown for each participant subgroup. (*Top*) Collision sport athletes (CSA) involved in boys' American football (N=38) and girls' soccer (N=19) were imaged at least five times around their competition season (*Pre*: during off-season conditioning; *In1*: during first half of the competition season (1-10 weeks after onset); *In2*: during second half of the competition season (5-15 weeks after onset); *Post1*: 1-2 months after end of the competition season (14-25 weeks after onset); *Post2*: 4-6 months after end of the competition season (24-38 weeks after onset); *Post3*: a subset of non-senior participants were imaged again 7-9 months after end of the competition season (44-52 weeks after onset). (*Bottom*) Non-collision sport athletes (NCA; N=29, F/M=14/15) involved in non-collision sports (see Table 3.1) were imaged twice during competition and conditioning (*Test* and *Retest* separated by 1-2 months).

3.1.3 Data Acquisition Protocol

MRI data acquisition: All imaging was conducted at the Purdue University MRI Facility (West Lafayette, IN) using a 3T General Electric Signa HDx (Waukesha, WI) with a 16-channel brain array (Nova Medical; Wilmington, MA). To assess longitudinal stability of anatomical volumes, a high-resolution T1 acquisition (3D fast spoiled gradient recalled-echo; 1mm isotropic resolution; TR/TE = 5.71/1.976msec; flip angle = 73°) was conducted at each session.

Head acceleration events data collection: CSA were monitored for head acceleration events (HAEs) in each official practice and game. Whilst there is no standard procedure for reporting head impact data (D. King et al., 2016b), this study documents telemetry data as PTA for each HAE. These were collected using one of two systems: head impact telemetry system (HITS; Simbex; Lebanon, NH), used only for American football athletes; or the xPatch (X2 Biosystems; Seattle, WA), used for both American football and soccer athletes. The collected data follows the head exposure distribution profile of previous studies (Bari et al., 2019b; Jang et al., 2019a; Svaldi et al., 2020; Lee et al. 2021). HITS encoders were used only with Riddell helmets, being placed prior to the season, and examined thereafter only to recharge batteries or replace encoders that had ceased nominal operation. When the xPatch was used, the device was placed on the athlete's right ear using an adhesive patch prior to each practice or game and collected after the activity. Regardless of the system being used, a researcher was present at every session (practice or game) to ensure proper function of sensors, as described in Talavage et al. (2014) and McCuen et al. (2015). The xPatch was affixed behind the athlete's right ear using an adhesive patch, applied after cleaning of the area with rubbing alcohol. A spray adhesive (Cavilon™) was applied on an as-needed basis.

Note: Two CSA were excluded from our analysis due to incomplete HAE data: one football athlete ceased participation in the sport during the season; a second football athlete had his HITS encoder fail, and no replacement was available for several weeks. Another 20 football players with an imaging session at *Post1* were added to strengthen and to an extent test the linear functional analysis of HAE against tissue volumetric change in the latter part of the analyses.

3.2 Data Pre-processing

3.2.1 MRI Pre-processing

Neuroimaging pre-processing was performed using existing analysis of functional neuroimages (AFNI; Cox et al., 1996) and FMRIB software library (FSL; Smith et al., 2004).

T1-weighted MRI pre-processing: A brain extraction tool (AFNI: *3dSkullStrip*) was applied to strip the skull from each anatomical T1-weighted scan. After skull-stripping, the T1-weighted image underwent bias field correction (AFNI: *3dUnifize*) to normalize tissue intensities and eliminate low-frequency noise components prior to image registration. All T1-weighted images were then registered via affine and high-dimensional nonlinear transformations (AFNI: *auto_warp.py*) along with 3-D spatial blurring (3mm full-width-at-half-maximum) to the MNI-152 nonlinear 6th generation atlas (Fonov et al., 2009).

MRI tissue mask generation: Tissue-specific masks were generated for the MNI-152 template using FSL-FAST (Smith et al., 2004) to yield gray matter (GM), white matter (WM), and cerebrospinal fluid (CSF) masks. Figure 3.2 depicts the pre-processing pipeline conducted on each T1-weighted scan (i.e., for every athlete, at each session) to produce a volumetric measure for a segmented standard-space ROI.

Note that NCA were not monitored for HAEs due to the absence of collisions from nominal participation in these activities, expected to lead to a substantial difference in exposure to RHI relative to CSA.

MRI regional volume generation: Regional volumes within each tissue were quantified using previously defined parcellations. GM volumes were computed based on the 278 region-of-interest (ROI) parcellation of (Shen et al., 2013). WM regional volumes were quantified using the 20 ROI parcellation of the white matter skeleton by (Mori et al., 2005). CSF was quantified using 2 templates, the first being the complete CSF segmented tissue of the MNI-152 template, and the second being a segmentation (Vrenken et al., 2014) of the deep brain/ventricular system CSF (dCSF) which included the lateral and third ventricles.

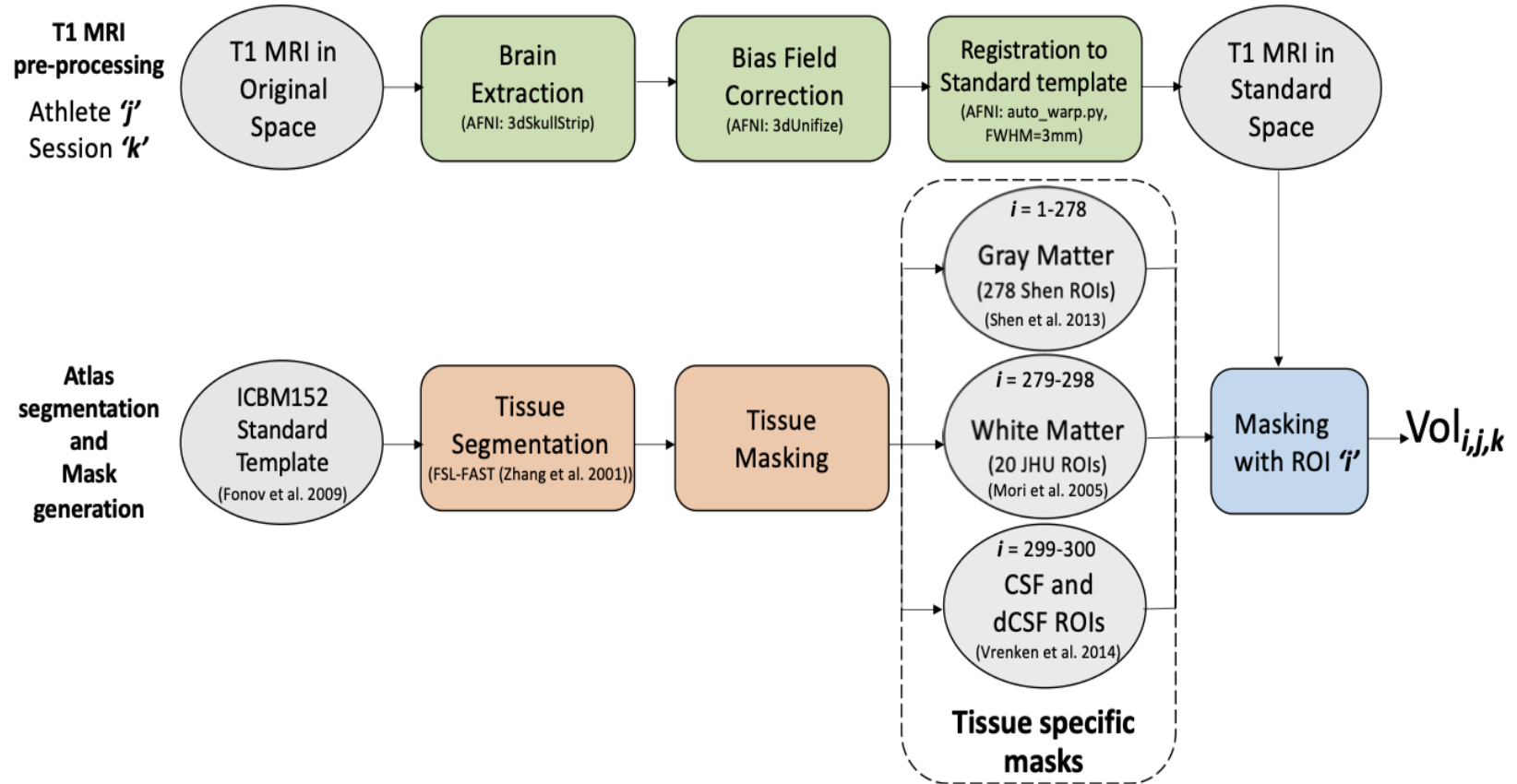


Figure 3.2 Pipelines for pre-processing, generation, and application of tissue-specific masks to T1-weighted images for calculation of volumetric changes as a function of time. (Top) For each athlete (j) and session (k), the native-space T1-weighted MRI is converted to the international consortium of brain mapping standard space template/atlas (ICBM152) for subsequent masking. (Bottom) Three tissue-specific masks are generated and subsequently parcellated into 300 total regions of interest (ROIs, i) for application to the standard space T1-weighted images, allowing quantification of volumetric measurements in each region for each athlete and session ($Vol_{i,j,k}$). Segmented tissues include gray matter (GM), white matter (WM), cerebrospinal fluid (CSF), and ventricular (or "deep") cerebrospinal fluid (dCSF). Tools used: Analysis of functional neuroimages (AFNI) and FMRIB software library (FSL).

MRI relative volume change computation: Relative volume changes were computed at three levels for each unique athlete-session. First, the rRVC was computed on an individual ROI basis, for each ROI associated with a given tissue type. Second, the rTVC was computed for each tissue type (GM, WM, CSF) by aggregating the relative volume changes in comprising ROIs. Third, the relative brain volume change (rBVC) was computed by aggregating over relative tissue volume changes (GM, WM, CSF) for the given athlete-session.

Equations of volumetric transformations: To examine volumetric changes on a normalized region-specific basis, a novel pipeline was implemented. First, the rRVC in the i^{th} ROI was computed for the j^{th} athlete at the k^{th} follow-up session (CSA: *In1*, *In2*, *Post1*, *Post2*, *Post3*; NCA: *Retest*) with normalization to baseline (CSA: *Pre*; NCA: *Test*) volume as:

$$rRVC_{i,j,k} = \frac{Vol_{i,j,k} - Vol_{i,j,Pre}}{Vol_{i,j,Pre}}$$

A closer look at the rRVC equation reveals a Z-score or t -statistic type transformation with the volumes from the follow-up session being normalized by the baseline session. The brain-wide measure of rTVC for a given athlete-session was computed at each session by a weighted sum of the rRVCs obtained for each of the N_X ROIs comprising tissue $X \in \{GM, WM, CSF, dCSF\}$:

$$rTVC_{X,j,k} = \sum_{i=1}^{N_X} c_i \times rRVC_{i,j,k}$$

The weight $c_i = \frac{v_i}{\sum_k v_k}$ is the relative fraction of the ROI volume (in voxels) represented by the ROI within the total volume of ROIs associated with the tissue.

$$rBVC_{j,k} = \sum_X w_X \times rTVC_{X,j,k}$$

The relative total brain volume change (rBVC) was similarly computed as the weighted sum of rTVC over the GM, WM, and CSF tissue masks, where $w_{GM}=0.4262$, $w_{WM}=0.3912$, and $w_{CSF}=0.1826$ represent the relative fraction of the entire brain encompassed by the GM, WM, and CSF masks, respectively for the MNI-152 nonlinear 6th generation atlas (Fonov et al. 2009).

3.2.2 HAE Pre-processing

HAE data were pooled over the HITS and xPatch sensors and subsequently pruned following the windowing and thresholding ($\geq 20G$) procedure of McCuen et al., (2015). Note that while both devices have been documented to exhibit low average error over large sample sizes (Broglia, Surma, et al., 2012; Cummiskey et al., 2017; O’Connor et al., 2017), both devices are also known to exhibit appreciable error levels on an individual measurement basis (Cummiskey et al., 2017). No analyses were performed based on singular events.

The count of HAEs exceeding a PTA threshold ($PTA_{Th} \in \{20G, 25G, 30G \dots 95G\}$) for the j^{th} athlete at the k^{th} ($k \in \{In1, In2, Post1\}$) follow-up session was computed as

$$nHAE_{Th,j,k} = \sum_{p=1}^{M_k} u(PTA_{p,j,k} - PTA_{Th})$$

where M_k represents the total number of HAEs experienced prior to the k^{th} session, and $u(\cdot)$ is the unit/Heaviside step function.

The evaluation of the skin-mounted and helmet sensors show that they have low resolution for each measurement (Tierman et al., 2019, O’Connor et al., 2017, Jadischke et al., 2013), but when averaged performance is measured over a season’s play, they are reliable for these population-based analyses (Cummiskey et al., 2019). Video-based monitoring and assisted telemetry can aid with the collection of on-field acceleration data (Campbell et al., 2020). In addition to quality assurance, it can record new information such as impact location, playing style, and direction of tackle, etc.

3.3 MRI Measurement Reliability

3.3.1 Ground Truth Measurements

SIENA estimates the percentage brain volume change (PBVC) between the T1-weighted images at two-time points. The SIENA PBVC is not normalized nor is it a local (no regional or tissue alternative) measure and inherently applies an analog of the boundary shift integral method (Freeborough & Fox, 1997) on the pre-processed T1-weighted whole-brain images. Traditional brain volume change (BVC) was also calculated as shown in the equations below with analogs for

regional (RVC) and tissue (TVC) levels. We will not be dealing with absolute volumes but instead, our ground truth analysis will include a comparison between the newly proposed normalized measure (rBVC) with BVC and SIENA.

$$\begin{aligned}
RVC_{i,j,k} &= Vol_{i,j,k} - Vol_{i,j,Pre} \\
TVC_{X,j,k} &= \sum_{i=1}^{N_X} c_i \times RVC_{i,j,k} \\
BVC_{j,k} &= \sum_X w_X \times TVC_{X,j,k} \\
SIENA_{j,k} &= FSL_SIENA(T1_{j,k}, T1_{j,Pre})
\end{aligned}$$

3.3.2 Data Quality Assurance

MRI images are corrupted by Rician distribution that arises from the complex Gaussian noise in the original frequency domain during data acquisition. A median filter is a simple and computation-efficient technique to denoise this corruption. Another form of noise is intensity inhomogeneity or nonuniformity. Termed as the low-frequency bias field (shading artifacts), it is an undesirable signal that blurs high-frequency contents (contours, edges) of MR images and decreases the fidelity of the image. The latter is more troublesome as it is not easily identifiable by the human eye and thus requires a mandatory pre-processing step for non-uniform intensity correction (Gispert et al., 2004).

AFNI's *3dUnifize* sub-routine solves both these issues by using local median white matter intensity values to uniformize the T1-weighted MRI and eradicate the shading artifacts. Other methods for denoising MR images exist (J. Yang et al., 2015; Zeng et al., 2020) but are not implemented in the final pre-processing pipeline as the latter part of the pipeline is involved with registration and blurring the images to a FWHM (full-width-half-max) of 3mm that denoises certain high-frequency noise components (Vibhakar et al., 2012).

MRI data quality checks are a crucial part of the pipeline. It requires constant eyes-on-data to spot errors in each stage of the pipeline. There exists no gold standard when it comes to denoising T1-weighted MRIs of all the possible noises that arise from data acquisition and pre-processing. Hence, it is up to the graduate student to ensure that all the slices of the T1-weighted

MRI are clean and of good quality. Coupled with post hoc checks for exaggerating results or volumetric measures, contrast-to-noise, and signal-to-noise ratios one can develop a healthy standard for good quality data.

3.3.3 Partial Volume Estimation

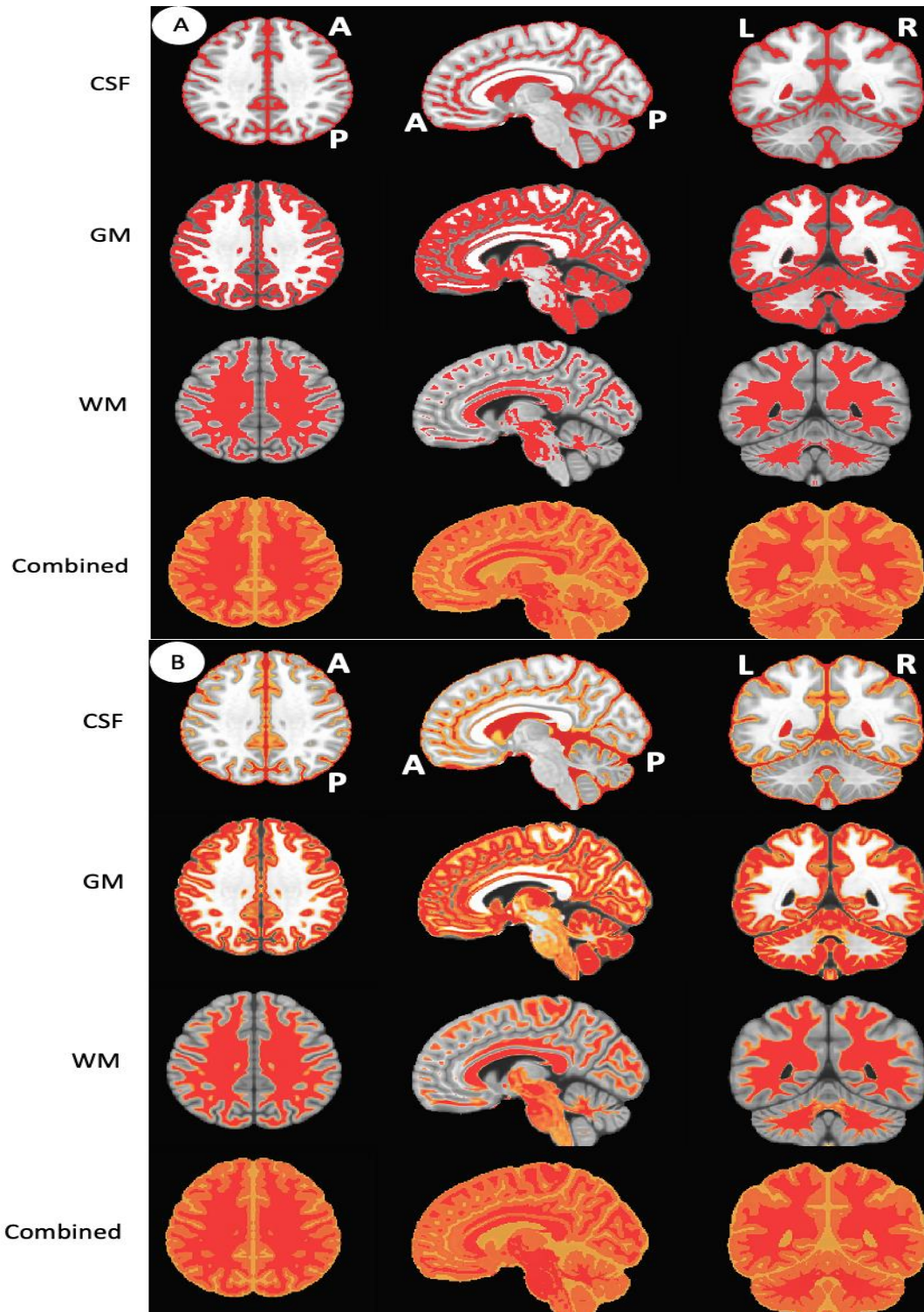


Figure 3.3 (Columns: Left to Right) Axial, sagittal, and coronal mask images of the FSL-FAST ICBM152 segmentations for (Rows: Top to Bottom) CSF, GM, WM, and Combined (CSF+GM+WM) (a) (Above) Without partial volume estimation (b) (Below) With partial volume estimation.

The FSL-FAST (Zhang et al., 2001) segmentation algorithm employs expectation maximization of hidden Markov random fields for the different tissues in the brain. This finite mixtures-based modeling technique also produces a probabilistic partial volume estimation. Essentially, the GM-CSF and GM-WM tissue boundaries/interfaces are continuously varying compared to the discrete masks segmented for these tissues without the partial volume estimation. Figure 3.3 depicts the differences between each tissue and the whole-brain mask.

We will only use the discrete masks in our calculations for normalized brain volumes since we are dealing with a singular standard atlas-specific segmentation that simplifies group-level analyses. It might be advised to employ the masks with partial volume estimation if one were segmenting the original space T1-weighted and not the group-level template (de Boer et al., 2010; Tohka, 2014). Additionally, CSF segmentations has the same intensity range as inflammation on T1-weighted MRI, a multi-modal approach with fluid-attenuated images can discern this difference whilst being cognizant of the test-retest reliability of different MRI pulse sequence and coil effects (Yan et al., 2020).

3.4 Statistical Analysis

Analyses were performed in MATLAB R2020a (Mathworks) using the statistical approaches described in *Primer of applied regression and analysis of variance*, Glantz 2016.

Linear regression analysis: The slope and intercept (b_1 , b_0) of a regression line for the dependent variable (y) as a function of the independent variable (x) for n samples is:

$$b_1 = \frac{n\sum XY - \sum X \sum Y}{n\sum X^2 - (\sum X)^2}$$

$$b_0 = Y_{mean} - b_1 X_{mean}$$

Testing if the slope of a regression line is different from zero i.e exhibits a linear relationship, we need to compare the t -statistic derived using the equation below with a standard two-tailed critical value t_α

$$t = \frac{b_1}{s_{b1}}$$

where s_{b1} is the standard error of the slope.

Relationship between regression and correlation: The square of the correlation coefficient a.k.a the coefficient of determination is the fraction of the total variance explained in the dependent variable by the regression equation.

$$R^2 = \frac{SS_{reg}}{SS_{Total}}$$

$$SS_{Total} = SS_{res} + SS_{reg}$$

Where, $SS_{Total} = \sum (Y - Y_{mean})^2$, $SS_{res} = \sum [(b_0 + b_1X) - Y_{mean}]^2$

4. RESULTS

4.1 Volumetric Measures Distribution Analysis

Independence of measurements: Independence of test classes is implied when comparing volumetric measures from different populations (CSA, NCA) and separate sessions (*In1*, *In2*, *Post1*, *Post2*, *Post3*), but not for separate tissues, as they are partitions of the complete brain.

Non-parametric normality analysis: To perform any statistical inference testing, we first need to understand the underlying distributions of the volumetric parameters: rTVC, rBVC, SIENA, TVC, and BVC. We used the non-parametric one-sample Kolmogorov-Smirnov (KS) test to ascertain if these distributions are indeed normally distributed. rTVC and TVC for every tissue (GM, WM, CSF, dCSF), rBVC, BVC, SIENA for an individual session (k : *In1*, *In2*, *Post1*, *Post2*, *Post3*, *Retest*), populations (NCA, CSA), and sport (Male: Football, Female: Soccer and pooled (across gender or sport) data) failed to reject the null hypothesis of a one-sample KS test (198 tests!) which stated that the original distribution came from a hypothesized normal distribution with the mean and variance of each respective volumetric parameter.

Pooling across gender or sport: Measurements of tissue and global volumes were found to be reliable in the control (NCA) population. Prior to conducting analyses across populations, NCA athletes at *Retest* were checked for any gender effects using an unpaired two-sample t -test. The pooling of male football and female soccer athletes was carried out as the sport-specific $SIENA_{Retest}$, BVC_{Retest} , TVC_{Retest} , $rTVC_{Retest}$, and $rBVC_{Retest}$ were not found to be with different means when tested using an unpaired two-sample t -test with $\alpha = 0.05$, degrees of freedom = 27 and for each method: SIENA ($p=0.66$), BVC (0.83), TVC (GM (0.81), WM (0.57), CSF (0.71), dCSF (0.62),), rTVC (GM (0.77), WM (0.61), CSF (0.74), dCSF (0.68),) and rBVC (0.57). Additionally, it is to be noted that pooled samples of $SIENA_{Retest}$, BVC_{Retest} , TVC_{Retest} , $rBVC_{Retest}$, and $rTVC_{Retest}$ values are not different in mean from zero over the 4-13-week time scale. Henceforth, the volumetric measures will be pooled for gender except for the last segment of HAE correlation analysis which explores the different HAE distribution profiles for each sport.

Sphericity: Mauchly's sphericity test was run on the pairwise difference of variances between the four sessions (*In1*, *In2*, *Post1*, *Post2*) for rTVC and TVC (each tissue GM, WM, CSF, dCSF), rBVC, BVC and SIENA. p -values resulting from Mauchly's W sphericity test for rTVC (WM (0.062), CSF (0.212), dCSF (0.191), GM (0.128)), TVC (WM (0.089), CSF (0.193), dCSF (0.246), GM (0.181)), rBVC (0.186), BVC (0.291) and SIENA (0.169). All tissues demonstrated a non-significant p -value at a significance level of $\alpha = 0.05$ thereby preserving the sphericity assumption and preventing the use of a correction.

This parametric sphericity analysis across balanced-sample CSA sessions will assist with longitudinal analysis of the volumetric data using a one-way repeated measures analysis of variance (rANOVA).

4.2 Ground Truth Analysis

As we have explored the background of the wide variety of morphometric techniques, we first need to understand if the proposed method of quantifying brain volume change using normalized regional measures performs differently from these existing techniques. Here, we demonstrate a comparison between global volumetric change calculated using SIENA (Smith et al., 2002), BVC (Bigler et al., 2004, 2019; Spitz et al., 2013; Whitwell et al., 2001), and the proposed rBVC for the control athletes (NCA). As we recall, the only difference between the proposed method and existing methods is a normalization with respect to the baseline volume in addition to the subtractive or differential volumetric calculation.

rANOVA (F -test with $F_{\text{critical}}(2, 56)=3.16$) was first performed over the *Retest* measures to yield $F=0.707$, and $p=0.49$ with prior verification for sphericity across measures (Mauchly's W on the pairwise differences of variances between the measures, $p=0.091$) preventing the use of a correction. Therefore, there were no overall differences between the related means of SIENA, BVC, and rBVC for the control population (NCA). Post hoc pairwise two-sample paired t -tests across the NCA population for these measures further verified that they were not different in means.

4.3 Atlas Specificity

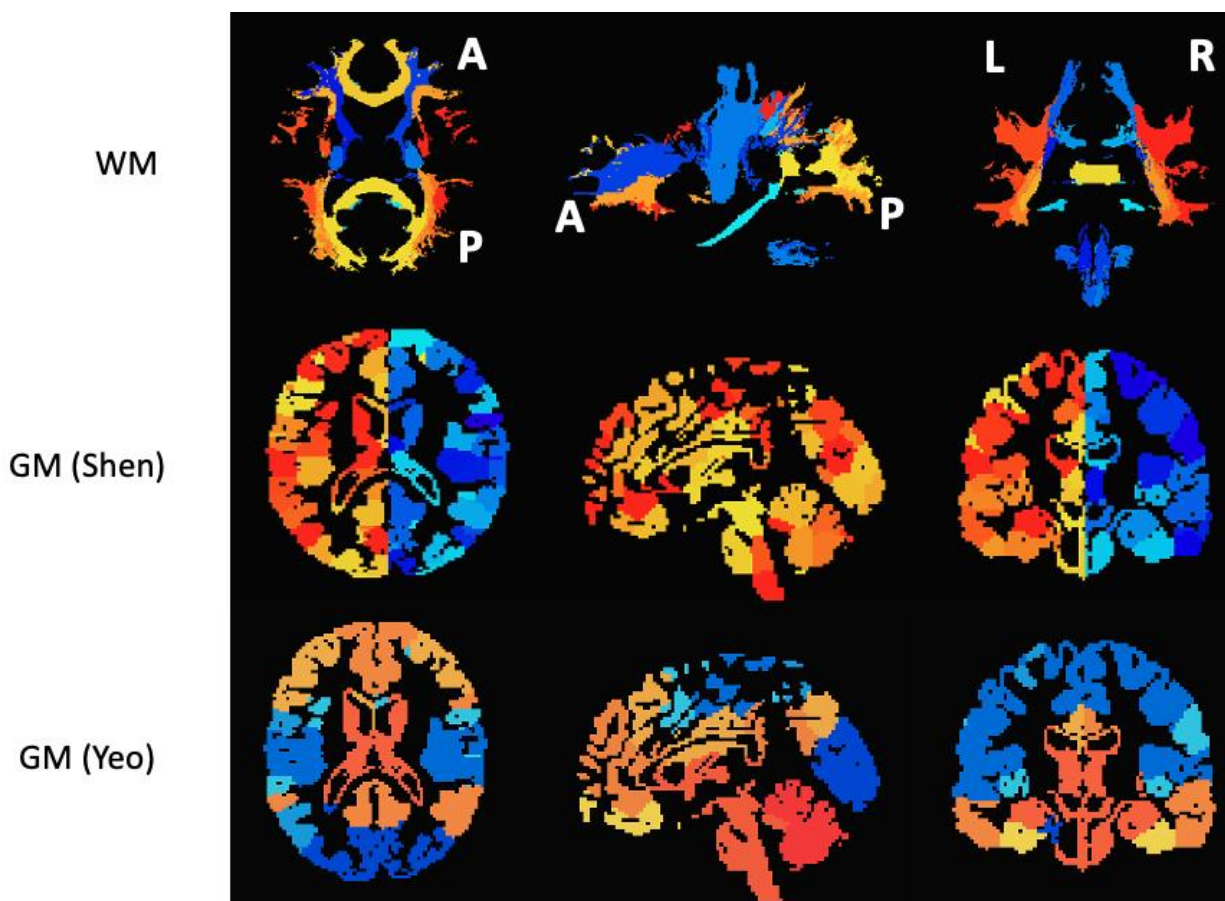


Figure 4.1 (Rows: Top to Bottom) Depiction of WM Johns Hopkins University (JHU) ROIs, GM Shen ROIs and GM Yeo ROIs for (Columns: Left to Right) axial, sagittal and coronal views.

There are 52 Brodmann areas that partition the brain into different anatomical structures based on their underlying cytoarchitecture. Linking these anatomical structures to functional networks (Baria et al., 2011) derived from resting state fMRI sequences has widely been practiced. Here resting-state networks (Shen et al., 2013) are demonstrated to reconcile with the normalized anatomical volumetric parameters. A deeper investigation must be conducted to understand why exactly this occurs. The resting-state networks are probably closely related to anatomically dependent delineation (Figure 1 and Figure 3 from (Tzourio-Mazoyer et al., 2002)) even though they are derived from resting state fMRI signals that are not based on cytoarchitecture or other anatomic distinctions.

In general, the choice of atlas for automatic segmentation methods can yield different performances (Yaakub et al., 2020). Here, we will depict a simple cross-comparison between two

GM atlases, specifically with largely varying average ROI sizes. Large scale resting-state networks (Yeo et al., 2011) do not show the same degree of GM volumetric detection as the high number of nodes in the Shen atlas (278 regions) forces a lower anatomical variance compared to the former (9 regions).

Intuitively, each yeo ROI consists of multiple Shen ROIs, thereby demonstrating a higher variance as seen in the scatter plots below for rRVC across ROIs in the two GM templates where each line represents a separate subject within a subplot for a specific session. Since the average slope of each subplot is flatter than the $y=x$ or *45-degree line* (black-dotted), we can infer that the variance of rRVC measure for the athletes is higher when computed using the Yeo atlas than compared to the Shen. Another way to interpret the figure is to visualize the distance between rRVC measures for each atlas, the Yeo atlas has a larger spread than the Shen atlas. Therefore, we are justified to employ a less noisy/lower variance alternative to compute the regional GM volumes.

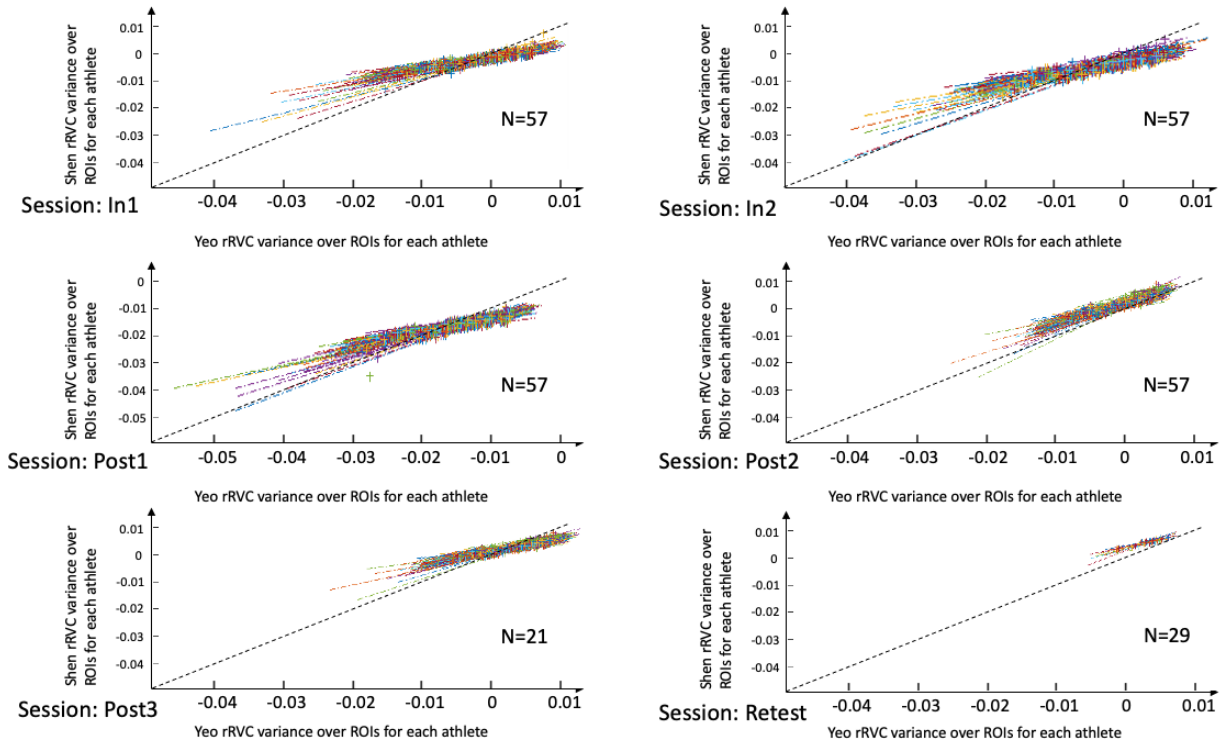


Figure 4.2 Visualizing template-specific variance in rRVC.

Moreover, the variance for CSA athletes for each template overshadowed the NCA athletes. Future work would involve exploring multiple WM atlases as well. The JHU 20 ROI atlas should suffice for the analyses performed here. It is also to be noted that WM structural changes are better visualized and detected by parameters computed from DTI images rather than volumetric measures from T1-weighted images.

4.4 Statistical Analysis of Volumetric Measures

There are multiple volumetric measures with a lot of degrees of freedom (subject, session, region, tissue, etc.). Visualizing the variation of these measures led us to explore longitudinal/session-wise analysis for a specific tissue as a function of subjects and regions/ROI. To understand the significant tissue-specific (GM, WM) longitudinal differences the following two analyses were performed.

4.4.1 Group-level ROI Analysis

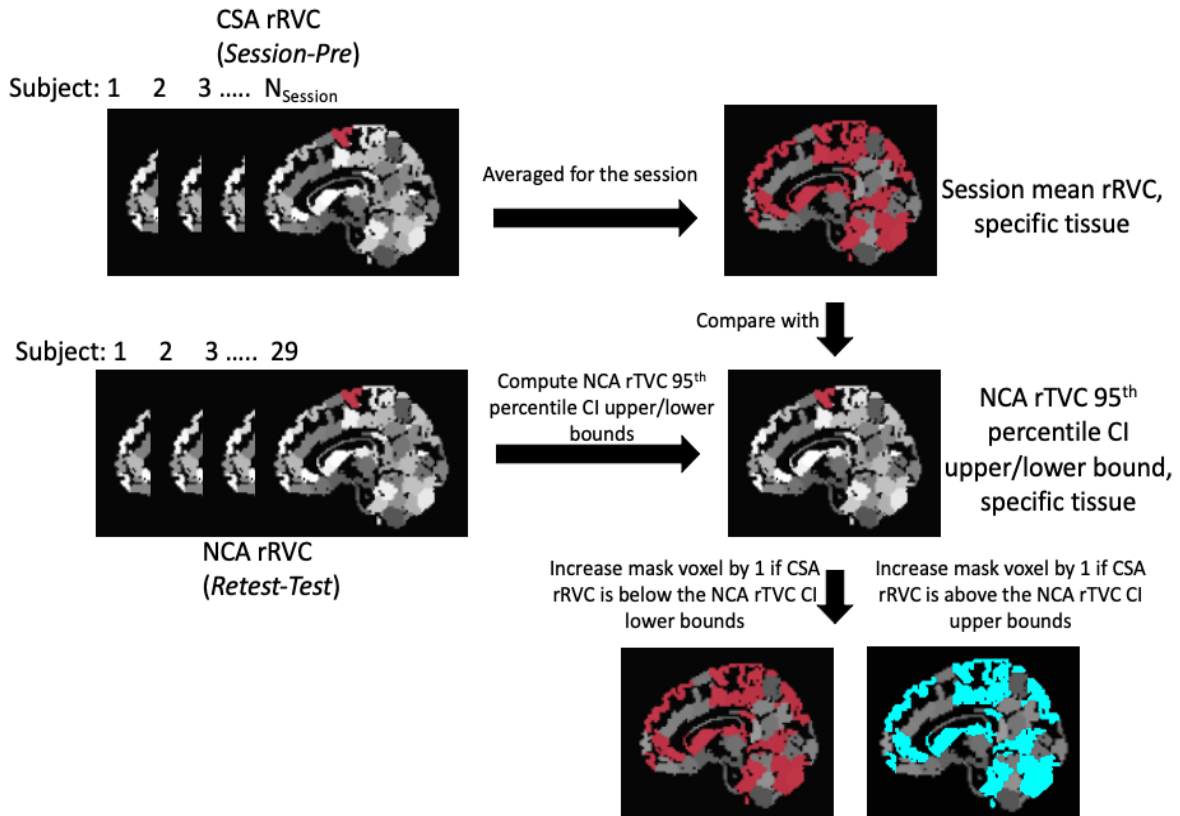


Figure 4.3 Flowchart for group-level ROI analysis.

Localization of region-specific longitudinal changes in rRVC was effected for CSA on a confidence interval (CI) basis, using the NCA population as a reference. In this case, each ROI in the CSA was assessed on a tissue-level basis to determine if the average rRVC for the given tissue exhibited a mean change that fell outside the 95% CI for the specific tissue (i.e., rTVC) for the NCA. Thus, two ROI maps were generated for each tissue in CSA, identifying those ROIs for which the average CSA rRVC changes were (1) more negative than the lower 95% CI bound of the rTVC for NCA, or (2) more positive than the upper 95% CI bound of the rTVC for NCA. Note that the WM assessment did not reveal any within-season ROIs falling outside the 95% CI and was omitted from further analysis.

Longitudinal volumetric measures of GM ROIs for CSA exhibited a concave up behavior. Values decreased from baseline (*Pre*) with maximum deviation at end-of-season, as collision-based activity ceased (*Post1*), followed by a neuroplastic return to baseline (*Pre*) after an extended period of rest (*Post3*).

Figure 4.4a illustrates GM ROIs for CSA exhibiting an average rRVC exceeding the upper 95% CI defined by rTVC of GM for NCA. The number of positively deviant ROIs peaked at *In1*, decreased with time until *Post1*, and then again increased across *Post2* and *Post3*. Figure 4.4b illustrates GM ROIs for CSA exhibiting an average rRVC falling below the lower 95% CI defined by rTVC of GM for NCA. The number of negatively deviant ROIs increased longitudinally across sessions *In1-Post1* but fell sharply for *Post2* and *Post3*.

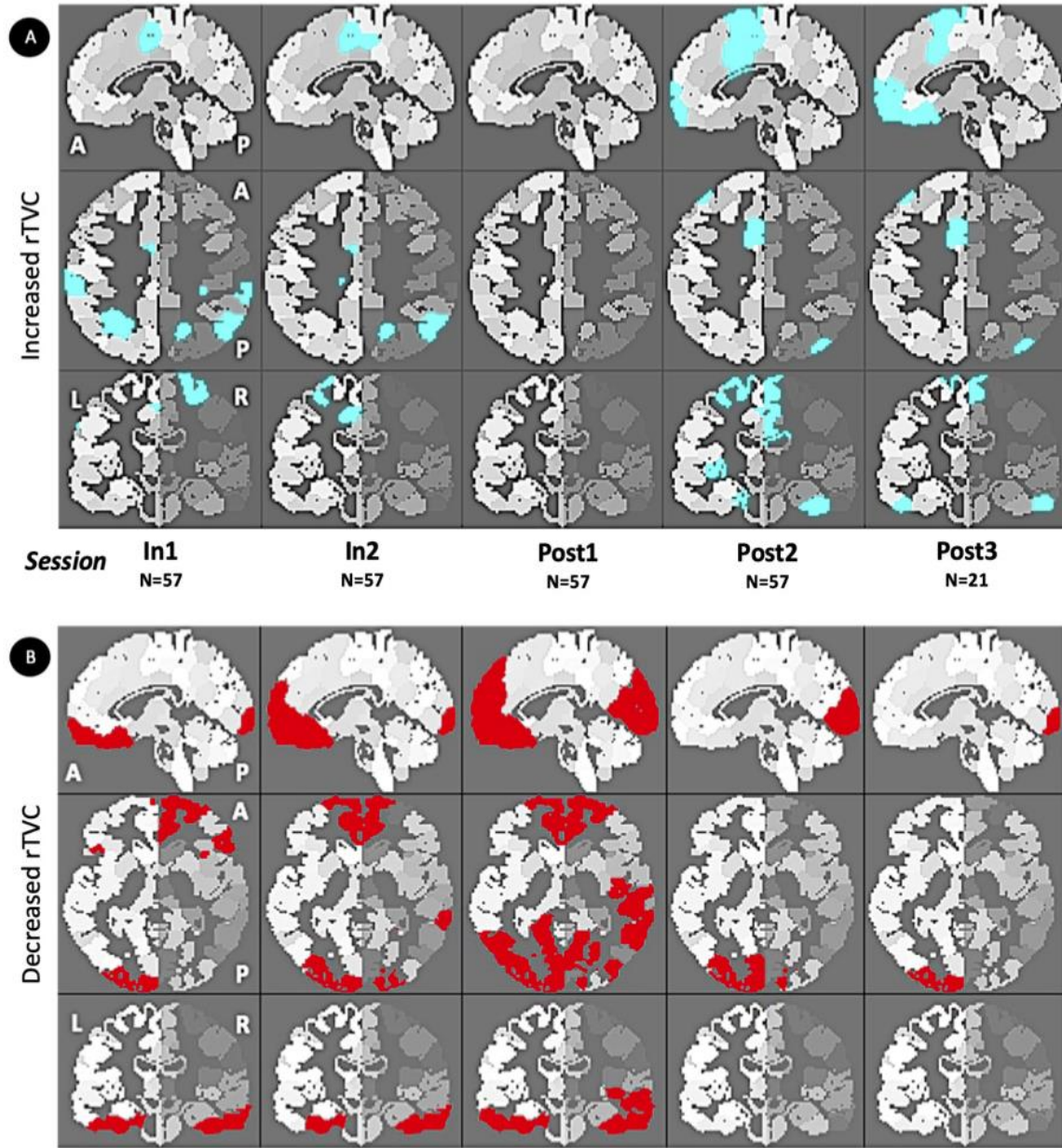


Figure 4.4 Gray matter regions of interest (ROIs) in collision sport athletes (CSA) at each given imaging session (see Figure 1) that exhibited an average relative regional volume change (rRVC), relative to *Pre*, that fell outside the 95% confidence interval defined from *Test-Retest* evaluation of non-collision athletes (NCA; N=29). (A) ROIs falling above the upper bound of the CI are depicted in cyan. (B) ROIs falling below the lower bound of the CI are depicted in red.

4.4.2 Subject-level ROI Distribution Analysis

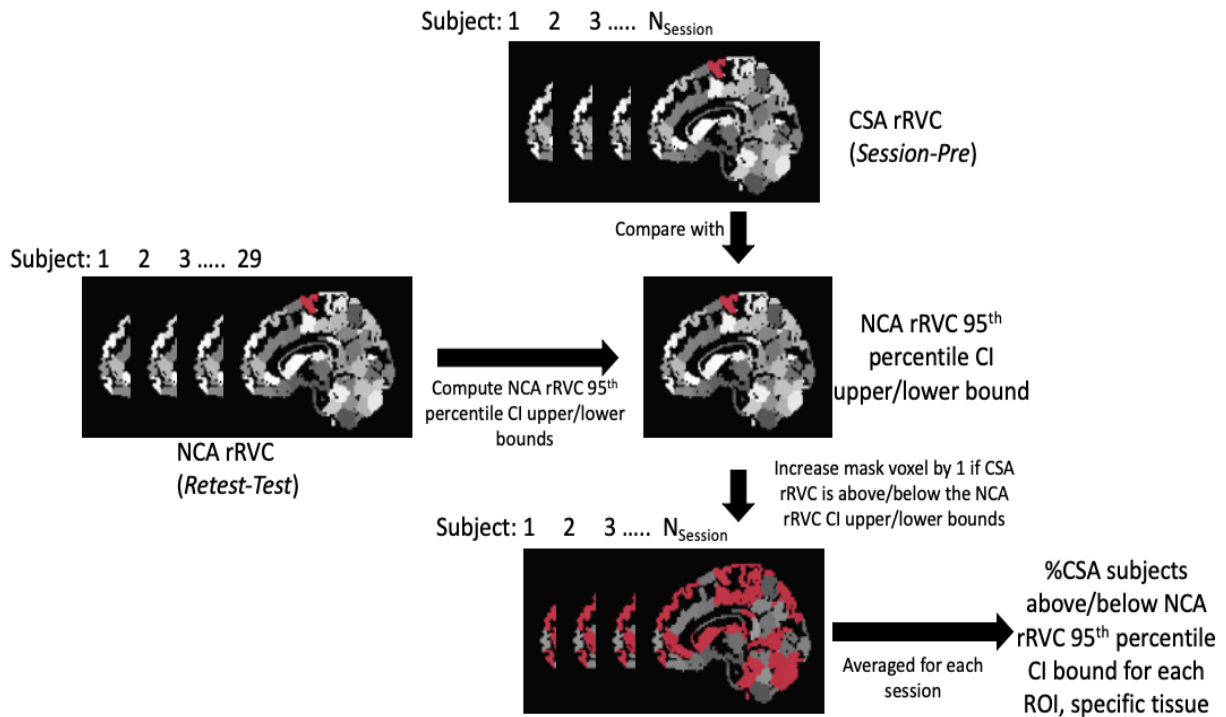


Figure 4.5 Flowchart for subject-level ROI distribution analysis.

Each CSA had a mask generated by comparing their rRVC for separate ROIs belonging to a tissue (GM, WM) with the corresponding NCA 95th percentile CI bound of rRVC for the respective ROI. If the rRVC was outside of the bound, i.e., abnormal change, a mask value of 1 was given and zero if not. The masks were then summed up over all CSA subjects and then normalized by the number of subjects at each session to yield a percentage value. The combined information of the session-wise distribution further explains the degree to which aberrant change is observed in the tissue-specific ROIs of CSA.

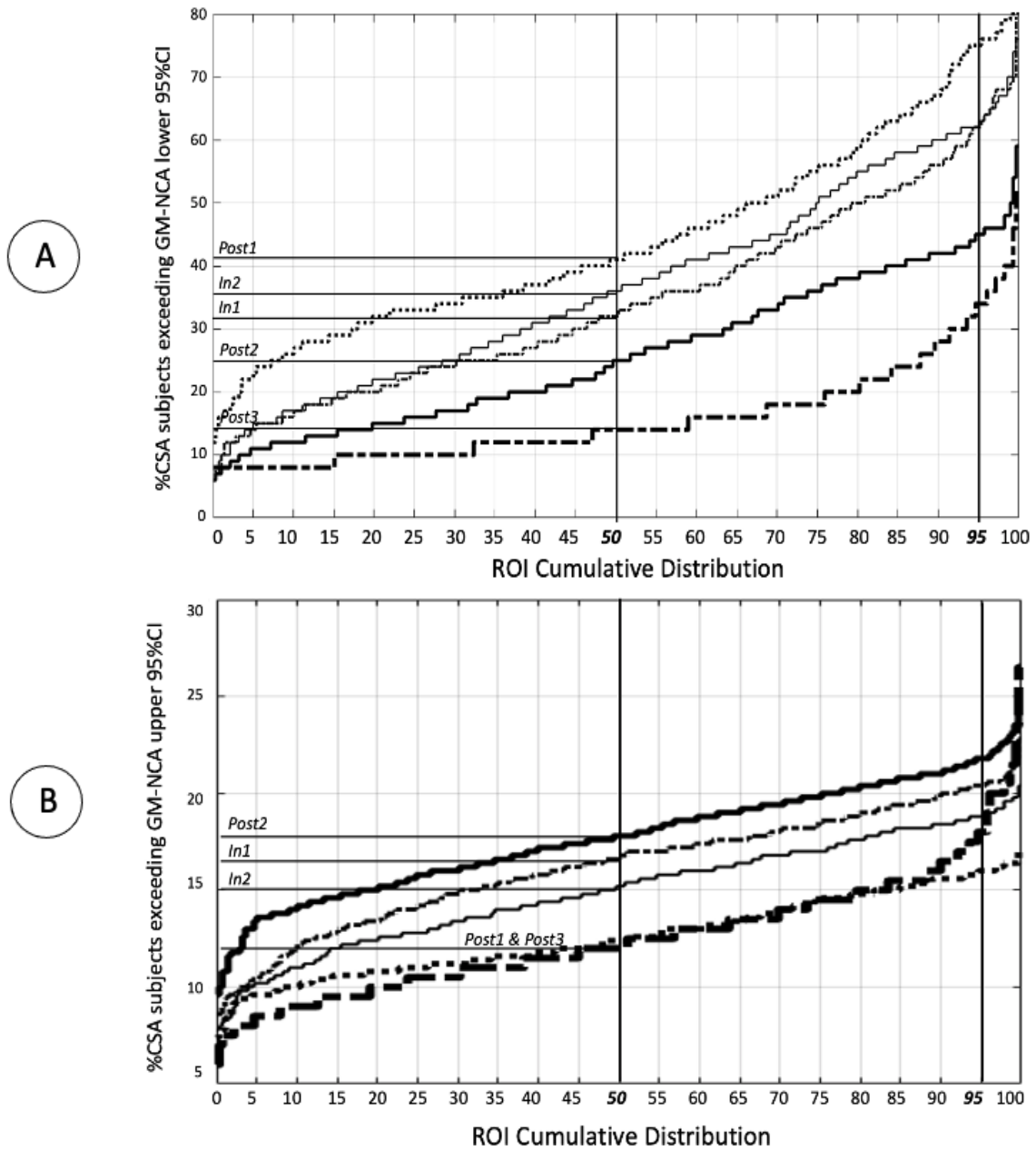


Figure 4.6 Cumulative distribution of ROIs with individual ROIs representing the percentage of CSA subjects exceeding the *NCA* 95th percentile CI bound of rRVC for that ROI for GM (a) Lower 95th and (b) Upper 95th.

Figure 4.6a illustrates the extent to which GM volumes decreased across sessions represented here in decreasing order: *Post1-In2-In1-Post2-Post3*. This demonstrates the longitudinal variation in the number of CSA subjects that exhibited decreases in regional GM volumes relative to *NCA*.

Figure 4.6b illustrates the extent to which GM volumes increased across sessions represented here in decreasing order: *Post2-In1-In2-Post1-Post3*. This demonstrates the longitudinal variation in the number of CSA subjects that exhibited increases in regional GM volumes relative to NCA.

Clearly, the *Post1* session showed the most detrimental change whereas the *Post2* session showed a reparative change of regional GM volume.

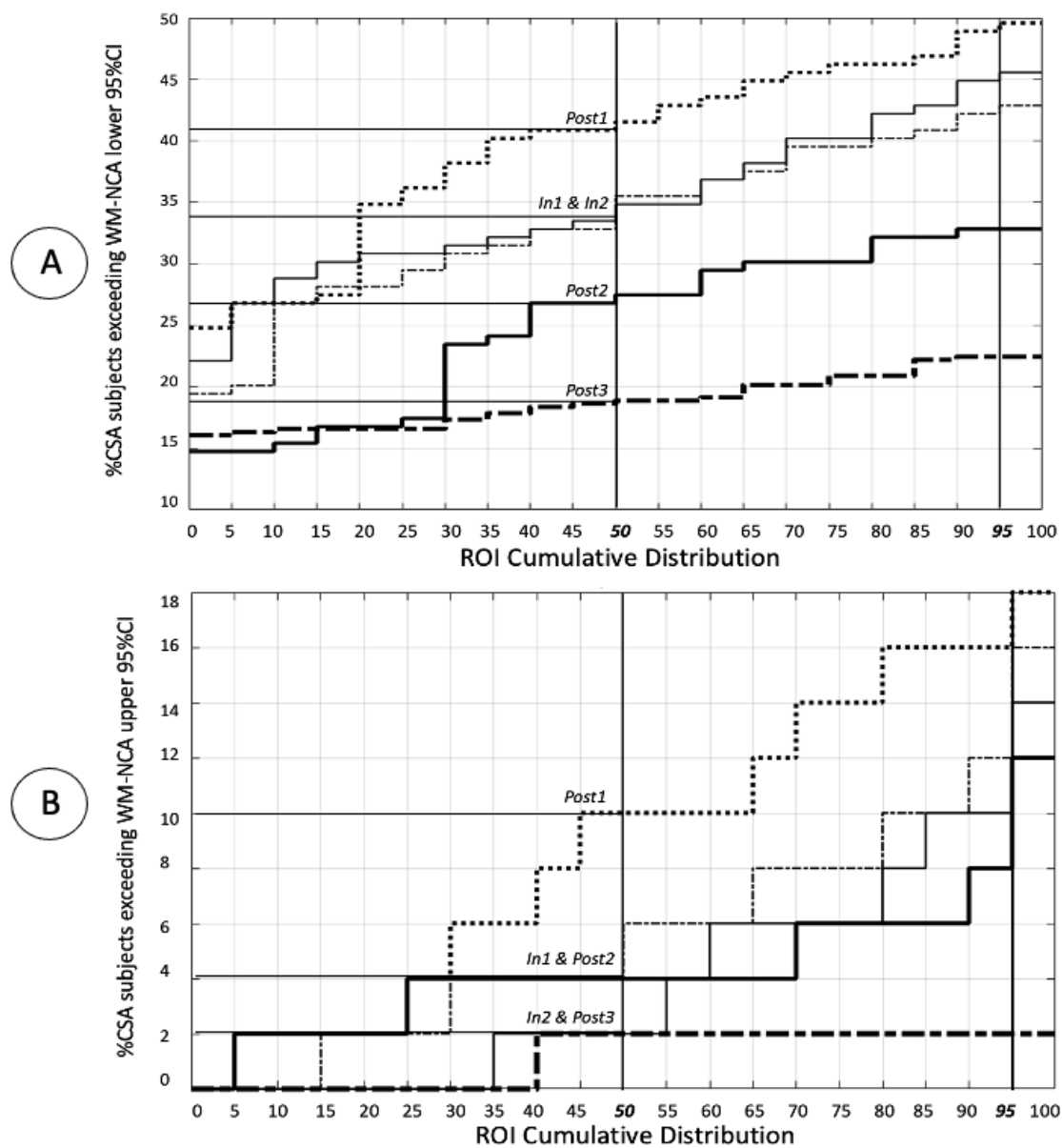


Figure 4.7 Cumulative distribution of ROIs with individual ROIs representing the percentage of CSA subjects exceeding/outside the NCA 95th percentile CI bound of rVC for that ROI for WM (a) Lower 95th and (b) Upper 95th.

Figure 4.7a illustrates the extent to which WM volumes decreased across sessions represented here in decreasing order: *Post1-In2-In1-Post2-Post3*. This demonstrates the longitudinal variation in the number of CSA subjects that exhibited decreases in regional WM volumes relative to NCA. Figure 4.7b illustrates the extent to which WM volumes increased across sessions represented here in decreasing order: *Post1-In1-Post2-In2-Post3*. This demonstrates the longitudinal variation in the number of CSA subjects that exhibited increases in regional WM volumes relative to NCA. The *Post1* session showed the most detrimental change and reparative change of regional WM volumes, although affecting at most 20% of the CSA subjects in the latter case.

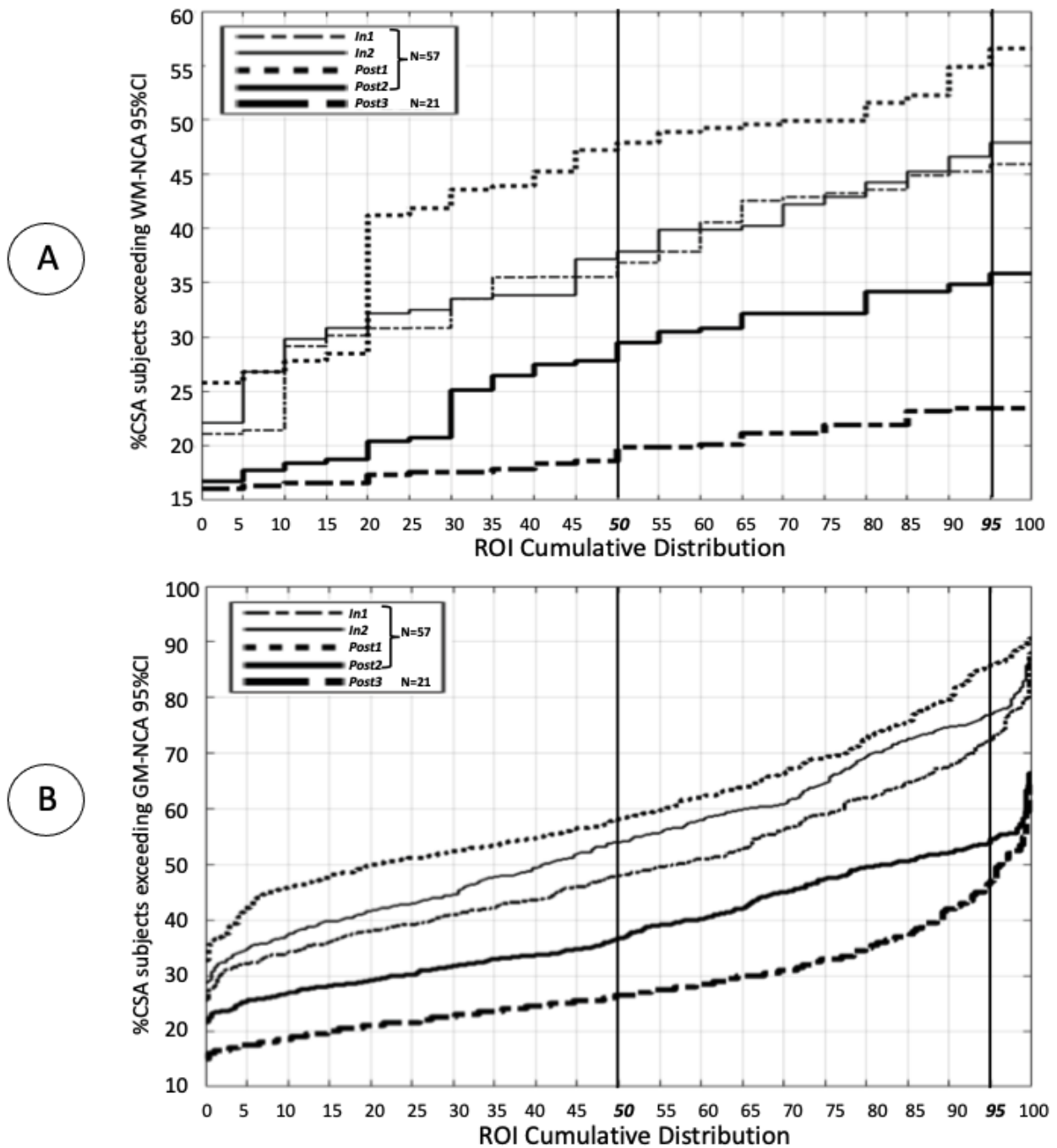


Figure 4.8 Cumulative distribution of ROIs with individual ROIs representing the percentage of CSA subjects exceeding the NCA 95th percentile CI bound of rRVC for that ROI for tissue (a) WM and (b) GM.

Table 4.1 represents the 50th and 95th percentile values of the percentage of CSA subjects exceeding NCA 95th percentile CI bound of rTVC at *Session* as seen in Figure 4.8.

Table 4.1 50th and 95th percentile values of percentage of CSA subjects exceeding NCA 95th percentile CI bound of rTVC at Session.

Tissue(X)	Percentile level	Percentage of CSA subjects exceeding NCA 95 th percentile CI bound at <i>Session</i>				
		<i>In1</i>	<i>In2</i>	<i>Post1</i>	<i>Post2</i>	<i>Post3</i>
<i>GM</i>	Top 50%	47.9	53.9	58.1	36.3	26.2
	Top 5%	72.0	77.6	85.2	53.3	46.2
<i>WM</i>	Top 50%	35.9	37.8	47.6	28.2	18.1
	Top 5%	45.6	47.4	56.1	35.5	23.7

Results for the cumulative distribution of ROIs with individual ROIs representing the percentage of CSA subjects exceeding the NCA 95th percentile CI bound of rRVC for that ROI for tissues WM, GM are depicted in Figure 4.8. Essentially, the Post1 session exhibited the most volumetric regional change for both tissues GM, WM with regards to the percentage of the CSA population. A finer analysis with just the individual upper, lower NCA 95th percentile CI ROI bounds is presented in Figures 4.6, 4.7 for GM and WM respectively. A two-sample KS test was run on the pairwise ROI distributions with the null hypothesis being that the data were sampled from the same distribution. All GM, WM session pairs, except *In1-In2* rejected this null hypothesis.

The group-level analysis looks to identify subject-averaged aberrant ROIs, whereas the subject-level analysis quantifies the percentage of subjects that show an aberrant change. The flowcharts of the computation schema also elucidate the difference in averaging methods that arrive at the result. Another difference between the two analyses is that the NCA 95th percentile pool bound of rTVC is a stricter threshold than the individual rRVC ROI bound and hence fewer ROIs survive than compared to the subject-level distributions. Essentially, we are visualizing the ROIs with the most deviation (greater than two standard deviations) from the NCA population mean of rTVC for the whole CSA population across sessions, thereby helping us understand the regions of the brain that are at most risk of volumetric changes.

4.4.3 Longitudinal Analysis

Note, *Post3* is excluded here onwards to promote sample-balanced statistical analysis for longitudinal detection amongst CSA. CSA athlete measures of rTVC were evaluated for sphericity (Mauchly's *W*) and normality (one-sample Kolmogorov-Smirnov) before rANOVA was used to determine if longitudinal differences in rTVC for CSA athletes were associated with session. Post hoc *t*-tests were conducted on a pairwise basis within the CSA population to identify session-specific changes (paired *t*-test), and across the CSA and NCA to detect any population differences (unpaired *t*-test). Refer to the boxplots in Figure 4.9 to get a brief understanding of each population's significant rTVC longitudinal deviations. The overall variance across populations of CSA, NCA is clearly distinctive and aligned with the normative variance of brain volume loss over time (Narayanan et al., 2020).

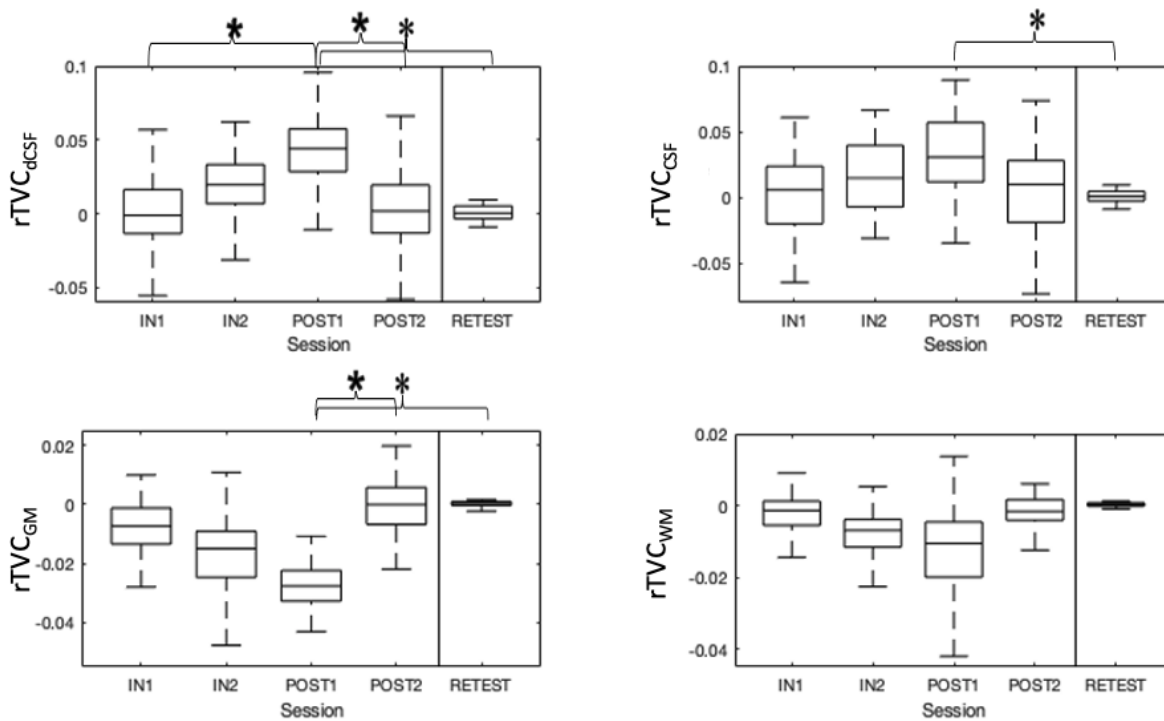


Figure 4.9 Boxplots depicting rTVC (GM, WM, CSF, dCSF) against sessions for NCA, CSA populations. (Significant differences for pairwise *t*-tests are highlighted by brackets)

Mean scores of rTVC for GM and dCSF exhibited significant session-wise differences within CSA and between CSA and NCA. Longitudinal assessment of rTVC for the CSA population were found to be significant for GM ($F(3,168) = 2.91$) and dCSF ($F(3,168) = 3.13$).

Post hoc Bonferroni corrected *t*-tests of rTVC within CSA population and across NCA-CSA populations are presented in Table 4.2.

4.4.4 Post hoc *t*-Tests

Inter-session tests were carried out across populations on the following basis:

CSA vs CSA: The *F*-test for each rTVC indicated significant changes for tissues: GM, dCSF across the four timepoints *In1-In2-Post1-Post2*. Post hoc paired *t*-tests further indicated the exact inter-session differences depicted in Table 4.2. All pairwise comparisons except the pairs involving *Post1* for WM exhibited uniform variance. The latter had DF corrected for by the Satterthwaite approximation. Paired *t*-tests were run on pairwise comparisons of CSA rTVC to ascertain the session-wise differences. Tests were corrected for multiple comparisons using Bonferroni correction (= 6) yielding a $T_{critical}=2.73$ at a significance level of 0.05. Tissues GM, dCSF having shown significant *F*-scores showed significant *T*-scores for inter-session comparisons of *Post1-Post2* and *In1-Post1, Post1-Post2* respectively.

CSA vs NCA: Across populations, unpaired *t*-tests were run on pairwise comparisons of *CSA-NCA* rTVC to ascertain the session-wise population differences. Tests were corrected for multiple comparisons using Bonferroni correction (= 4) yielding a $T_{critical}=2.61$ at a significance level of 0.05 with degrees of freedom corrected for by Satterthwaite approximation due to unequal variances of rTVC across populations (*CSA, NCA*) for each case. Tissues GM, CSF, dCSF showed significant *T*-scores for inter-session comparisons of *Post1-Retest*. All significant differences for the post hoc *t*-tests are highlighted in Figure 4.9. Table 4.2 summarizes the results of the rANOVA ($F(3,168)$) for each *CSA* rTVC (X: GM, WM, CSF, dCSF) as the continuous dependent variable and sessions (*In1-In2-Post1-Post2*) as the repeated measures independent variable or conditions. Means of each rTVC were tested for equality under the null hypothesis. Only GM, dCSF showed a significant deviation exceeding $F_{critical} = 2.66$ for DF= 3 (conditions), 168 (error/residuals term) at a significance level of 0.05.

Table 4.2 Comparisons, by tissue type, of relative tissue volumetric changes (rTVC) as a function of group and session. For each tissue of gray matter (GM), cerebrospinal fluid (CSF), white matter (WM) and deep (ventricular), CSF (*dCSF*), results are presented for both within-group analyses of the collision sport athletes (CSA), and for an across group analysis of CSA with the non-collision sports athletes (NCA). To evaluate within-group differences for CSA, Bonferroni corrected paired *t*-tests were conducted to compare the mean difference in rTVC on a pair-wise basis between follow-up sessions (*In1*, *In2*, *Post1*, *Post2*). To evaluate CSA relative to NCA, Bonferroni corrected unpaired *t*-tests were conducted to compare the mean difference in rTVC on a pair-wise basis between CSA follow-up session and the NCA follow-up session (*Retest*).

Tissue	Mean Difference in rTVC (%)									
	CSA vs. CSA						CSA vs. NCA			
	<i>In2</i>	<i>Post1</i>	<i>Post2</i>	<i>Post1</i>	<i>Post2</i>	<i>Post2</i>	<i>In1</i>	<i>In2</i>	<i>Post1</i>	<i>Post2</i>
	vs. <i>In1</i>	vs. <i>In1</i>	vs. <i>In1</i>	vs. <i>In2</i>	vs. <i>In2</i>	vs. <i>Post1</i>	vs. <i>Retest</i>	vs. <i>Retest</i>	vs. <i>Retest</i>	vs. <i>Retest</i>
GM	-0.91	-1.55	0.88	-0.64	1.79	2.43*	-0.89	-1.80	-2.44*	-0.01
CSF	0.42	1.86	0.01	1.44	-0.41	-1.85	0.78	1.20	2.64*	0.79
dCSF	1.34	3.68*	0.05	2.34	-1.29	-3.63*	-0.02	1.32	3.66*	0.03
WM	-0.68	-1.08	0.01	-0.40	0.69	1.09	-0.04	-0.72	-1.12	-0.03

* Values in bold are statistically significant at $p < 0.05$ after Bonferroni correction

Table 4.3 Longitudinal statistical analysis (*F*-test and *t*-tests) of global volumetric measures rBVC, SIENA, and BVC representing the mean percentage difference across sessions. All datasets are relative normalized volumes and hence have no units.

Volumetric measure	Mean Difference in measure (%)									
	CSA vs. CSA						CSA vs. NCA			
	<i>In2</i>	<i>Post1</i>	<i>Post2</i>	<i>Post1</i>	<i>Post2</i>	<i>Post2</i>	<i>In1</i>	<i>In2</i>	<i>Post1</i>	<i>Post2</i>
	vs. <i>In1</i>	vs. <i>In1</i>	vs. <i>In1</i>	vs. <i>In2</i>	vs. <i>In2</i>	vs. <i>Post1</i>	vs. <i>Retest</i>	vs. <i>Retest</i>	vs. <i>Retest</i>	vs. <i>Retest</i>
rBVC	-0.51	-0.72	0.23	-0.21	0.74	0.95	-0.02	-0.53	-0.74	0.21
SIENA	-0.53	-0.69	0.28	-0.16	0.81	0.97	-0.02	-0.55	0.71	0.26
BVC	-0.54	-1.02	-0.35	-0.48	0.19	0.67	0.34	-0.2	-0.68	-0.01

rBVC ($F = 1.49$), SIENA (1.47), BVC (0.87). According to the Monro-Kellie hypothesis, the total brain volume (brain parenchyma (GM, WM) and brain fluids (CSF)) is conserved and hence we probably do not see a significant longitudinal change across the global volumetric measures.

Table 4.4 Comparisons, by tissue type, of tissue volumetric changes (TVC) as a function of group and session. For each tissue of gray matter (GM), cerebrospinal fluid (CSF), white matter (WM), and deep (ventricular) CSF (dCSF), results are presented for both within-group analysis of the collision sport athletes (CSA), and for an across group analysis of CSA with the non-collision sports athletes (NCA). To evaluate within-group differences for CSA, Bonferroni corrected paired *t*-tests were conducted to compare the mean difference in TVC on a pair-wise basis between follow-up sessions (*In1*, *In2*, *Post1*, *Post2*). To evaluate CSA relative to NCA, Bonferroni corrected unpaired *t*-tests were conducted to compare the mean difference in TVC on a pair-wise basis between CSA follow-up session and the NCA follow-up session (*Retest*).

Tissue	Mean Difference in TVC (%)									
	CSA vs. CSA						CSA vs. NCA			
	<i>In2</i>	<i>Post1</i>	<i>Post2</i>	<i>Post1</i>	<i>Post2</i>	<i>Post2</i>	<i>In1</i>	<i>In2</i>	<i>Post1</i>	<i>Post2</i>
	vs. <i>In1</i>	vs. <i>In1</i>	vs. <i>In1</i>	vs. <i>In2</i>	vs. <i>In2</i>	vs. <i>Post1</i>	vs. <i>Retest</i>	vs. <i>Retest</i>	vs. <i>Retest</i>	vs. <i>Retest</i>
GM	-0.82	-1.30	0.42	-0.48	1.24	1.72	-0.38	-1.20	-1.68	0.04
CSF	0.72	1.23	-0.36	0.51	-1.08	-1.59	0.44	1.16	1.67	0.08
dCSF	0.74	1.39	-0.40	0.65	-1.14	-1.79	0.48	1.21	1.87	0.07
WM	-0.54	-0.99	0.21	-0.45	0.75	1.20	-0.21	-0.75	-1.19	0.01

* Values in bold are statistically significant at $p < 0.05$ after Bonferroni correction

The above table provides an extension to the sensitivity of traditional volumetric measures (TVC) as compared to the one proposed here (rTVC). As we can see (Table 4.2 vs. Table 4.4) the normalized measure (rTVC) increases longitudinal detection that would have been absent with traditional (TVC) measures.

4.5 HAE Regression Analysis

Note, *Post2* and *Post3* are excluded here onwards because of the negligible change in volumetric measures from *Post1* in addition to an absence of HAE profiles after *Post1*.

Outline: Assessment of the correlation of volumetric changes (rTVC) with HAE exposure (across multiple PTA thresholds) was effected by the computation of Pearson's *r* at each session. A linear predictor was subsequently modeled for rTVC as a function of nHAE at each session, only for those PTA_{Th} for which a significant *r* was observed. All statistical results from these assessments were corrected for multiple comparisons using the FWER (Family-wise Error Rate) Bonferroni correction procedure, the *p*-values are corrected for four tissues (GM, WM, CSF, dCSF) at each session. It is to be noted that this procedure gives the same performance as for a Benjamini-Hochberg procedure of False Discovery Rate = 5%.

Assessments of rTVC for dCSF demonstrated a linear relationship with accumulated RHI (nHAE) at a PTA_{Th} of 50G. The predictor modeling of rTVC as a function of nHAE for the significant PTA_{Th} , session is illustrated in Figure 4.10 with respective 95% CIs.

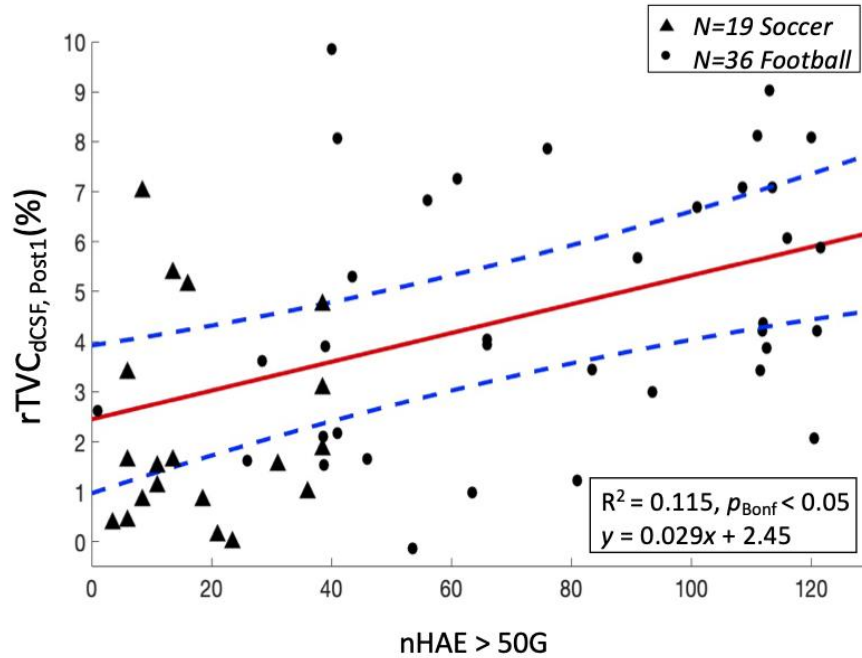


Figure 4.10 Linear dependence ($p_{Bonf} < 0.05$) at *Post1* (N=55) for percentage relative tissue volume change (rTVC) of ventricular cerebrospinal fluid (*dCSF*) as a function of the number of head acceleration events (nHAE) exceeding 50 G. Female soccer athletes (N=19), male football athletes (N=36) are represented by solid triangles and solid circles respectively. Red solid and blue dashed lines represent the mean regression line and corresponding 95% confidence interval.

Note: Two football athletes with incomplete HAE data are excluded from this analysis.

Table 4.5 Effect sizes of Pearson's r ($\alpha = 0.05$ /adjusted $p_{corrected(FWER)} = 0.0125$; N=55) for rTVC against nHAE at respective PTA threshold.

	$PTA_{Th} (G)$															
	20	25	30	35	40	45	50	55	60	65	70	75	80	85	90	95
<i>GM</i>	.281	.284	.280	.272	.268	.254	.321	.290	.293	.311	.314	.334	.322	.323	.295	.281
<i>dCSF</i>	.226	.231	.242	.241	.268	.283	.339	.311	.289	.252	.271	.241	.220	.199	.177	.134

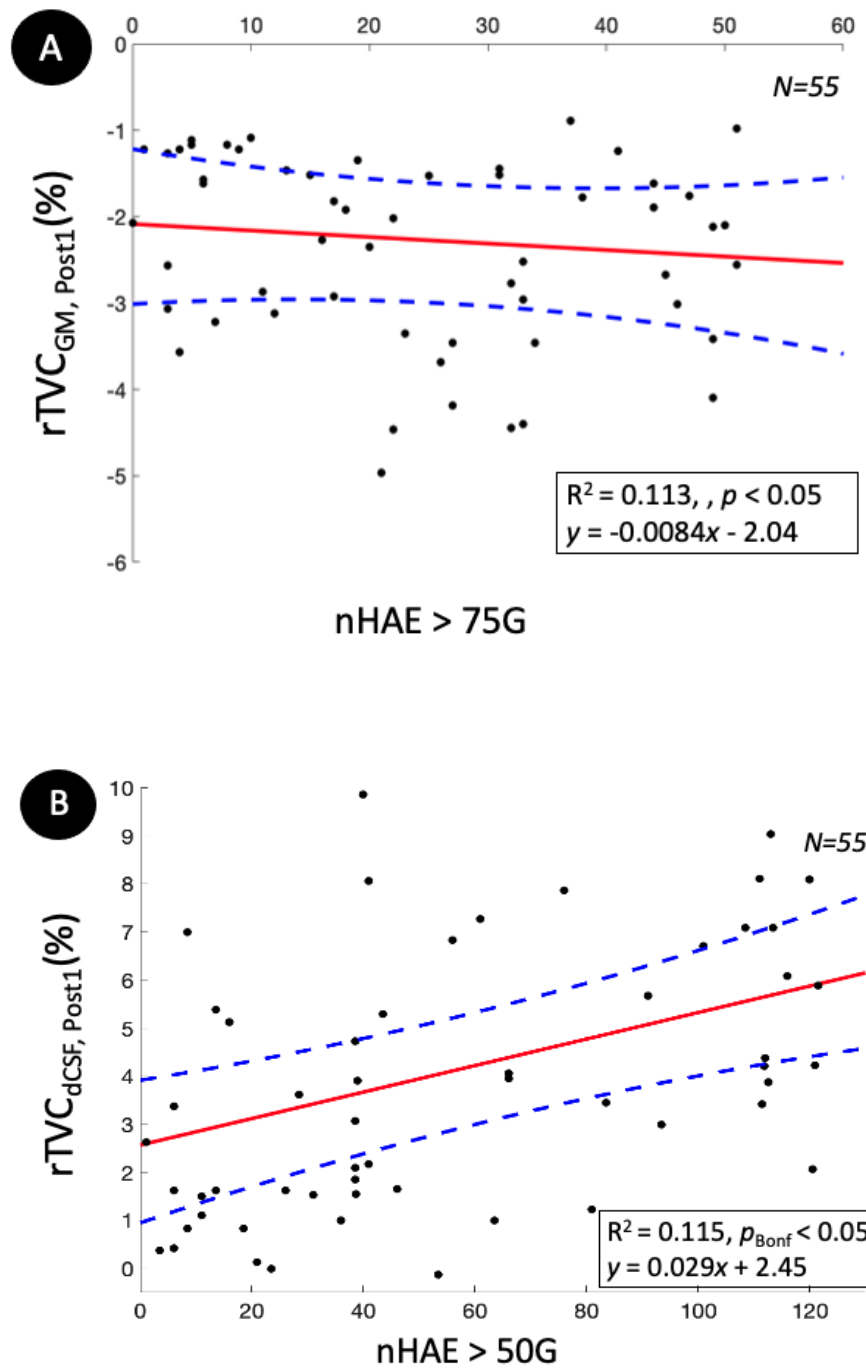


Figure 4.11 Linear predictor plots for rTVC at session *Post1* of GM, dCSF against nHAE at 75G, 50G respectively.

Significant changes observed within dCSF: As depicted in Table 4.5, the GM rTVC was also highly (but not strongly or significantly) correlated ($p_{Bonf} > 0.05$, $p < 0.05$) at the 75G PTA threshold, thereby indicating accrued damage to the GM at a higher threshold than compared to the dCSF tissue. Given the negligible slope (Figure 4.11a) and its derived t -statistic (slope normalized by the standard error of the slope), we can see that the regression line does not demonstrate a significant linear relationship.

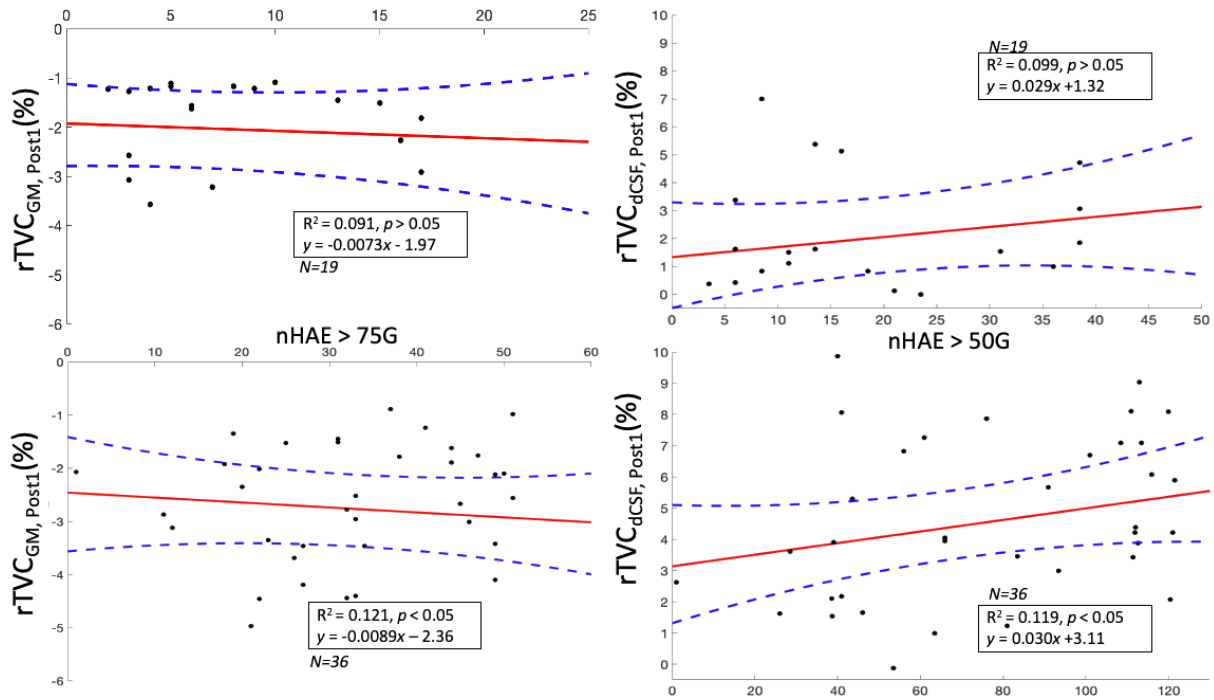


Figure 4.12 Linear predictor plots for rTVC at session *Post1* of GM (Left), dCSF (Right) against nHAE at 75G, 50G respectively. Top row for N=19 soccer athletes, bottom row for N=36 football athletes.

Analysis across sports: Figure 4.12 illustrates the sport-specific changes depicted in Figure 4.11 for soccer and football. Highlighting that the majority of the correlation of nHAE with rTVC is contributed by the football athletes, who are exposed to a larger (close to 2-3 fold) number of high-G HAE than compared to their soccer counterparts. Figure 4.13b provides a counterintuitive argument when compared to Figure 4.11b, proving that the combined cohort of soccer and football athletes produce a more meaningful correlation of nHAE with rTVC of dCSF at session *Post1* than just the football athletes with similar degrees of freedom. And Figure 4.13a, the larger combined sample size of N=75 provides the strongest correlation of this section of regression analysis.

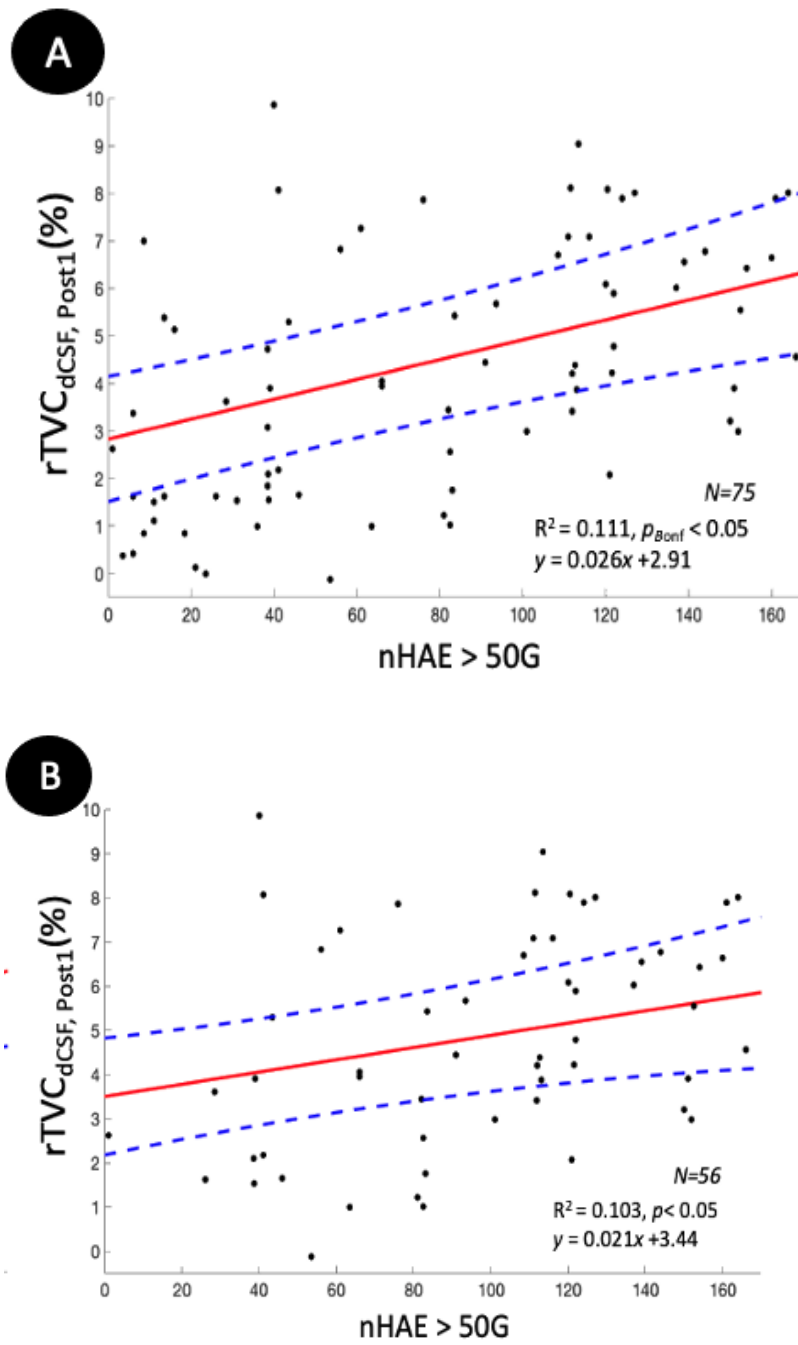
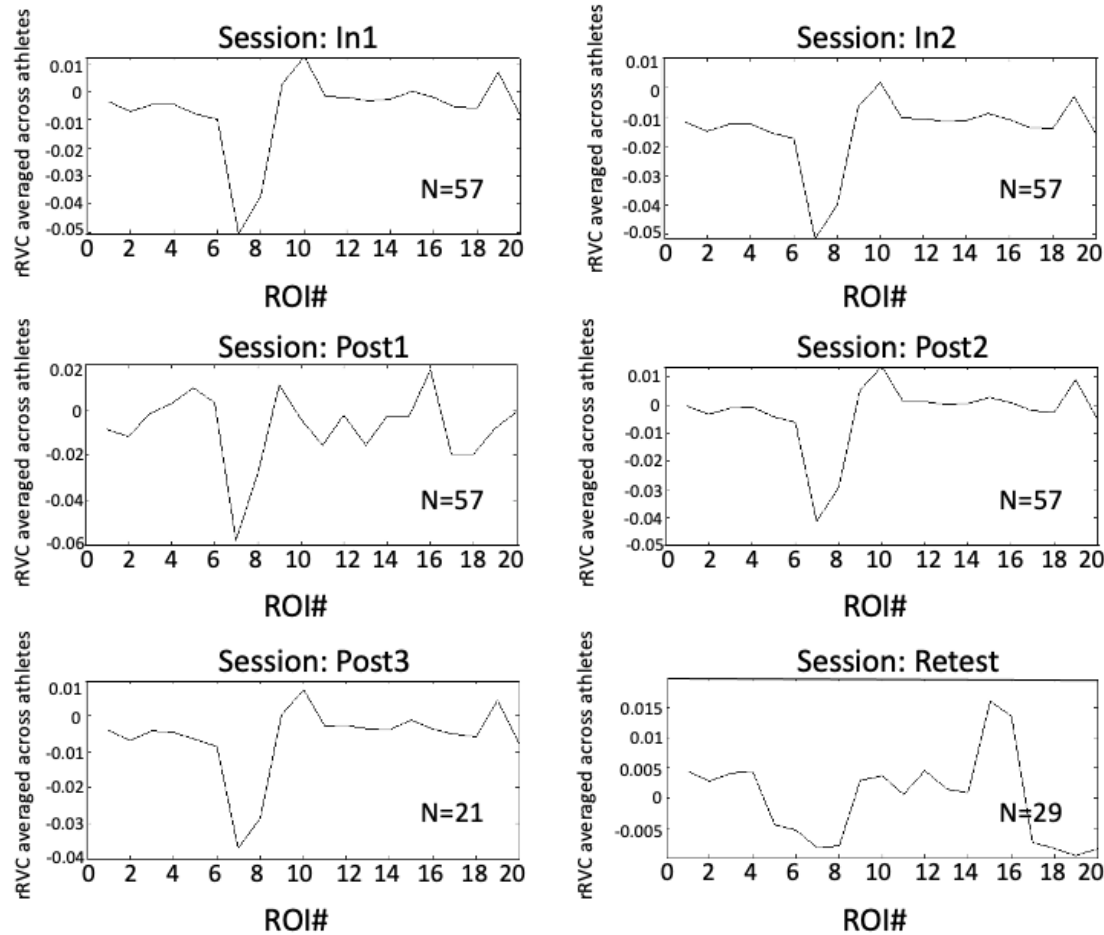


Figure 4.13 Linear predictor plots for rTVC at session *Post1* of dCSF against nHAE at 50G for (a) larger (Post hoc) cohort of athletes, (b) football only.

4.6 WM ROI Distribution



ROI# in ascending order:

1. ACR: Anterior corona radiata
2. ALIC: Anterior limb of internal capsule
3. BCC: Body of corpus callosum
4. CgC: Cingulum in the cingulate cortex
5. CgH: Cingulum in the hippocampus
6. CP: Cerebral peduncle
7. CST: Corticospinal tract
8. EC: External capsule
9. FX: Fornix
10. GCC: Genu of the corpus callosum
11. ICP: Inferior cerebellar peduncle
12. MCP: Middle cerebellar peduncle
13. ML: Medial lemniscus
14. PLIC: Posterior limb of the internal capsule
15. RLIC: Retrolenticular part of the internal capsule
16. PTR: Posterior thalamic radiation
17. SCC: Splenium of the corpus callosum
18. SCP: Superior cerebellar peduncle
19. SCR: Superior corona radiata
20. SLF: Superior longitudinal fasciculus

Figure 4.14 WM rVC ROI distribution by session.

Figure 4.14 explores the distribution rRVC of WM JHU ROIs. Possibly driving some insights into the sensitivity of the volumetric algorithm for WM. We can see a symmetric variation in the rRVC of individual ROIs across CSA sessions with only a slight change in means and a higher variance for session *Post1*, probably explaining the lack of findings with any of the previous longitudinal, distribution, and correlational analyses. Although the rRVC of ROIs 7, 8 exhibit volumetric changes (methods described by section 4.4.1 and Figure 4.3) future work would need to factor in DTI tractography measures to yield a more sensitive and clearer understanding of the WM structural alterations.

In summary, collision-sport athletes exhibit different rTVC than Controls i.e., NCA-rTVC and CSA-rTVC were different at *Post1*. Changes in collision-sport athletes are time-dependent i.e., CSA rTVC at *Post1* differs from *In1* and *Post2*. These time-dependent changes in collision-sport athletes are correlated with HAE exposure: nHAE was strongly correlated with changes in dCSF at *Post1* for HAEs for $PTA_{Th} = 50G$. The longitudinal trend observed in volumetric changes because of accumulated head trauma should urge athletes and coaches to allow for sufficient rest during the season to prevent the incidence of these short-term session-specific changes. The long-term fatigue induced by the repeated stress of the short-term season-specific reversible changes remains yet to be explored.

5. DISCUSSION

Summary: This investigation sought to characterize and explain variations in brain volume measures from RHI experienced by the participation of high school-aged youth in collision sports (CSA). Using MRI, volumetric changes were assessed across a season of collision-sport participation and compared with the session-to-session variability of age-matched peers who participate only in sports that do not involve purposeful collisions (NCA). Statistically significant regional tissue-level volumetric changes (rTVC) were observed for gray matter (GM) and deep (ventricular) cerebrospinal fluid (dCSF) in CSA at the post-season (*Post1*) measure, relative to measures obtained prior to the season's onset of collision exposure (*Pre*). Further, longitudinal volumetric dCSF increases in these athletes were found to be significantly correlated with exposure to RHI (i.e., nHAE). Consistent with previous observations of changes in brain health in this population, the changes observed in dCSF did not return to baseline/normative levels until several months after the cessation of collision-based activities (*Post2*, *Post3*). While persistent alterations such as those suggesting accrual of changes year-over-year were not observed, concern remains for the neural health of CSA given the relatively long duration of the observed alterations in brain volume.

5.1 Volumetric Changes

Volumetric changes and normal aging: Volumetric changes for CSA documented here are suggestive of at least transient deleterious alterations to brain physiology brought about by repetitive HAEs. Decreases in GM volume and increases in dCSF volume are not consistent with previous literature quantifying year-to-year normative brain development (Blatter et al., 1997; Ge et al., 2002.; Good et al., 2001; Lenroot et al., 2007). Further, volumetric changes in dCSF were linked to cumulative exposure to RHI. Given the inter-session time intervals and the subsequent neuroplastic return to baseline after extended rest from collision-based activity, it is unlikely that these observed changes are a consequence of maturation in adolescents.

Note that we are here assuming that normative changes for youth athletes over the interval between imaging sessions are captured by our test-retest measures with the NCA. The observation of significant tissue-level (GM, CSF, dCSF) population-specific volumetric changes (CSA vs.

NCA) for CSA at *Post1* can thus be reasonably posited to be attributable to accumulated physiological changes caused by HAEs, which are expected to be absent (or at least substantially lesser) in NCA.

Volumetric changes and HAE thresholds: Near-term post-season measurements of volumetric changes in dCSF for asymptomatic CSA were predicted by cumulative exposure to RHI. The longitudinal tissue-level changes seen in mean rTVC for dCSF were strongly correlated at *Post1* with nHAE at a PTA threshold of 50G. These findings are not dependent on the athlete's gender even after factoring in the difference in hit distribution profiles across the populations of football and soccer athletes (Lee et al., 2021). At this 50G PTA threshold, these volumetric findings complement the previous detection of CVR changes (Svaldi et al., 2015) and MR spectroscopic changes (Bari et al., 2019) for the asymptomatic CSA population.

Further, similar PTA thresholds (e.g., 60G) have been found to induce functional changes in previous biomarker studies involving this CSA population using verbal, visual task-based fMRI (Robinson et al., 2015; Talavage et al., 2014b) and MR spectroscopy (Poole et al., 2015). The amalgamation of these various findings moves us closer to understanding the threshold at which HAEs meaningfully affect the brain health of CSA.

Regional variation of volumetric changes: Regional variation of GM volumetric measures was sparsely scattered across all areas of the brain as opposed to the localized dCSF changes. Longitudinal measurements of volumetric changes in GM for CSA primarily showed a decrease in the temporal, occipital, and prefrontal cortices coupled with a slight increase in the parietal cortex. At a regional level, similar longitudinal distributions of deviant ROIs have been recorded for task-based fMRI (Robinson et al., 2015), CVR (Svaldi et al., 2017), DTI (Bazarian et al., 2014; Jang et al., 2019a; Lipton et al., 2013; Tremblay et al., 2019) and neurophysiological impairment (Breedlove et al., 2012) for the CSA population.

The lack of consistent localization of these volumetric changes could be attributed to the varying patterns of head impact history (location, magnitude, and frequency). Determining the underlying mechanism (coup, contrecoup, resonance cavitation) of the observed changes would be the next steps of the in-depth impact location analysis. Some literature observing posterior

changes in cortical gray matter with frontal impact loading favor the contrecoup explanation (Gong et al., 2018).

The mechanical stress of cumulative HAEs is observed here to cause a tissue-specific (dCSF) relative volumetric change, specifically within the ventricles. Regional brain mechanical responses to randomly incident HAE exhibit a primary intersection of induced strain near the center of the brain (Ji et al., 2014; Gurdjian and Gurdjian 1976). This accumulated strain might explain the observation of localized dCSF increase as opposed to a significant global change in CSF.

Documenting and validating the loci of these volumetric changes should aid future investigations to explore regional alterations in brain physiology. Lack of volumetric changes in WM could be explained by the absence of immediate large-scale axonal loss (Smits et al., 2011), the sensitivity of MRI as opposed to DTI to detect WM changes (Jang et al., 2019), and the relatively long duration for neuroinflammation to manifest as WM degeneration (Mouzon et al., 2014). Similar trends of GM-CSF changes with a lack of significant WM findings were observed in a ROI approach study involving severe vs. mild TBI children (Berryhill et al., 1995)

Therefore, asymptomatic CSA are likely to exhibit regional volumetric alterations significantly different from NCA that take several months to return to baseline levels. Here, these alterations are best explained by the accumulation of HAE which is absent in NCA. Continual participation in collision-based activities may represent a risk wherein recovery cannot occur. Even when present, the degree of the eventual recovery remains to be explored but has strong implications for the well-being of collision-sport participants.

5.2 Pathophysiological Modeling

Similar findings in other pathologies: The exploration to ascertain a mechanism explaining this pathology is best supplemented by studying the pathophysiology of similar neurological conditions. Similar volumetric changes have previously been observed in cases with mTBI specifically quantifying ventricular CSF increase (Blatter et al., 1997; Brezova et al., 2014; N. D. Davenport et al., 2018; T. C. Harris et al., 2019; Ledig et al., 2017; Spitz et al., 2013) and GM atrophy in temporal, parietal, subcortical ROIs (Bigler et al., 2019; Burrowes et al., 2020; Levine et al., 2006; Patel et al., 2020; Sussman et al., 2017), cortical ROIs (Bigler et al., 2004; Epstein et al., 2016; Dean et al., 2015; Gale et al., 2005; Mackenzie et al., 2002.; Patel et al., 2020;

Spitz et al., 2013; Zhou et al., 2013). Studies of Anorexia Nervosa (AN), dehydration have also been documented with similar longitudinally reversible GM and dCSF volume changes (Boto et al., 2017; Frintrop et al., 2019; Reyes-Haro et al., 2015; Seitz et al., 2015). Here, we build on the above findings and demonstrate similar volumetric changes in a dataset of asymptomatic youth athletes experiencing RHI.

Moving forward in investigating other more severe neurological conditions. Longitudinal GM atrophy has also been observed on a regional, global level in pathologies related to moderate-severe TBI (Bendlin et al., 2008; Blatter et al., 1997; Cole et al., 2018; T. C. Harris et al., 2019; Lannsjö et al., 2013; Ledig et al., 2017; Meysami et al., 2019; Raji et al., 2016; Tremblay et al., 2013, 2019; Trivedi et al., 2007) mainly affecting the temporal, parietal, sub-cortical and cortical regions. It has additionally been quantified on a regional basis in the hippocampus, amygdala (Anstey et al., 2003; Bottino et al., 2002) for Alzheimer's disease, cognitive impairment (Labayru et al., 2019; Lee et al., 2013; Anderson et al., 2012; Bottino et al., 2002) and multiple sclerosis (MS) (Nakamura et al., 2014; Rudick et al., 1999). Furthermore, instances of cortical thinning are witnessed in cases of chronic smokers (Kuhn et al., 2010), schizophrenia (Giuliani et al., 2005), and other psychiatric disorders (Raine et al., 2000; Huebner et al., 2008). Ventricular CSF increase, on the other hand, has been observed in cases of CTE (McKee et al., 2009; Omalu et al. 2011), sports concussions (Tremblay et al., 2013), MS (Rudick et al., 1999), and acute dehydration (Streitbürger et al., 2012; Dickson et al., 2005). Linking the neuromodulation of these underlying pathologies with mTBI (Graham et al., 2019; Raji et al., 2016; Gooijers et al., 2016) and RHT should provide insight into the mechanism driving the changes observed here.

Understanding the pathophysiological mechanisms: Future intervention strategies to prevent or treat changes, such as were observed here, require us to explore possible mechanisms governing these volumetric changes. Longitudinal changes in volumetric measures of GM and dCSF reach a maximum of 4-8 weeks after the cessation of collision activity and return to normal after 15-20 weeks of rest from collision-related activity. Similar results in cortical gray matter have been observed in a slightly older mTBI cohort wherein the neurobehavioral symptoms start to subside after a 4-month interval (Ling et al., 2013).

GM changes could be perfusion induced (Holmin et al., 1995; Holmin et al., 1998; Unterberg et al., 2004) with apoptosis of cortical cells peaking only after 1-week post-injury (Conti

et al., 1998). dCSF increase could be attributed to improper waste metabolism within the glymphatic system (Christensen et al., 2020; Plog et al., 2015) leading to a progressive enlargement of the ventricles. The cumulative effect of these asymptomatic volumetric changes could lead to the manifestation of a more gross and recognizable symptomatic pathology.

The exact mechanism of interaction of these tissue-specific volumetric changes and how they play a combined role in explaining asymptomatic repetitive HAE-induced injury remains yet to be quantified, but several hypothesized key pathways linking these neurological observations are presented in Figure 5.1. Pathologies such as anorexia nervosa (Blasel et al., 2012; Boghi et al., 2011; Boto et al., 2017; Seitz et al., 2015) and dehydration (Biller et al., 2015; Kempton et al., 2011) present with similar volumetric observations and therefore might help narrow down the actively involved metabolic regulatory mechanisms.

The acute edema, neuroinflammation (Jang et al., 2019), oxidative stress (Fehily & Fitzgerald, 2017) from the RHI could possibly lead to reactive astrogliosis (Chen et al., 2020), microglial activation (Kou & VandeVord, 2014), astrocyte density (Fintrop et al., 2019; Reyes-Haro et al., 2015) and metabolism (J. L. Harris et al., 2015) alteration coupled with reduced neurogenesis (Costa et al., 2010; Diotel et al., 2020; Redell et al., 2020), mitochondrial dysfunction (Lindfors et al., 2011; Rinholm et al., 2016) and excitotoxicity (Blasel et al., 2012). Finding an intersection for most of these mechanisms leads us to hypothesize a connection between glymphatic system dysregulation and RHT. These mechanisms are possible precursors which when accumulated over longer periods of collision-based activity could cause large-scale systemic alterations.

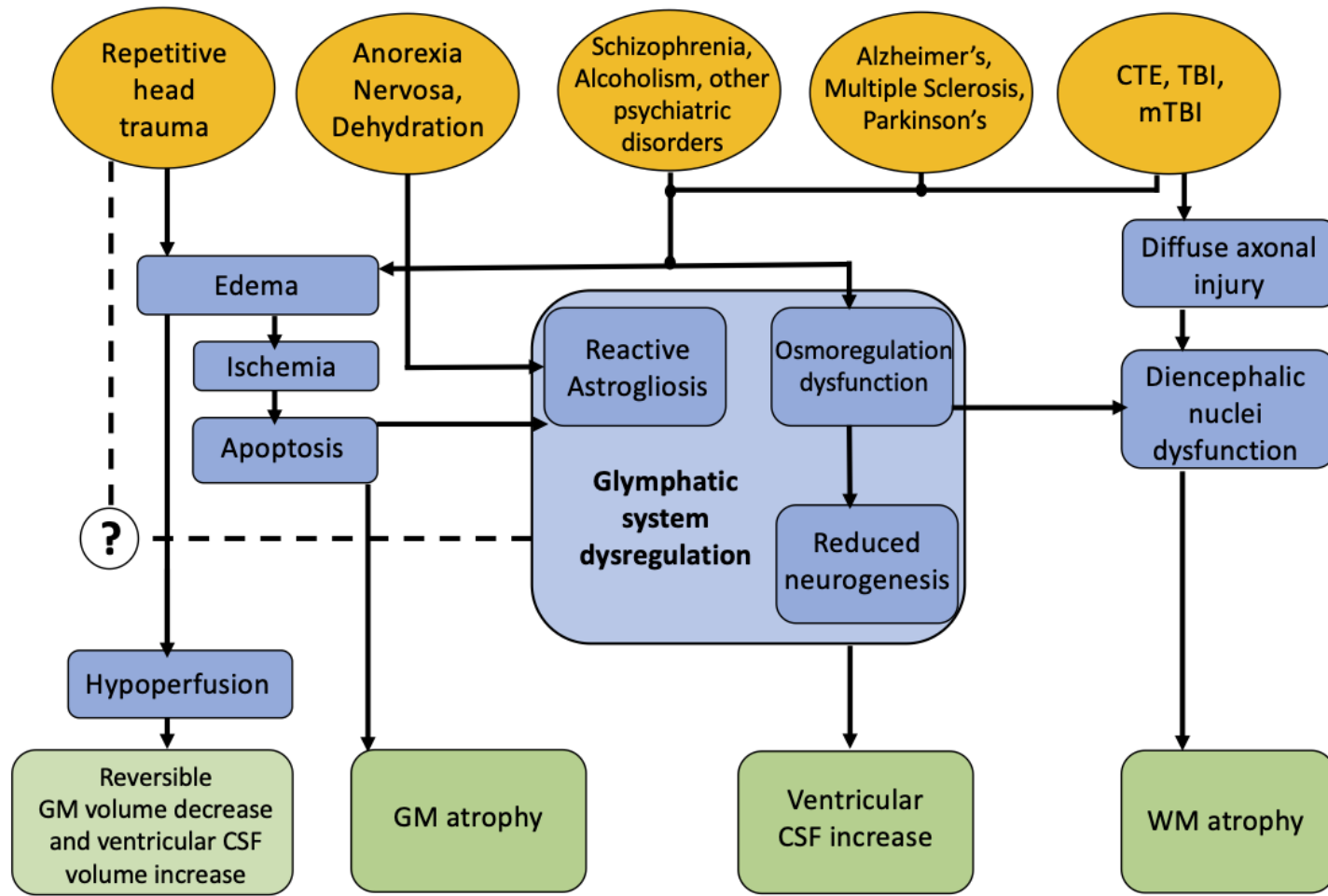


Figure 5.1 Hypothesis of pathophysiological mechanisms linking RHT (as associated with exposure to HAEs) to observed reversible changes in GM and dCSF volumes. Other disorders (yellow) known to effect similar changes in GM and dCSF, in addition to changes in WM that were not observed herein, are depicted along with key pathways (blue) hypothesized to lead to these neurological observations (green).

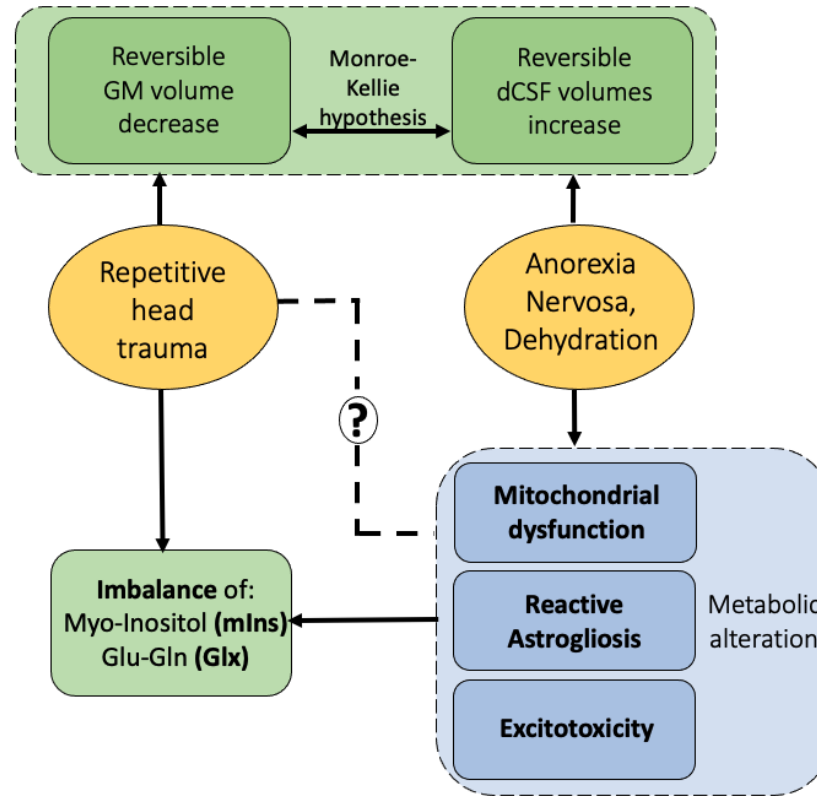


Figure 5.2 Hypothesis of metabolic regulatory pathways as associated with repeated exposure to HAEs to observations of altered. The pathophysiological metabolic regulatory mechanisms (Blue) of the conditions (yellow) anorexia nervosa, dehydration, and RHT hypothesized due to the observation of similar metabolites (Myo-Inositol, Glutamine-Glutamate) concentration imbalance (Green).

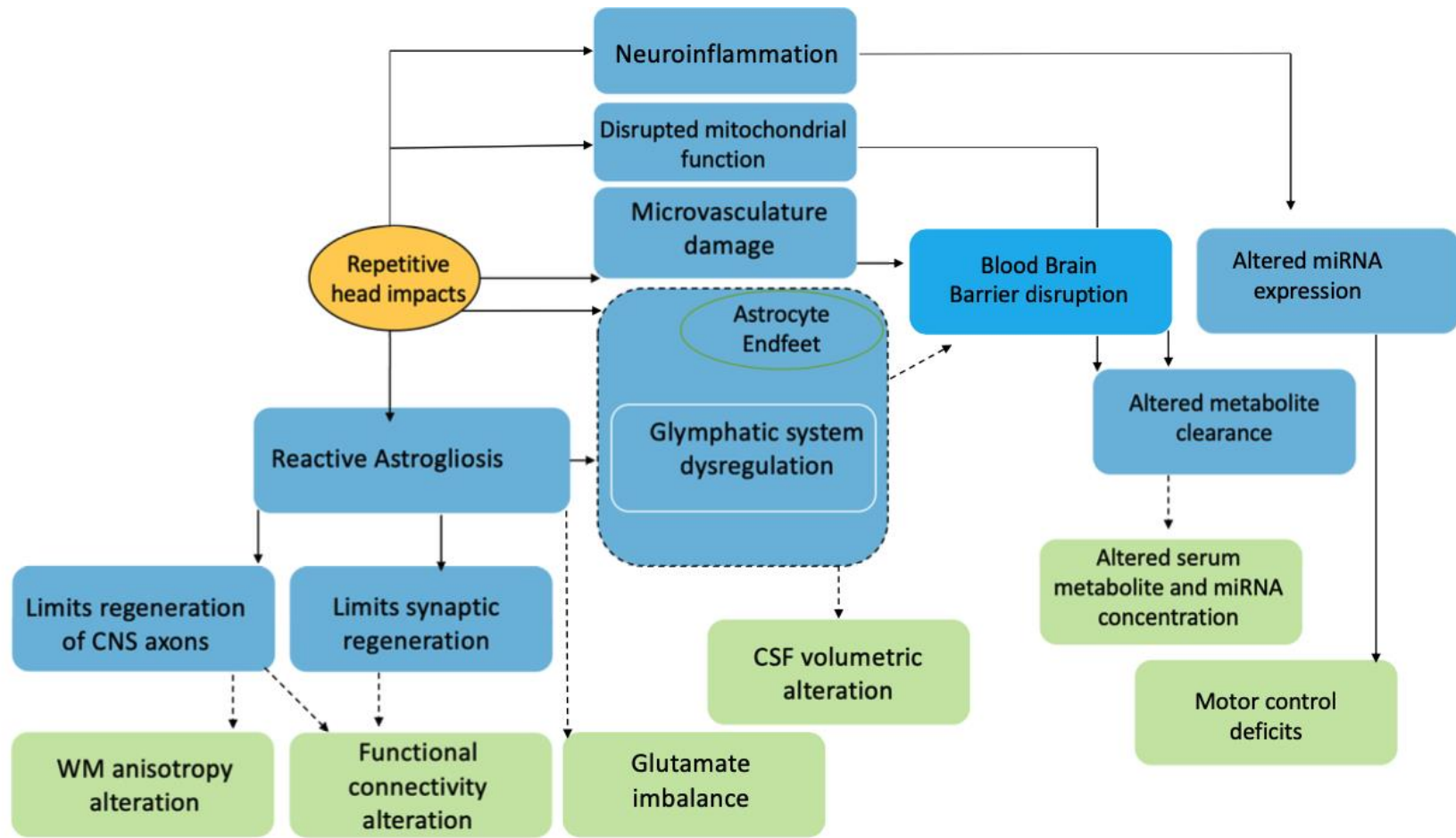


Figure 5.3 Hypothesis of reactive astrogliosis and glymphatic system dysfunction as an explanation for the changes observed with head trauma. *Green* depicting the observed outcomes with repetitive head trauma, *sky blue* pinpointing an adverse outcome and *transparent dark blue* representing key metabolic processes.

Understanding the metabolic regulatory pathways: Investigating possible mechanisms governing these volumetric changes in GM, dCSF further led us to explore the pathophysiology of similar neuropathological conditions. Studies of Anorexia Nervosa (AN), dehydration have also been documented with similar longitudinally reversible GM and dCSF volume changes. Moreover, the imbalance in biomarkers such as concentration of myo-Inositol and Glutamine-Glutamate as seen in subjects experiencing RHI (Bari et al., 2019; Fischer, Hylin, et al., 2016; J. L. Harris et al., 2015; Lefebvre et al., 2018) are observed separately as an outcome of metabolic alteration caused by mitochondrial dysfunction (Rinholm et al., 2016; Lindfors et al., 2010), reactive astrogliosis (Hellerhoff et al., 2021; Chen et al., 2017) and excitotoxicity (Blasel et al., 2012) in AN. Glutamate excitotoxicity is also observed after severe neurotrauma resulting in elevated intracellular calcium, mitochondrial failure, ischemia that can cause memory impairment (Atkins et al., 2006) astrocytic dysfunction (Ma et al., 2013). Reconciling these findings across the pathologies could unearth an underlying explanation (Figure 5.2) that explores the metabolic regulation mechanisms and pathways of the RHT condition.

All of these within-season changes are consistent with prior studies of acute dehydration (Dickson et al., 2005) but observed in a more chronic form here. Another possible route for future studies would be to investigate the glymphatic system. The glial-lymphatic system is responsible for waste management above the cervical lymph nodes. Quantifying CSF flow and correlating it with acquired fMRI/MRI data should be an interesting question for future research.

Reactive astrogliosis and other physiological implications: A small hit to the cranial compartment can compress the axon fibers of the neurons and affect the nodes of Ranvier which assist with normal nerve impulse conduction. Large hits on the other hand can fracture the skull, cause a subdural hematoma, and break the axon fibers. At a smaller scale the initial biomechanical and physiological changes would be changes in intracranial pressure, microvasculature damage, axonal injury from shear stresses coupled with neuronal and glial stress. With sufficient damage, these can cause secondary mechanisms such as mitochondrial alteration, protein aggregation, oxidative stress, synaptic dysfunction, and excitotoxicity.

Neuroinflammation and microvasculature damage are the first signs of physical trauma in the central nervous system. These affect the glial cells (astrocytes, microglia, oligodendrocytes that support axon fibers), especially the astrocytes (Burda et al., 2016) which affect normal

neuronal functioning and cause reactive astrogliosis which in turn affects the glymphatic system (Ren et al. 2021, Mira et al., 2021, Benveniste et al., 2019) that can disrupt the blood brain barrier.

Reactive astrogliosis is one of the active mechanisms involved with tissue damage to the central nervous system (Pekny et al., 2016, Sofroniew et al., 2015, Li et al., 2020, Moulson et al., 2021). Reactive astrogliosis is known to limit regeneration of axons and synapses (Pekny et al., 2014). A possible pathway highlighting the alterations observed in functional connectivity of CSA: Abbas et al. (2015), white matter structural integrity: Jang et al. (2019), metabolite concentration and microRNAs: Vike et al. (2021) and volumetric changes from the current study are presented in Figure 5.3. With the latter also being observed as inflammation-dependent in posthemorrhagic hydrocephalus (Karimy et al., 2017).

Given the prominence of such mechanisms, biomarkers such as glial fibrillary acidic protein should be explored to quantify the extent of injury (Huebschmann et al., 2020, Papa et al., 2016, Meier et al., 2017) as it plays a major role in astrocyte development. Other biomarkers such as salivary S100B (Janigro et al. 2020, Meier et al., 2017) can function as surrogates for regulating neuronal development after a TBI.

Multiple mechanical injury models for blast-related injury (Rosenfeld et al., 2013) have demonstrated dysfunction of neurotransmitter receptors mainly in the hippocampus and other excitatory synaptic neurotransmission (Aungst et al., 2014). GM volume change could be a result of short-term acute cerebral ischemia, cerebral autoregulation and reperfusion which eventually lead to edema. Hypoperfusional zones exhibit secondary neuronal damage coupled glial and axonal degeneration. Moreover, vasogenic blood brain barrier breakdown occurs a few hours (6-16) after a TBI (Holmin et al., 1995) with cytotoxic alterations like mitochondrial dysfunction, micro hemorrhages and cerebral aquaporin4 channel disruption, the latter playing a key role in glymphatic system functioning (Unterberg et al., 2004). These short-term changes can accumulate over time to cause cortical atrophy coupled with changes in intracranial and cerebral perfusion pressures. Additionally, apoptosis of cortical cells peaks at 1 week in rat models, with severe head trauma leading to glutamate increase, hyper glycolysis and fast excitotoxicity to cellular calcium imbalance (Bullock et al., 1998). Similar physiological cascades could be created with milder head trauma.

The lack of significant WM volume reduction could be because large-scale volume loss only occurs 6-12 months after severe injury (Mouzon et al., 2014) whereas micro alterations are

best detected using DTI images (Jang et al., 2019). In addition, to alterations in serum miRNAs and metabolite concentrations, CSF cytokine levels are known to increase in cases of TBI (Lindqvist et al., 2014, Kumar et al., 2014, Juengst et al., 2014). The reactive oxidative stress that follows TBI can lead to DNA fragmentation then to alteration in mitochondrial function finally leading to apoptosis and even necrosis (Tran et al., 2014). Other neurodegenerative pathologies such as Alzheimer's have presented with B-amyloid depositions that likely contribute to apoptosis and inflammation (Faden et al., 2015, Roberts et al., 1990), linking mTBI to Alzheimer's via a pathophysiological pathway will burgeon other research opportunities in the field of neuroscience. The chronic nature of these alterations and their relation to the health of youth athletes remains yet to be explored. It is to be noted that late exercise reduces neuroinflammation after TBI in mice (Piao et al., 2013) and could be a possible intervention for youth athletes to reduce the effects of neurotoxic inflammatory response.

CSF flow implications: The Monro-Kellie hypothesis states that the sum of the brain parenchymal volume, CSF and intracranial blood is constant if the intracranial pressure remains constant. The hypothesis's contributions are mainly with increased intracranial pressure and decreased CSF volume observed in MRI abnormalities (Mokri, 2001), tissue-compliance changes during hypoxic-ischemic conditions such as stroke (Kalisvaart et al., 2020) and other surgical applications (Dobrocky et al., 2020). Here, it can be posited that if the intracranial pressure and blood volumes (related to cerebral perfusion pressure) remain constant over long periods of time (months to a year), the reversible changes observed in CSF are coupled with complementary changes in the brain parenchyma, mainly GM ROIs.

To pinpoint the causative mechanism would require further exploration with multi-modal techniques of MR perfusion and CSF flow imaging. It is also observed that increased CSF volumes are correlated with increased glymphatic waste clearances in neurodegenerative disorders (Tarasoff-Conway et al., 2015). The extent of this change and possible chronic complications remains yet to be explored. There have been other studies trying to quantify CSF flow using fMRI techniques (H.-C. Yang et al., 2021.) linking them to vascular low frequency oscillations and respiration (Vijayakrishnan Nair et al., 2021). But the lack of reproducibility and reliability when it comes to using fMRI signals to quantify cerebral blood volume is low, as it's often confounded with cerebral flow and other metabolic regulatory processes (Murphy & Fox, 2017). Therefore,

the use of 3-D phase contrast imaging and other MR perfusion techniques will provide a better ground truth when it comes to quantifying CSF flow within the glymphatic system. Additionally, not only are the subcortical regions affected with the glymphatic dysregulation but also the perivascular spaces (Ramirez et al. 2016), hence the latter could be considered as an alternative for imaging strategy to quantify glymphatic functioning for RHT.

6. FUTURE DIRECTIONS

Considering the recent findings using multiple MRI protocols (MRS, DTI, CVR, fMRI, working memory and T1-weighted MRI) within this study cohort, it would be in the interest to re-assess all the data using these different approaches to create a more integrated and complete model explaining the neuroradiological observations. Following which, the construction of a more comprehensive pathophysiological model explaining the biological pathways that regulate these observations would be a vital contribution in this field.

From a morphometric perspective, it would be great if a structural model was created coupling the GM-CSF sensitive T1-weighted MRI and WM-sensitive DTI thereby explaining the volumetric aspects of RHT. Using other techniques to quantify GM cortical thickness and surface area would also add to the volumetric findings.

The resolution of the MRI images increases with increasing magnetic field strength, specifically with the square root of the B0 field. Therefore, collecting longitudinal data with a magnet of higher field strength would greatly improve the optics of these findings. Additionally, exploring the variation of these longitudinal volumetric changes over greater lengths of time (>2 years or seasons of collision-based activity) using mediating statistical models would give a complete picture of the temporal aspect of RHT. This study also uses a relatively small sample (N<100) of youth athletes, quantifying volumetric changes with a larger cohort (N>200) while being cognizant of the reliability across different data acquisition protocols would increase the statistical power of the results.

$$rRVC_{p,i,j,k} = \frac{Vol_{i,j,k}^{1/p} - Vol_{i,j,Pre}^{1/p}}{Vol_{i,j,Pre}^{1/p}}$$

A significant contribution of this thesis is the mathematical approach towards brain volumetry wherein the regional volumes are normalized with respect to the baseline volumes. Employing other kernels and mathematical transformations (example: Lp normalization for RVC as described above) and quantifying its sensitivity statistically across populations would be a worthy next step.

Additionally, exploring the physiological modeling with regards to the changes observed in the CSF, employing a multi-model approach to quantify CSF flow, cerebral blood volume and brain parenchymal volumes will produce more meaningful results. Possible alternatives could include arterial spin-labeling or other MR perfusion techniques coupled with phase contrast imaging, DTI, dynamic susceptibility contrast imaging and T1-weighted MRI. This way, it would be easier to quantify CSF flow and its implications to the neural health of these athletes. Since the CSF is mainly regulated during sleep, collecting MRI and EEG data while the subjects are asleep will provide a better picture of the subject's waste clearance system. Constructing causal statistical models tracking various RHT biomarkers with other evidence-based mediators and outcomes should culminate the research in this field. Specifically, using short-term serum-based biomarkers and longitudinal imaging assessments of athletes participating in collision sports. Testing the sensitivity, reliability, and temporal evolution of the neuroradiological observations is an important next step.

Finally, the current study is limited by the error introduced by its pre-processing, post-processing methods, scanner noise, head coil noise, patient variability and the sensitivity of T1-weighted MRI. Patient/inter-subject variability encompassing factors such as hit distribution history profile, active game time, position on the field, skull geometry, intracranial tissue distribution, neck strength, BMI, and other covariates are crucial for understanding this pathology. Factoring in all these variables and quantifying their variances would help future analyses and statistical models. The possible inclusion of MR-phantom based techniques to improve the reliability of the underlying data would be useful as well.

REFERENCES

- Abbas, K., Shenk, T. E., Poole, V. N., Breedlove, E. L., Leverenz, L. J., Nauman, E. A., Talavage, T. M., & Robinson, M. E. (2015). Alteration of default mode network in high school football athletes due to repetitive subconcussive mild traumatic brain injury: A resting-state functional magnetic resonance imaging study. *Brain Connectivity*, 5(2), 91–101. <https://doi.org/10.1089/brain.2014.0279>
- Abbas, K., Shenk, T. E., Poole, V. N., Robinson, M. E., Leverenz, L. J., Nauman, E. A., & Talavage, T. M. (2015). Effects of repetitive sub-concussive brain injury on the functional connectivity of default mode network in high school football athletes. *Developmental Neuropsychology*, 40(1), 51–56. <https://doi.org/10.1080/87565641.2014.990455>
- Adduru, V., Baum, S. A., Zhang, C., Helguera, M., Zand, R., Lichtenstein, M., Griessenauer, C. J., & Michael, A. M. (2020). A method to estimate brain volume from head CT images and application to detect brain atrophy in alzheimer disease. *American Journal of Neuroradiology*, 41(2), 224–230. <https://doi.org/10.3174/AJNR.A6402>
- Akudjedu, T. N., Nabulsi, L., Makelyte, M., Scanlon, C., Hehir, S., Casey, H., Ambati, S., Kenney, J., O'Donoghue, S., McDermott, E., Kilmartin, L., Dockery, P., McDonald, C., Hallahan, B., & Cannon, D. M. (2018). A comparative study of segmentation techniques for the quantification of brain subcortical volume. *Brain Imaging and Behavior*, 12(6), 1678–1695. <https://doi.org/10.1007/s11682-018-9835-y>
- Alexander M. P. (1995). Mild traumatic brain injury: pathophysiology, natural history, and clinical management. *Neurology*, 45(7), 1253–1260. <https://doi.org/10.1212/wnl.45.7.1253>
- Alosco, M. L., Kasimis, A. B., Stamm, J. M., Chua, A. S., Baugh, C. M., Daneshvar, D. H., Robbins, C. A., Mariani, M., Hayden, J., Conneely, S., Au, R., Torres, A., McClean, M. D., McKee, A. C., Cantu, R. C., Mez, J., Nowinski, C. J., Martin, B. M., Chaisson, C. E., ... Stern, R. A. (2017). Age of first exposure to American football and long-term neuropsychiatric and cognitive outcomes. *Translational Psychiatry*, 7(9), e1236. <https://doi.org/10.1038/tp.2017.197>
- Andersson, M. Jenkinson and S. Smith (2007) Non-linear registration, aka Spatial normalisation. FMRIB technical report TR07JA2 from www.fmrib.ox.ac.uk/analysis/techrep
- Ashburner, J. (2010). VBM Tutorial. <http://www.brain-development.org/>
- Ashburner, J., & Friston, K. J. (2000). Voxel-based morphometry--the methods. *NeuroImage*, 11(6-1), 805–821. <https://doi.org/10.1006/nimg.2000.0582>
- Ashburner, J., & Friston, K. J. (2001). Why voxel-based morphometry should be used. *NeuroImage*, 14(6), 1238–1243. <https://doi.org/10.1006/nimg.2001.0961>

- Bader, J. M., Geyer, P. E., Müller, J. B., Strauss, M. T., Koch, M., Leypoldt, F., Koertvelyessy, P., Bittner, D., Schipke, C. G., Incesoy, E. I., Peters, O., Deigendesch, N., Simons, M., Jensen, M. K., Zetterberg, H., & Mann, M. (2020). Proteome profiling in cerebrospinal fluid reveals novel biomarkers of Alzheimer's disease. *Molecular Systems Biology*, 16(6). <https://doi.org/10.15252/msb.20199356>
- Bahrami, N., Sharma, D., Rosenthal, S., Davenport, E. M., Urban, J. E., Wagner, B., Jung, Y., Vaughan, C. G., Gioia, G. A., Stitzel, J. D., Whitlow, C. T., & Maldjian, J. A. (2016). Subconcussive head impact exposure and white matter tract changes over a single season of youth football. *Radiology*, 281(3), 919–926. <https://doi.org/10.1148/radiol.2016160564>
- Bailes, J. E., Petraglia, A. L., Omalu, B. I., Nauman, E., & Talavage, T. (2013). Role of subconcussion in repetitive mild traumatic brain injury. *Journal of Neurosurgery*, 119(5), 1235–1245. <https://doi.org/10.3171/2013.7.JNS121822>
- Bailes, J., Bravo, S., Breiter, H., Kaufman, D., Lu, Z., Molfese, D., Perrish, T., Slobounov, S., Talavage, T., & Zhu, D. (2015). Editorial: A call to arms: The need to create an inter-institutional concussion neuroimaging consortium to discover clinically relevant diagnostic biomarkers and develop evidence-based interventions to facilitate recovery. *Developmental Neuropsychology*, 40(2), 59–62. <https://doi.org/10.1080/87565641.2015.1018090>
- Bari, S., Svaldi, D. O., Jang, I., Shenk, T. E., Poole, V. N., Lee, T., Dydak, U., Rispoli, J., Nauman, E. A., & Talavage, T. M. (2019). Dependence on subconcussive impacts of brain metabolism in collision sport athletes: an MR spectroscopic study. *Brain Imaging and Behavior*, 13(3), 735–749. <https://doi.org/10.1007/s11682-018-9861-9>
- Baria, A. T., Baliki, M. N., Parrish, T., & Apkarian, A. V. (2011). Anatomical and functional assemblies of brain BOLD oscillations. *Journal of Neuroscience*, 31(21), 7910–7919. <https://doi.org/10.1523/JNEUROSCI.1296-11.2011>
- Baugh, C. M., Kiernan, P. T., Kroshus, E., Daneshvar, D. H., Montenigro, P. H., McKee, A. C., & Stern, R. A. (2015). Frequency of head-impact-related outcomes by position in NCAA division I collegiate football players. *Journal of Neurotrauma*, 32(5), 314–326. <https://doi.org/10.1089/neu.2014.3582>
- Baugh, C. M., Stamm, J. M., Riley, D. O., Gavett, B. E., Shenton, M. E., Lin, A., Nowinski, C. J., Cantu, R. C., McKee, A. C., & Stern, R. A. (2012). Chronic traumatic encephalopathy: Neurodegeneration following repetitive concussive and subconcussive brain trauma. *Brain Imaging and Behavior*, 6(2), 244–254. <https://doi.org/10.1007/s11682-012-9164-5>
- Bazarian, J. J., Zhu, T., Zhong, J., Janigro, D., Rozen, E., Roberts, A., Javien, H., Merchant-Borna, K., Abar, B., & Blackman, E. G. (2014). Persistent, long-term cerebral white matter changes after sports-related repetitive head impacts. *Plos one*, 9(4), e94734. <https://doi.org/10.1371/journal.pone.0094734>

- Bendlin, B. B., Ries, M. L., Lazar, M., Alexander, A. L., Dempsey, R. J., Rowley, H. A., Sherman, J. E., & Johnson, S. C. (2008). Longitudinal changes in patients with traumatic brain injury assessed with diffusion-tensor and volumetric imaging. *NeuroImage*, 42(2), 503–514. <https://doi.org/10.1016/j.neuroimage.2008.04.254>
- Benson, B. W., Hamilton, G. M., Meeuwisse, W. H., McCrory, P., & Dvorak, J. (2009). Is protective equipment useful in preventing concussion? A systematic review of the literature. *British Journal of Sports Medicine*, 43(Suppl. 1), i56–67. <https://doi.org/10.1136/bjsm.2009.058271>
- Bernier, M., Cunnane, S. C., & Whittingstall, K. (2018). The morphology of the human cerebrovascular system. *Human Brain Mapping*, 39(12), 4962–4975. <https://doi.org/10.1002/hbm.24337>
- Bigler, E. D. (2013). Traumatic brain injury, neuroimaging, and neurodegeneration. *Frontiers in human neuroscience*, 7, 1662–516. <https://doi.org/10.3389/fnhum.2013.00395>
- Bigler, E. D., & Maxwell, W. L. (2012). Neuropathology of mild traumatic brain injury: relationship to neuroimaging findings. *Brain imaging and behavior*, 6(2), 108–136. <https://doi.org/10.1007/s11682-011-9145-0>
- Bigler, E. D., Abildskov, T. J., Eggleston, B., Taylor, B. A., Tate, D. F., Petrie, J. A., Newsome, M. R., Scheibel, R. S., Levin, H., Walker, W. C., Goodrich-Hunsaker, N., Tustison, N. J., Stone, J. R., Mayer, A. R., Duncan, T. D., York, G. E., & Wilde, E. A. (2019). Structural neuroimaging in mild traumatic brain injury: A chronic effects of neurotrauma consortium study. *International Journal of Methods in Psychiatric Research*, 28(3). <https://doi.org/10.1002/mpr.1781>
- Bigler, E. D., Neeley, E. S., Miller, M. J., Tate, D. F., Rice, S. A., Cleavinger, H., Wolfson, L., Tschanz, J., & Welsh-Bohmer, K. (2004). Cerebral volume loss, cognitive deficit and neuropsychological performance: Comparative measures of brain atrophy: I. Dementia. *Journal of the International Neuropsychological Society*, 10(3), 442–452. <https://doi.org/10.1017/S1355617704103111>
- Biller, A., Reuter, M., Patenaude, B., Homola, G. A., Breuer, F., Bendszus, M., & Bartsch, A. J. (2015). Responses of the human brain to mild dehydration and rehydration explored in vivo by 1H-MR imaging and spectroscopy. *American Journal of Neuroradiology*, 36(12), 2277–2284. <https://doi.org/10.3174/ajnr.A4508>
- Bitar, R., Leung, G., Perng, R., Tadros, S., Moody, A. R., Sarrazin, J., McGregor, C., Christakis, M., Symons, S., Nelson, A., & Roberts, T. P. (2006). MR pulse sequences: What every radiologist wants to know but is afraid to ask. *Radiographics*, 26(2), 513–537. <https://doi.org/10.1148/rg.262055063>
- Blasel, S., Pilatus, U., Magerkurth, J., von Stauffenberg, M., Vronski, D., Mueller, M., Woeckel, L., & Hattingen, E. (2012). Metabolic gray matter changes of adolescents with anorexia nervosa in combined MR proton and phosphorus spectroscopy. *Neuroradiology*, 54(7), 753–764. <https://doi.org/10.1007/s00234-011-1001-9>

- Blatter, D. D., Bigler, E. D., Gale, S. D., Johnson, S. C., Anderson, C. V., Burnett, B. M., Ryser, D., Macnamara, S. E., & Bailey, B. J. (1997). MR-based brain and cerebrospinal fluid measurement after traumatic brain injury: correlation with neuropsychological outcome. *AJNR. American journal of neuroradiology*, 18(1), 1–10.
- Blyth, B. J., & Bazarian, J. J. (2010). Traumatic Alterations in Consciousness: Traumatic Brain Injury. *Emergency Medicine Clinics of North America*, 28(3), 571–594. <https://doi.org/10.1016/j.emc.2010.03.003>
- Boghi, A., Sterpone, S., Sales, S., D’Agata, F., Bradac, G. B., Zullo, G., & Munno, D. (2011). In vivo evidence of global and focal brain alterations in anorexia nervosa. *Psychiatry Research - Neuroimaging*, 192(3), 154–159. <https://doi.org/10.1016/j.psychresns.2010.12.008>
- Bookstein, F. L. (2001). “voxel-based morphometry” should not be used with imperfectly registered images. *NeuroImage*, 14(6), 1454–1462. <https://doi.org/10.1006/nimg.2001.0770>
- Boto, J., Gkinis, G., Roche, A., Kober, T., Maréchal, B., Ortiz, N., Lövblad, K. O., Lazeyras, F., & Vargas, M. I. (2017). Evaluating anorexia-related brain atrophy using MP2RAGE-based morphometry. *European Radiology*, 27(12), 5064–5072. <https://doi.org/10.1007/s00330-017-4914-9>
- Breedlove, E. L., Robinson, M., Talavage, T. M., Morigaki, K. E., Yoruk, U., O’Keefe, K., King, J., Leverenz, L. J., Gilger, J. W., & Nauman, E. A. (2012). Biomechanical correlates of symptomatic and asymptomatic neurophysiological impairment in high school football. *Journal of Biomechanics*, 45(7), 1265–1272. <https://doi.org/10.1016/j.jbiomech.2012.01.034>
- Brett, B. L., Bobholz, S. A., España, L. Y., Huber, D. L., Mayer, A. R., Harezlak, J., Broglio, S. P., McAllister, T. W., McCrea, M. A., Meier, T. B., & CARE Consortium Investigators (2020). Cumulative Effects of Prior Concussion and Primary Sport Participation on Brain Morphometry in Collegiate Athletes: A Study From the NCAA-DoD CARE Consortium. *Frontiers in neurology*, 11, 673. <https://doi.org/10.3389/fneur.2020.00673>
- Brezova, V., Gørn Moen, K., Skandsen, T., Vik, A., Brewer, J. B., Salvesen, Ø., & Håberg, A. K. (2014). Prospective longitudinal MRI study of brain volumes and diffusion changes during the first year after moderate to severe traumatic brain injury. *NeuroImage: Clinical*, 5, 128–140. <https://doi.org/10.1016/j.nicl.2014.03.012>
- Briggs, D. I., Angoa-Pérez, M., & Kuhn, D. M. (2016). Prolonged Repetitive Head Trauma Induces a Singular Chronic Traumatic Encephalopathy–Like Pathology in White Matter Despite Transient Behavioral Abnormalities. *American Journal of Pathology*, 186(11), 2869–2886. <https://doi.org/10.1016/j.ajpath.2016.07.013>
- Brock, J. B., Yanuck, S., Pierce, M., Powell, M., Geanopoulos, S., Noseworthy, S., Kharrazian, D., Turnpaugh, C., Comey, A., Zielinski, G., & Brock, J. B. (2013). The potential impact of various physiological mechanisms on outcomes in TBI, mTBI, concussion and PPCS. *Functional Neurological Rehabilitation*, 3(2-3), 215-256.

- Broglio, S. P., Eckner, J. T., Paulson, H. L., & Kutcher, J. S. (2012). Cognitive decline and aging: The role of concussive and subconcussive impacts. *Exercise and Sport Sciences Reviews*, 40(3), 138–144. <https://doi.org/10.1097/JES.0b013e3182524273>
- Broglio, S. P., Surma, T., & Ashton-Miller, J. A. (2012). High school and collegiate football athlete concussions: A biomechanical review. *Annals of Biomedical Engineering*, 40(1), 37–46. <https://doi.org/10.1007/s10439-011-0396-0>
- Budday, S., Ovaert, T. C., Holzapfel, G. A., Steinmann, P., & Kuhl, E. (2019). Fifty Shades of Brain: A Review on the Mechanical Testing and Modeling of Brain Tissue. *Archives of Computational Methods in Engineering*, 27(10), 1187-1230. <https://doi.org/10.1007/s11831-019-09352-w>
- Burda, J. E., Bernstein, A. M., & Sofroniew, M. V. (2016). Astrocyte roles in traumatic brain injury. *Experimental neurology*, 275 (3), 305–315. <https://doi.org/10.1016/j.expneurol.2015.03.020>
- Burrowes, S. A. B., Rhodes, C. S., Meeker, T. J., Greenspan, J. D., Gullapalli, R. P., & Seminowicz, D. A. (2020). Decreased grey matter volume in mTBI patients with post-traumatic headache compared to headache-free mTBI patients and healthy controls: a longitudinal MRI study. *Brain Imaging and Behavior*, 14(5), 1651–1659. <https://doi.org/10.1007/s11682-019-00095-7>
- Cai, X., Qiao, J., Kulkarni, P., Harding, I. C., Ebong, E., & Ferris, C. F. (2020). Imaging the effect of the circadian light-dark cycle on the glymphatic system in awake rats. *Proceedings of the National Academy of Sciences of the United States of America*, 117(1), 668–676. <https://doi.org/10.1073/pnas.1914017117>
- Campbell, K. R., Marshall, S. W., Luck, J. F., Pinton, G. F., Stitzel, J. D., Boone, J. S., Guskiewicz, K. M., & Mihalik, J. P. (2020). Head Impact Telemetry System's Video-based Impact Detection and Location Accuracy. *Medicine and science in sports and exercise*, 52(10), 2198–2206. <https://doi.org/10.1249/MSS.0000000000002371>
- Cancelliere, C., Hincapié, C. A., Keightley, M., Godbolt, A. K., Côté, P., Kristman, V. L., Stålnacke, B. M., Carroll, L. J., Hung, R., Borg, J., Nygren-De Boussard, C., Coronado, V. G., Donovan, J., & Cassidy, J. D. (2014). Systematic review of prognosis and return to play after sport concussion: Results of the international collaboration on mild traumatic brain injury prognosis. *Archives of Physical Medicine and Rehabilitation*, 95(3) SUPPL. <https://doi.org/10.1016/j.apmr.2013.06.035>
- Carroll, L. J., Cassidy, J. D., Holm, L., Kraus, J., Coronado, V. G., & WHO Collaborating Centre Task Force on Mild Traumatic Brain Injury (2004). Methodological issues and research recommendations for mild traumatic brain injury: the WHO Collaborating Centre Task Force on Mild Traumatic Brain Injury. *Journal of rehabilitation medicine*, 43(Suppl), 113–125. <https://doi.org/10.1080/16501960410023877>
- Cernak I. (2005). Animal models of head trauma. *NeuroRx : the journal of the American Society for Experimental NeuroTherapeutics*, 2(3), 410–422. <https://doi.org/10.1602/neurorx.2.3.410>

- Champagne, A. A., Coverdale, N. S., Germuska, M., Bhogal, A. A., & Cook, D. J. (2020). Changes in volumetric and metabolic parameters relate to differences in exposure to sub-concussive head impacts. *Journal of Cerebral Blood Flow and Metabolism*, 40(7), 1453–1467. <https://doi.org/10.1177/0271678X19862861>
- Chen, Y., Dai, Z., Fan, R., Mikulis, D. J., Qiu, J., Shen, Z., Wang, R., Lai, L., Tang, Y., Li, Y., Jia, Y., Yan, G., & Wu, R. (2020). Glymphatic System Visualized by Chemical-Exchange-Saturation-Transfer Magnetic Resonance Imaging. *ACS Chemical Neuroscience*, 11(13), 1978–1984. <https://doi.org/10.1021/acscchemneuro.0c00222>
- Chiu, C. C., Liao, Y. E., Yang, L. Y., Wang, J. Y., Tweedie, D., Karnati, H. K., Greig, N. H., & Wang, J. Y. (2016). Neuroinflammation in animal models of traumatic brain injury. *Journal of Neuroscience Methods*, 272, 38–49. <https://doi.org/10.1016/j.jneumeth.2016.06.018>
- Christensen, J., Wright, D. K., Yamakawa, G. R., Shultz, S. R., & Mychasiuk, R. (2020). Repetitive Mild Traumatic Brain Injury Alters Glymphatic Clearance Rates in Limbic Structures of Adolescent Female Rats. *Scientific Reports*, 10(1). <https://doi.org/10.1038/s41598-020-63022-7>
- Chun, I. Y., Mao, X., Breedlove, E. L., Leverenz, L. J., Nauman, E. A., & Talavage, T. M. (2015). DTI detection of longitudinal WM abnormalities due to accumulated head impacts. *Developmental Neuropsychology*, 40(2), 92–97. <https://doi.org/10.1080/87565641.2015.1020945>
- Cole, J. H., Jolly, A., de Simoni, S., Bourke, N., Patel, M. C., Scott, G., & Sharp, D. J. (2018). Spatial patterns of progressive brain volume loss after moderate-severe traumatic brain injury. *Brain*, 141(3), 822–836. <https://doi.org/10.1093/brain/awx354>
- Conti, A. C., Raghupathi, R., Trojanowski, J. Q., & McIntosh, T. K. (1998). Experimental brain injury induces regionally distinct apoptosis during the acute and delayed post-traumatic period. *The Journal of neuroscience : the official journal of the Society for Neuroscience*, 18(15), 5663–5672. <https://doi.org/10.1523/JNEUROSCI.18-15-05663.1998>
- Corrigan, F., Ziebell, J. M., & Vink, R. (2011). Models of rodent cortical traumatic brain injury. *Neuromethods*, 62, 193–209. https://doi.org/10.1007/978-1-61779-301-1_11
- Costa, M. R., Götz, M., & Berninger, B. (2010). What determines neurogenic competence in glia? *Brain Research Reviews*, 63(1–2), 47–59. <https://doi.org/10.1016/j.brainresrev.2010.01.002>
- Cummiskey, B., Sankaran, G. N., McIver, K. G., Shyu, D., Markel, J., Talavage, T. M., Leverenz, L., Meyer, J. J., Adams, D., & Nauman, E. A. (2019). Quantitative evaluation of impact attenuation by football helmets using a modal impulse hammer. *Proceedings of the Institution of Mechanical Engineers, Part P: Journal of Sports Engineering and Technology*, 233(2), 301–311. <https://doi.org/10.1177/1754337118823603>

- Daneshvar, D. H., Baugh, C. M., Nowinski, C. J., McKee, A. C., Stern, R. A., & Cantu, R. C. (2011). Helmets and Mouth Guards: The Role of Personal Equipment in Preventing Sport-Related Concussions. *Clinics in Sports Medicine*, 30(1), 145–163. <https://doi.org/10.1016/j.csm.2010.09.006>
- Daneshvar, D. H., Nowinski, C. J., McKee, A. C., & Cantu, R. C. (2011). The Epidemiology of Sport-Related Concussion. *Clinics in Sports Medicine*, 30(1), 1–17. <https://doi.org/10.1016/j.csm.2010.08.006>
- Das, A., Murphy, K., & Drew, P. J. (2021). Rude mechanicals in brain hemodynamics: non-neural actors that influence blood flow. *Philosophical Transactions of the Royal Society B: Biological Sciences*, 376(1815), 20190635. <https://doi.org/10.1098/rstb.2019.0635>
- Dashnaw, M. L., Petraglia, A. L., & Bailes, J. E. (2012). An overview of the basic science of concussion and subconcussion: where we are and where we are going. *Neurosurgical focus*, 33(6), 1–9. <https://doi.org/10.3171/2012.10.FOCUS12284>
- Davenport, E. M., Apkarian, K., Whitlow, C. T., Urban, J. E., Jensen, J. H., Szuch, E., Espeland, M. A., Jung, Y., Rosenbaum, D. A., Gioia, G. A., Powers, A. K., Stitzel, J. D., & Maldjian, J. A. (2016). Abnormalities in diffusional kurtosis metrics related to head impact exposure in a season of high school varsity football. *Journal of Neurotrauma*, 33(23), 2133–2146. <https://doi.org/10.1089/neu.2015.4267>
- Davenport, E. M., Urban, J. E., Mokhtari, F., Lowther, E. L., Van Horn, J. D., Vaughan, C. G., Gioia, G. A., Whitlow, C. T., Stitzel, J. D., & Maldjian, J. A. (2016). Subconcussive impacts and imaging findings over a season of contact sports. *Concussion (London, England)*, 1(4), CNC19. <https://doi.org/10.2217/cnc-2016-0003>
- Davenport, E. M., Whitlow, C. T., Urban, J. E., Espeland, M. A., Jung, Y., Rosenbaum, D. A., Gioia, G. A., Powers, A. K., Stitzel, J. D., & Maldjian, J. A. (2014). Abnormal white matter integrity related to head impact exposure in a season of high school varsity football. *Journal of Neurotrauma*, 31(19), 1617–1624. <https://doi.org/10.1089/neu.2013.3233>
- Davenport, N. D., Gullickson, J. T., Grey, S. F., Hirsch, S., & Sponheim, S. R. (2018). Longitudinal evaluation of ventricular volume changes associated with mild traumatic brain injury in military service members. *Brain Injury*, 32(10), 1245–1255. <https://doi.org/10.1080/02699052.2018.1494854>
- Dayon, L., Núñez Galindo, A., Wojcik, J., Cominetti, O., Corthésy, J., Oikonomidi, A., Henry, H., Kussmann, M., Migliavacca, E., Severin, I., Bowman, G. L., & Popp, J. (2018). Alzheimer disease pathology and the cerebrospinal fluid proteome. *Alzheimer's Research and Therapy*, 10(1). <https://doi.org/10.1186/s13195-018-0397-4>
- de Boer, R., Vrooman, H. A., Ikram, M. A., Vernooij, M. W., Breteler, M. M. B., van der Lugt, A., & Niessen, W. J. (2010). Accuracy and reproducibility study of automatic MRI brain tissue segmentation methods. *NeuroImage*, 51(3), 1047–1056. <https://doi.org/10.1016/j.neuroimage.2010.03.012>

- Dean, P. J., & Sterr, A. (2013). Long-term effects of mild traumatic brain injury on cognitive performance. *Frontiers in human neuroscience*, 7, 30. <https://doi.org/10.3389/fnhum.2013.00030>
- Dean, P. J. A., Sato, J. R., Vieira, G., McNamara, A., & Sterr, A. (2015). Multimodal imaging of mild traumatic brain injury and persistent postconcussion syndrome. *Brain and Behavior*, 5(1), 45–61. <https://doi.org/10.1002/brb3.292>
- Dean, P., Sato, J. R., Vieira, G., McNamara, A., & Sterr, A. (2015). Long-term structural changes after mTBI and their relation to post-concussion symptoms. *Brain injury*, 29(10), 1211–1218. <https://doi.org/10.3109/02699052.2015.1035334>
- DeSimone, J. C., Davenport, E. M., Urban, J., Xi, Y., Holcomb, J. M., Kelley, M. E., Whitlow, C. T., Powers, A. K., Stitzel, J. D., & Maldjian, J. A. (2021). Mapping default mode connectivity alterations following a single season of subconcussive impact exposure in youth football. *Human Brain Mapping*, 42(8), 2529–2545. <https://doi.org/10.1002/hbm.25384>
- di Virgilio, T. G., Ietswaart, M., Wilson, L., Donaldson, D. I., & Hunter, A. M. (2019). Understanding the Consequences of Repetitive Subconcussive Head Impacts in Sport: Brain Changes and Dampened Motor Control Are Seen After Boxing Practice. *Frontiers in Human Neuroscience*, 13. <https://doi.org/10.3389/fnhum.2019.00294>
- Diaz-de-Grenu, L. Z., Acosta-Cabronero, J., Williams, G. B., & Nestor, P. J. (2014). Comparing voxel-based iterative sensitivity and voxel-based morphometry to detect abnormalities in T2-weighted MRI. *NeuroImage*, 100, 379–384. <https://doi.org/10.1016/j.neuroimage.2014.06.030>
- Dickson, J. M., Weavers, H. M., Mitchell, N., Winter, E. M., Wilkinson, I. D., van Beek, E. J. R., Wild, J. M., & Griffiths, P. D. (2005). The effects of dehydration on brain volume - Preliminary results. *International Journal of Sports Medicine*, 26(6), 481–485. <https://doi.org/10.1055/s-2004-821318>
- Diotel, N., Lübke, L., Strähle, U., & Rastegar, S. (2020). Common and Distinct Features of Adult Neurogenesis and Regeneration in the Telencephalon of Zebrafish and Mammals. *Frontiers in neuroscience*, 14, 568930. <https://doi.org/10.3389/fnins.2020.568930>
- Dobrocky, T., Rebsamen, M., Rummel, C., Häni, L., Mordasini, P., Raabe, A., Ulrich, C. T., Gralla, J., Piechowiak, E. I., & Beck, J. (2020). Monro-kellie hypothesis: Increase of ventricular CSF volume after surgical closure of a spinal dural leak in patients with spontaneous intracranial hypotension. *American Journal of Neuroradiology*, 41(11), 2055–2061. <https://doi.org/10.3174/ajnr.A6782>
- Mac Donald, C. L., Dikranian, K., Song, S. K., Bayly, P. V., Holtzman, D. M., & Brody, D. L. (2007). Detection of traumatic axonal injury with diffusion tensor imaging in a mouse model of traumatic brain injury. *Experimental neurology*, 205(1), 116–131. <https://doi.org/10.1016/j.expneurol.2007.01.035>

- Dvorak, J., McCrory, P., & Kirkendall, D. T. (2007). Head injuries in the female football player: incidence, mechanisms, risk factors and management. *British journal of sports medicine*, 41(Suppl 1), i44–i46. <https://doi.org/10.1136/bjism.2007.037960>
- Eide, P. K., & Ringstad, G. (2019). Delayed clearance of cerebrospinal fluid tracer from entorhinal cortex in idiopathic normal pressure hydrocephalus: A glymphatic magnetic resonance imaging study. *Journal of Cerebral Blood Flow and Metabolism*, 39(7), 1355–1368. <https://doi.org/10.1177/0271678X18760974>
- Eierud, C., Craddock, R. C., Fletcher, S., Aulakh, M., King-Casas, B., Kuehl, D., & Laconte, S. M. (2014). Neuroimaging after mild traumatic brain injury: Review and meta-analysis. *NeuroImage: Clinical*, 4, 283–294. <https://doi.org/10.1016/j.nicl.2013.12.009>
- Eisele, A., Hill-Strathy, M., Michels, L., & Rauen, K. (2020). Magnetic Resonance Spectroscopy following Mild Traumatic Brain Injury: A Systematic Review and Meta-Analysis on the Potential to Detect Posttraumatic Neurodegeneration. *Neuro-degenerative diseases*, 20(1), 2–11. <https://doi.org/10.1159/000508098>
- Epstein, D. J., Legarreta, M., Bueler, E., King, J., McGlade, E., & Yurgelun-Todd, D. (2016). Orbitofrontal cortical thinning and aggression in mild traumatic brain injury patients. *Brain and Behavior*, 6(12). <https://doi.org/10.1002/brb3.581>
- Fehily, B., & Fitzgerald, M. (2017). Repeated mild traumatic brain injury: Potential mechanisms of damage. *Cell Transplantation*, 26(7), 1131–1155. <https://doi.org/10.1177/0963689717714092>
- Filipek, P. A., Kennedy, D. N., Caviness, V. S., Jr, Rossnick, S. L., Spraggins, T. A., & Starewicz, P. M. (1989). Magnetic resonance imaging-based brain morphometry: development and application to normal subjects. *Annals of neurology*, 25(1), 61–67. <https://doi.org/10.1002/ana.410250110>
- Fischer, T. D., Hylin, M. J., Zhao, J., Moore, A. N., Waxham, M. N., & Dash, P. K. (2016). Altered mitochondrial dynamics and TBI pathophysiology. *Frontiers in Systems Neuroscience*, 10(3). <https://doi.org/10.3389/fnsys.2016.00029>
- Fischer, T. D., Red, S. D., Chuang, A. Z., Jones, E. B., McCarthy, J. J., Patel, S. S., & Sereno, A. B. (2016). Detection of Subtle Cognitive Changes after mTBI Using a Novel Tablet-Based Task. *Journal of Neurotrauma*, 33(13), 1237–1246. <https://doi.org/10.1089/neu.2015.3990>
- Fisher, E., Lee, J. C., Nakamura, K., & Rudick, R. A. (2008). Gray matter atrophy in multiple sclerosis: A longitudinal study. *Annals of Neurology*, 64(3), 255–265. <https://doi.org/10.1002/ana.21436>
- Freeborough, P. A., & Fox, N. C. (1997). The boundary shift integral: an accurate and robust measure of cerebral volume changes from registered repeat MRI. *IEEE transactions on medical imaging*, 16(5), 623–629. <https://doi.org/10.1109/42.640753>

- Frintrop, L., Trinh, S., Liesbrock, J., Leunissen, C., Kempermann, J., Etdöger, S., Kas, M. J., Tolba, R., Heussen, N., Neulen, J., Konrad, K., Päfgen, V., Kiessling, F., Herpertz-Dahlmann, B., Beyer, C., & Seitz, J. (2019). The reduction of astrocytes and brain volume loss in anorexia nervosa—the impact of starvation and refeeding in a rodent model. *Translational Psychiatry*, 9(1). <https://doi.org/10.1038/s41398-019-0493-7>
- Fultz, N. E., Bonmassar, G., Setsompop, K., Stickgold, R. A., Rosen, B. R., Polimeni, J. R., & Lewis, L. D. (2019). Coupled electrophysiological, hemodynamic, and cerebrospinal fluid oscillations in human sleep. *Science (New York, N.Y.)*, 366(6465), 628–631. <https://doi.org/10.1126/science.aax5440>
- Gale, S. D., Baxter, L., Roundy, N., & Johnson, S. C. (2005). Traumatic brain injury and grey matter concentration: A preliminary voxel-based morphometry study. *Journal of Neurology, Neurosurgery and Psychiatry*, 76(7), 984–988. <https://doi.org/10.1136/jnnp.2004.036210>
- Garcia, M., Gloor, M., Bieri, O., Radue, E. W., Lieb, J. M., Cordier, D., & Stippich, C. (2015). Imaging of Primary Brain Tumors and Metastases with Fast Quantitative 3-Dimensional Magnetization Transfer. *Journal of neuroimaging*, 25(6), 1007–1014. <https://doi.org/10.1111/jon.12222>
- Gardner, R. C., & Yaffe, K. (2015). Epidemiology of mild traumatic brain injury and neurodegenerative disease. *Molecular and cellular neurosciences*, 66(PtB), 75–80. <https://doi.org/10.1016/j.mcn.2015.03.001>
- Gavett, B. E., Stern, R. A., & McKee, A. C. (2011). Chronic traumatic encephalopathy: a potential late effect of sport-related concussive and subconcussive head trauma. *Clinics in sports medicine*, 30(1), 179–xi. <https://doi.org/10.1016/j.csm.2010.09.007>
- Ge, Y., Grossman, R. I., Babb, J. S., Rabin, M. L., Mannon, L. J., & Kolson, D. L. (2002). Age-related total gray matter and white matter changes in normal adult brain. Part I: volumetric MR imaging analysis. *AJNR. American journal of neuroradiology*, 23(8), 1327–1333.
- Ghali, M. G. Z., & Ghali, G. Z. (2020). Mechanisms Contributing to the Generation of Mayer Waves. *Frontiers in Neuroscience*, 14, 1662-453X <https://doi.org/10.3389/fnins.2020.00395>
- Giorgio, A., & de Stefano, N. (2013). Clinical use of brain volumetry. *Journal of Magnetic Resonance Imaging*, 37(1), 1–14. <https://doi.org/10.1002/jmri.23671>
- Gispert, J. D., Reig, S., Pascau, J., Vaquero, J. J., García-Barreno, P., & Desco, M. (2004). Method for bias field correction of brain T1-weighted magnetic images minimizing segmentation error. *Human Brain Mapping*, 22(2), 133–144. <https://doi.org/10.1002/hbm.20013>
- Giuliani, N. R., Calhoun, V. D., Pearlson, G. D., Francis, A., & Buchanan, R. W. (2005). Voxel-based morphometry versus region of interest: A comparison of two methods for analyzing gray matter differences in schizophrenia. *Schizophrenia Research*, 74(2–3), 135–147. <https://doi.org/10.1016/j.schres.2004.08.019>

- Giza, C. C., & Hovda, D. A. (2014). The new neurometabolic cascade of concussion. *Neurosurgery*, 75, S24–S33. <https://doi.org/10.1227/NEU.0000000000000505>
- Gong, N. J., Kuzminski, S., Clark, M., Fraser, M., Sundman, M., Guskiewicz, K., Petrella, J. R., & Liu, C. (2018). Microstructural alterations of cortical and deep gray matter over a season of high school football revealed by diffusion kurtosis imaging. *Neurobiology of Disease*, 119, 79–87. <https://doi.org/10.1016/j.nbd.2018.07.020>
- Good, C. D., Johnsrude, I. S., Ashburner, J., Henson, R. N. A., Friston, K. J., & Frackowiak, R. S. J. (2001). A voxel-based morphometric study of ageing in 465 normal adult human brains. *Neuroimage*, 14(1), 21–36. <https://doi.org/10.1006/nimg.2001.0786>
- Guskiewicz, K. M., Bruce, S. L., Cantu, R. C., Ferrara, M. S., Kelly, J. P., McCrea, M., Putukian, M., & McLeod, T. C. V. (2006). Research based recommendations on management of sport related concussion: Summary of the National Athletic Trainers' Association position statement. *British Journal of Sports Medicine*, 40(1), 6–11. <https://doi.org/10.1136/bjsm.2005.021683>
- Guskiewicz, K. M., Bruce, S. L., Cantu, R. C., Ferrara, M. S., Kelly, J. P., McCrea, M., Putukian, M., & Valovich McLeod, T. C. (2004). National Athletic Trainers' Association Position Statement: Management of Sport-Related Concussion. *Journal of athletic training*, 39(3), 280–297.
- Gysland, S. M., Mihalik, J. P., Register-Mihalik, J. K., Trulock, S. C., Shields, E. W., & Guskiewicz, K. M. (2012). The relationship between subconcussive impacts and concussion history on clinical measures of neurologic function in collegiate football players. *Annals of Biomedical Engineering*, 40(1), 14–22. <https://doi.org/10.1007/s10439-011-0421-3>
- Harris, J. L., Choi, I. Y., & Brooks, W. M. (2015). Probing astrocyte metabolism in vivo: Proton magnetic resonance spectroscopy in the injured and aging brain. *Frontiers in Aging Neuroscience*, 7(10). <https://doi.org/10.3389/fnagi.2015.00202>
- Harris, T. C., de Rooij, R., & Kuhl, E. (2019). The Shrinking Brain: Cerebral Atrophy Following Traumatic Brain Injury. *Annals of Biomedical Engineering*, 47(9), 1941–1959. <https://doi.org/10.1007/s10439-018-02148-2>
- Haug H. (1986). History of neuromorphometry. *Journal of neuroscience methods*, 18(1-2), 1–17. [https://doi.org/10.1016/0165-0270\(86\)90110-x](https://doi.org/10.1016/0165-0270(86)90110-x)
- Henninger, N., Dützmänn, S., Sicard, K. M., Kollmar, R., Bardutzky, J., & Schwab, S. (2005). Impaired spatial learning in a novel rat model of mild cerebral concussion injury. *Experimental Neurology*, 195(2), 447–457. <https://doi.org/10.1016/j.expneurol.2005.06.013>
- Hevia-Montiel, N., Rodriguez-Perez, P. I., Lamothe-Molina, P. J., Arellano-Reynoso, A., Bribiesca, E., & Alegria-Loyola, M. A. (2015). Neuromorphometry of primary brain tumors by magnetic resonance imaging. *Journal of Medical Imaging*, 2(2), 024503. <https://doi.org/10.1117/1.jmi.2.2.024503>

- Hootman, J. M., Dick, R., & Agel, J. (2007). Epidemiology of collegiate injuries for 15 sports: summary and recommendations for injury prevention initiatives. *Journal of athletic training*, 42(2), 311–319.
- Horie, T., Kajihara, N., Matsumae, M., Obara, M., Hayashi, N., Hirayama, A., Takizawa, K., Takahara, T., Yatsushiro, S., & Kuroda, K. (2017). Magnetic Resonance Imaging Technique for Visualization of Irregular Cerebrospinal Fluid Motion in the Ventricular System and Subarachnoid Space. *World Neurosurgery*, 97, 523–531. <https://doi.org/10.1016/j.wneu.2016.07.062>
- Howden, L., Giddings, D., Power, H., Aroussi, A., Vloeberghs, M., Garnett, M., & Walker, D. (2008). Three-dimensional cerebrospinal fluid flow within the human ventricular system. *Computer Methods in Biomechanics and Biomedical Engineering*, 11(2), 123–133. <https://doi.org/10.1080/10255840701492118>
- Hunter, J. V., Wilde, E. A., Tong, K. A., & Holshouser, B. A. (2012). Emerging imaging tools for use with traumatic brain injury research. *Journal of Neurotrauma*, 29(4), 654–671. <https://doi.org/10.1089/neu.2011.1906>
- Hunter, L. E., Branch, C. A., & Lipton, M. L. (2019). The neurobiological effects of repetitive head impacts in collision sports. *Neurobiology of Disease*, 123, 122–126. <https://doi.org/10.1016/j.nbd.2018.06.016>
- Iliff, J. J., Wang, M., Liao, Y., Plogg, B. A., Peng, W., Gundersen, G. A., Benveniste, H., Vates, G. E., Deane, R., Goldman, S. A., Nagelhus, E. A., & Nedergaard, M. (2012). A paravascular pathway facilitates CSF flow through the brain parenchyma and the clearance of interstitial solutes, including amyloid β . *Science Translational Medicine*, 4(147). <https://doi.org/10.1126/scitranslmed.3003748>
- Irimia, A., Wang, B., Aylward, S. R., Prastawa, M. W., Pace, D. F., Gerig, G., Hovda, D. A., Kikinis, R., Vespa, P. M., & van Horn, J. D. (2012). Neuroimaging of structural pathology and connectomics in traumatic brain injury: Toward personalized outcome prediction. *NeuroImage: Clinical*, 1(1), 1–17. <https://doi.org/10.1016/j.nicl.2012.08.002>
- Jadischke, R., Viano, D. C., Dau, N., King, A. I., & McCarthy, J. (2013). On the accuracy of the Head Impact Telemetry (HIT) System used in football helmets. *Journal of biomechanics*, 46(13), 2310–2315. <https://doi.org/10.1016/j.jbiomech.2013.05.030>
- Jang, I., Chun, I. Y., Brosch, J. R., Bari, S., Zou, Y., Cummiskey, B. R., Lee, T. A., Lycke, R. J., Poole, V. N., Shenk, T. E., Svaldi, D. O., Tamer, G. G., Dydak, U., Leverenz, L. J., Nauman, E. A., & Talavage, T. M. (2019b). Every hit matters: White matter diffusivity changes in high school football athletes are correlated with repetitive head acceleration event exposure. *NeuroImage: Clinical*, 24. <https://doi.org/10.1016/j.nicl.2019.101930>
- Jessen, N. A., Munk, A. S. F., Lundgaard, I., & Nedergaard, M. (2015). The Glymphatic System: A Beginner's Guide. *Neurochemical Research*, 40(12), 2583–2599. <https://doi.org/10.1007/s11064-015-1581-6>

- Ji, S., Ghadyani, H., Bolander, R. P., Beckwith, J. G., Ford, J. C., McAllister, T. W., Flashman, L. A., Paulsen, K. D., Ernstrom, K., Jain, S., Raman, R., Zhang, L., & Greenwald, R. M. (2014). Parametric comparisons of intracranial mechanical responses from three validated finite element models of the human head. *Annals of Biomedical Engineering*, 42(1), 11–24. <https://doi.org/10.1007/s10439-013-0907-2>
- Johanson, C., Stopa, E., Baird, A., & Sharma, H. (2011). Traumatic brain injury and recovery mechanisms: Peptide modulation of periventricular neurogenic regions by the choroid plexus-CSF nexus. *Journal of Neural Transmission*, 118(1), 115–133. <https://doi.org/10.1007/s00702-010-0498-0>
- Johnson, B., Zhang, K., Gay, M., Neuberger, T., Horovitz, S., Hallett, M., Sebastianelli, W., & Slobounov, S. (2012). Metabolic alterations in corpus callosum may compromise brain functional connectivity in MTBI patients: An 1H-MRS study. *Neuroscience Letters*, 509(1), 5–8. <https://doi.org/10.1016/j.neulet.2011.11.013>
- Kalisvaart, A. C. J., Wilkinson, C. M., Gu, S., Kung, T. F. C., Yager, J., Winship, I. R., van Landeghem, F. K. H., & Colbourne, F. (2020). An update to the Monro–Kellie doctrine to reflect tissue compliance after severe ischemic and hemorrhagic stroke. *Scientific Reports*, 10(1). <https://doi.org/10.1038/s41598-020-78880-4>
- Kane, M. J., Angoa-Pérez, M., Briggs, D. I., Viano, D. C., Kreipke, C. W., & Kuhn, D. M. (2012). A mouse model of human repetitive mild traumatic brain injury. *Journal of Neuroscience Methods*, 203(1), 41–49. <https://doi.org/10.1016/j.jneumeth.2011.09.003>
- Karimy, J. K., Zhang, J., Kurland, D. B., Theriault, B. C., Duran, D., Stokum, J. A., Furey, C. G., Zhou, X., Mansuri, M. S., Montejo, J., Vera, A., DiLuna, M. L., Delpire, E., Alper, S. L., Gunel, M., Gerzanich, V., Medzhitov, R., Simard, J. M., & Kahle, K. T. (2017). Inflammation-dependent cerebrospinal fluid hypersecretion by the choroid plexus epithelium in posthemorrhagic hydrocephalus. *Nature medicine*, 23(8), 997–1003. <https://doi.org/10.1038/nm.4361>
- Kempton, M. J., Ettinger, U., Foster, R., Williams, S. C. R., Calvert, G. A., Hampshire, A., Zelaya, F. O., O’Gorman, R. L., McMorris, T., Owen, A. M., & Smith, M. S. (2011). Dehydration affects brain structure and function in healthy adolescents. *Human Brain Mapping*, 32(1), 71–79. <https://doi.org/10.1002/hbm.20999>
- Kennedy, D. N., Makris, N., Herbert, M. R., Takahashi, T., & Caviness, V. S., Jr. (2002). Basic principles of MRI and morphometry studies of human brain development. *Developmental Science*, 5(3), 268–278. <https://doi.org/10.1111/1467-7687.00366>
- Khong, E., Odenwald, N., Hashim, E., & Cusimano, M. D. (2016). Diffusion Tensor Imaging Findings in Post-Concussion Syndrome Patients after Mild Traumatic Brain Injury: A Systematic Review. *Frontiers in neurology*, 7, 156. <https://doi.org/10.3389/fneur.2016.00156>
- Khurana, V. G., & Kaye, A. H. (2012). An overview of concussion in sport. *Journal of clinical neuroscience : official journal of the Neurosurgical Society of Australasia*, 19(1), 1–11. <https://doi.org/10.1016/j.jocn.2011.08.002>

- King, D. A., Hume, P. A., Gissane, C., & Clark, T. N. (2016). Similar head impact acceleration measured using instrumented ear patches in a junior rugby union team during matches in comparison with other sports. *Journal of Neurosurgery: Pediatrics*, 18(1), 65–72. <https://doi.org/10.3171/2015.12.PEDS15605>
- King, D., Brughelli, M., Hume, P., & Gissane, C. (2014). Assessment, management and knowledge of sport-related concussion: Systematic review. *Sports Medicine*, 44(4), 449–471. <https://doi.org/10.1007/s40279-013-0134-x>
- King, D., Hume, P., Gissane, C., Brughelli, M., & Clark, T. (2016). The Influence of Head Impact Threshold for Reporting Data in Contact and Collision Sports: Systematic Review and Original Data Analysis. *Sports Medicine*, 46(2), 151–169. <https://doi.org/10.1007/s40279-015-0423-7>
- Koerte, I. K., Esopenko, C., Hinds, S. R., Shenton, M. E., Bonke, E. M., Bazarian, J. J., Bickart, K. C., Bigler, E. D., Bouix, S., Buckley, T. A., Choe, M. C., Echlin, P. S., Gill, J., Giza, C. C., Hayes, J., Hodges, C. B., Irimia, A., Johnson, P. K., Kenney, K., ... Baron, D. (2021). The ENIGMA sports injury working group:– an international collaboration to further our understanding of sport-related brain injury. *Brain Imaging and Behavior*, 15(2), 576–584. <https://doi.org/10.1007/s11682-020-00370-y>
- Koerte, I. K., Lin, A. P., Muehlmann, M., Merugumala, S., Liao, H., Starr, T., Kaufmann, D., Mayinger, M., Steffinger, D., Fisch, B., Karch, S., Heinen, F., Ertl-Wagner, B., Reiser, M., Stern, R. A., Zafonte, R., & Shenton, M. E. (2015). Altered Neurochemistry in Former Professional Soccer Players without a History of Concussion. *Journal of Neurotrauma*, 32(17), 1287–1293. <https://doi.org/10.1089/neu.2014.3715>
- Kou, Z., & Iraj, A. (2014). Imaging brain plasticity after trauma. *Neural Regeneration Research*, 9(7), 693–700. <https://doi.org/10.4103/1673-5374.131568>
- Kou, Z., & VandeVord, P. J. (2014). Traumatic white matter injury and glial activation: From basic science to clinics. *Glia*, 62(11), 1831–1855. <https://doi.org/10.1002/glia.22690>
- Kou, Z., Wu, Z., Tong, K. A., Holshouser, B., Benson, R. R., Hu, J., & Haacke, E. M. (2010). The role of advanced MR imaging findings as biomarkers of traumatic brain injury. *The Journal of head trauma rehabilitation*, 25(4), 267–282. <https://doi.org/10.1097/HTR.0b013e3181e54793>
- Langlois, J. A., Rutland-Brown, W., & Wald, M. M. (2006). The epidemiology and impact of traumatic brain injury: a brief overview. *The Journal of head trauma rehabilitation*, 21(5), 375–378. <https://doi.org/10.1097/00001199-200609000-00001>
- Lannsjö, M., Raininko, R., Bustamante, M., Seth, C. von, & Borg, J. (2013). Brain pathology after mild traumatic brain injury: An exploratory study by repeated magnetic resonance examination. *Journal of Rehabilitation Medicine*, 45(8), 721–728. <https://doi.org/10.2340/16501977-1169>

- Ledig, C., Kamnitsas, K., Koikkalainen, J., Posti, J. P., Takala, R. S. K., Katila, A., Frantzén, J., Ala-Seppälä, H., Kyllönen, A., Maanpää, H. R., Tallus, J., Lötjönen, J., Glocker, B., Tenovuo, O., & Rueckert, D. (2017). Regional brain morphometry in patients with traumatic brain injury based on acute- and chronic-phase magnetic resonance imaging. *Plos one*, 12(11). <https://doi.org/10.1371/journal.pone.0188152>
- Lee, H., Wintermark, M., Gean, A. D., Ghajar, J., Manley, G. T., & Mukherjee, P. (2008). Focal lesions in acute mild traumatic brain injury and neurocognitive outcome: CT versus 3T MRI. *Journal of Neurotrauma*, 25(9), 1049–1056. <https://doi.org/10.1089/neu.2008.0566>
- Lee, Y. K., Hou, S. W., Lee, C. C., Hsu, C. Y., Huang, Y. S., & Su, Y. C. (2013). Increased Risk of Dementia in Patients with Mild Traumatic Brain Injury: A Nationwide Cohort Study. *Plos one*, 8(5). <https://doi.org/10.1371/journal.pone.0062422>
- Lefebvre, G., Chamard, E., Proulx, S., Tremblay, S., Halko, M., Soman, S., de Guise, E., Pascual-Leone, A., & Théoret, H. (2018). Increased myo-inositol in primary motor cortex of contact sports athletes without a history of concussion. *Journal of Neurotrauma*, 35(7), 953–962. <https://doi.org/10.1089/neu.2017.5254>
- Leker, R. R., & Shohami, E. (2002). Cerebral ischemia and trauma-different etiologies yet similar mechanisms: neuroprotective opportunities. *Brain research. Brain research reviews*, 39(1), 55–73. [https://doi.org/10.1016/s0165-0173\(02\)00157-1](https://doi.org/10.1016/s0165-0173(02)00157-1)
- Lenroot, R. K., Gogtay, N., Greenstein, D. K., Wells, E. M., Wallace, G. L., Clasen, L. S., Blumenthal, J. D., Lerch, J., Zijdenbos, A. P., Evans, A. C., Thompson, P. M., & Giedd, J. N. (2007). Sexual dimorphism of brain developmental trajectories during childhood and adolescence. *NeuroImage*, 36(4), 1065–1073. <https://doi.org/10.1016/j.neuroimage.2007.03.053>
- Levine, B., Fujiwara, E., O'Connor, C., Richard, N., Kovacevic, N., Mandic, M., Restagno, A., Easdon, C., Robertson, I. H., Graham, S. J., Cheung, G., Gao, F., Schwartz, M. L., & Black, S. E. (2006). In vivo characterization of traumatic brain injury neuropathology with structural and functional neuroimaging. *Journal of neurotrauma*, 23(10), 1396–1411. <https://doi.org/10.1089/neu.2006.23.1396>
- Li, L., Chopp, M., Ding, G., Davoodi-Bojd, E., Zhang, L., Li, Q., Zhang, Y., Xiong, Y., & Jiang, Q. (2020). MRI detection of impairment of glymphatic function in rat after mild traumatic brain injury. *Brain Research*, 1747, 147062. <https://doi.org/10.1016/j.brainres.2020.147062>
- Lin, A. P., Ramadan, S., Stern, R. A., Box, H. C., Nowinski, C. J., Ross, B. D., & Mountford, C. E. (2015). Changes in the neurochemistry of athletes with repetitive brain trauma: Preliminary results using localized correlated spectroscopy. *Alzheimer's Research and Therapy*, 7(1). <https://doi.org/10.1186/s13195-015-0094-5>
- Lincoln, A. E., Caswell, S. V., Almquist, J. L., Dunn, R. E., Norris, J. B., & Hinton, R. Y. (2011). Trends in Concussion Incidence in High School Sports: A Prospective 11-Year Study. *The American Journal of Sports Medicine*, 39(5), 958–963. <https://doi.org/10.1177/0363546510392326>

- Lindfors, C., Nilsson, I. A. K., Garcia-Roves, P. M., Zuberi, A. R., Karimi, M., Donahue, L. R., Roopenian, D. C., Mulder, J., Uhlén, M., Ekström, T. J., Davisson, M. T., Hökfelt, T. G. M., Schalling, M., & Johansen, J. E. (2011). Hypothalamic mitochondrial dysfunction associated with anorexia in the anx/anx mouse. *Proceedings of the National Academy of Sciences of the United States of America*, 108(44), 18108–18113. <https://doi.org/10.1073/pnas.1114863108>
- Ling, J. M., Klimaj, S., Toulouse, T., & Mayer, A. R. (2013). A prospective study of gray matter abnormalities in mild traumatic brain injury. *Neurology*, 81(24), 2121–2127. <https://doi.org/10.1212/01.wnl.0000437302.36064.b1>
- Lipton, M. L., Kim, N., Zimmerman, M. E., Kim, M., Stewart, W. F., Branch, C. A., & Lipton, R. B. (2013). Soccer heading is associated with white matter microstructural and cognitive abnormalities. *Radiology*, 268(3), 850–857. <https://doi.org/10.1148/radiol.13130545>
- Luo, J., Nguyen, A., Villeda, S., Zhang, H., Ding, Z., Lindsey, D., Bieri, G., Castellano, J. M., Beaupre, G. S., & Wyss-Coray, T. (2014). Long-term cognitive impairments and pathological alterations in a mouse model of repetitive mild traumatic brain injury. *Frontiers in Neurology*, 5(2). <https://doi.org/10.3389/fneur.2014.00012>
- MacKenzie, J. D., Siddiqi, F., Babb, J. S., Bagley, L. J., Mannon, L. J., Sinson, G. P., & Grossman, R. I. (2002). Brain atrophy in mild or moderate traumatic brain injury: a longitudinal quantitative analysis. *AJNR. American journal of neuroradiology*, 23(9), 1509–1515.
- Maher, M. E., Hutchison, M., Cusimano, M., Comper, P., & Schweizer, T. A. (2014). Concussions and heading in soccer: A review of the evidence of incidence, mechanisms, biomarkers and neurocognitive outcomes. *Brain Injury*, 28(3), 271–285. <https://doi.org/10.3109/02699052.2013.865269>
- Mainwaring, L., Ferdinand Pennock, K. M., Mylabathula, S., & Alavie, B. Z. (2018). Subconcussive head impacts in sport: A systematic review of the evidence. *International Journal of Psychophysiology*, 132, 39–54. <https://doi.org/10.1016/j.ijpsycho.2018.01.007>
- Marchi, N., Bazarian, J. J., Puvenna, V., Janigro, M., Ghosh, C., Zhong, J., Zhu, T., Blackman, E., Stewart, D., Ellis, J., Butler, R., & Janigro, D. (2013). Consequences of Repeated Blood-Brain Barrier Disruption in Football Players. *Plos one*, 8(3). <https://doi.org/10.1371/journal.pone.0056805>
- Masoumi, N., Framanzad, F., Zamanian, B., Seddighi, A. S., Moosavi, M. H., Najarian, S., & Bastani, D. (2013). 2D Computational Fluid Dynamic Modeling of Human Ventricle System Based on Fluid-Solid Interaction and Pulsatile Flow. *Basic and clinical neuroscience*, 4(1), 64–75.
- Matsumae, M., Hirayama, A., Atsumi, H., Yatsushiro, S., & Kuroda, K. (2014). Velocity and pressure gradients of cerebrospinal fluid assessed with magnetic resonance imaging - Clinical article. *Journal of Neurosurgery*, 120(1), 218–227. <https://doi.org/10.3171/2013.7.JNS121859>

- Matsumae, M., Kuroda, K., Yatsushiro, S., Hirayama, A., Hayashi, N., Takizawa, K., Atsumi, H., & Sorimachi, T. (2019). Changing the currently held concept of cerebrospinal fluid dynamics based on shared findings of cerebrospinal fluid motion in the cranial cavity using various types of magnetic resonance imaging techniques. *Neurologia Medico-Chirurgica*, 59(4), 133–146. <https://doi.org/10.2176/nmc.ra.2018-0272>
- Mccrory, P., Matser, E., Cantu, R., & Ferrigno, M. (2004). Football neurology. *Neurology*, 3(7), 435-440. <http://neurology.thelancet.com>
- McCrory, P., Davis, G., & Makdissi, M. (2012). Second impact syndrome or cerebral swelling after sporting head injury. *Current sports medicine reports*, 11(1), 21–23. <https://doi.org/10.1249/JSR.0b013e3182423bfd>
- McCrory, P., Meeuwisse, W. H., Echemendia, R. J., Iverson, G. L., Dvořák, J., & Kutcher, J. S. (2013). What is the lowest threshold to make a diagnosis of concussion? *British Journal of Sports Medicine*, 47(5), 268–271. <https://doi.org/10.1136/bjsports-2013-092247>
- McCuen, E., Svaldi, D., Breedlove, K., Kraz, N., Cummiskey, B., Breedlove, E. L., Traver, J., Desmond, K. F., Hannemann, R. E., Zanath, E., Guerra, A., Leverenz, L., Talavage, T. M., & Nauman, E. A. (2015). Collegiate women's soccer players suffer greater cumulative head impacts than their high school counterparts. *Journal of Biomechanics*, 48(13), 3720–3723. <https://doi.org/10.1016/j.jbiomech.2015.08.003>
- McDonald, B. C., Saykin, A. J., & McAllister, T. W. (2012). Functional MRI of mild traumatic brain injury (mTBI): Progress and perspectives from the first decade of studies. *Brain Imaging and Behavior*, 6(2), 193–207. <https://doi.org/10.1007/s11682-012-9173-4>
- Mckee, A. C., & Daneshvar, D. H. (2015). The neuropathology of traumatic brain injury. *Handbook of Clinical Neurology*, 127, 45–66. <https://doi.org/10.1016/B978-0-444-52892-6.00004-0>
- McKee, A. C., Alosco, M. L., & Huber, B. R. (2016). Repetitive Head Impacts and Chronic Traumatic Encephalopathy. *Neurosurgery Clinics of North America*, 27(4), 529–535. <https://doi.org/10.1016/j.nec.2016.05.009>
- McKee, A. C., Cantu, R. C., Nowinski, C. J., Hedley-Whyte, E. T., Gavett, B. E., Budson, A. E., Santini, V. E., Lee, H. S., Kubilus, C. A., & Stern, R. A. (2009). Chronic traumatic encephalopathy in athletes: progressive tauopathy after repetitive head injury. *Journal of neuropathology and experimental neurology*, 68(7), 709–735. <https://doi.org/10.1097/NEN.0b013e3181a9d503>
- Meier, T. B., Brummel, B. J., Singh, R., Nerio, C. J., Polanski, D. W., & Bellgowan, P. S. F. (2015). The underreporting of self-reported symptoms following sports-related concussion. *Journal of Science and Medicine in Sport*, 18(5), 507–511. <https://doi.org/10.1016/j.jsams.2014.07.008>

- Meier, T. B., Nelson, L. D., Huber, D. L., Bazarian, J. J., Hayes, R. L., & McCrea, M. A. (2017). Prospective Assessment of Acute Blood Markers of Brain Injury in Sport-Related Concussion. *Journal of neurotrauma*, 34(22), 3134–3142. <https://doi.org/10.1089/neu.2017.5046>
- Messé, A., Caplain, S., Paradot, G., Garrigue, D., Mineo, J. F., Soto Ares, G., Ducreux, D., Vignaud, F., Rozec, G., Desal, H., Pélégri-issac, M., Montreuil, M., Benali, H., & Lehericy, S. (2011). Diffusion tensor imaging and white matter lesions at the subacute stage in mild traumatic brain injury with persistent neurobehavioral impairment. *Human Brain Mapping*, 32(6), 999–1011. <https://doi.org/10.1002/hbm.21092>
- Mestre, H., Mori, Y., & Nedergaard, M. (2020). The Brain's Glymphatic System: Current Controversies. *Trends in Neurosciences*, 43(7), 458–466. <https://doi.org/10.1016/j.tins.2020.04.003>
- Meysami, S., Raji, C. A., Merrill, D. A., Porter, V. R., & Mendez, M. F. (2019). MRI Volumetric Quantification in Persons with a History of Traumatic Brain Injury and Cognitive Impairment. *Journal of Alzheimer's Disease*, 72(1), 293–300. <https://doi.org/10.3233/JAD-190708>
- Mietchen, D., & Gaser, C. (2009). Computational morphometry for detecting changes in brain structure due to development, aging, learning, disease and evolution. *Frontiers in neuroinformatics*, 3, 25. <https://doi.org/10.3389/neuro.11.025.2009>
- Mihalik, J. P., Lynall, R. C., Teel, E. F., & Carneiro, K. A. (2014). Concussion management in soccer. *Journal of Sport and Health Science*, 3(4), 307–313. <https://doi.org/10.1016/j.jshs.2014.07.005>
- Mills, A. F., Sakai, O., Anderson, S. W., & Jara, H. (2017). Principles of quantitative MR imaging with illustrated review of applicable modular pulse diagrams. *Radiographics*, 37(7), 2083–2105. <https://doi.org/10.1148/rg.2017160099>
- Mills, B. D., Goubran, M., Parivash, S. N., Dennis, E. L., Rezaii, P., Akers, C., Bian, W., Mitchell, L. A., Boldt, B., Douglas, D., Sami, S., Mouchawar, N., Wilson, E. W., DiGiacomo, P., Parekh, M., Do, H., Lopez, J., Rosenberg, J., Camarillo, D., ... Zeineh, M. (2020). Longitudinal alteration of cortical thickness and volume in high-impact sports. *NeuroImage*, 217. <https://doi.org/10.1016/j.neuroimage.2020.116864>
- Mokri B. (2001). The Monro-Kellie hypothesis: applications in CSF volume depletion. *Neurology*, 56(12), 1746–1748. <https://doi.org/10.1212/wnl.56.12.1746>
- Moore, R. D., Lepine, J., & Ellemberg, D. (2017). The independent influence of concussive and sub-concussive impacts on soccer players' neurophysiological and neuropsychological function. *International Journal of Psychophysiology*, 112, 22–30. <https://doi.org/10.1016/j.ijpsycho.2016.11.011>

- Mori, S., Oishi, K., Jiang, H., Jiang, L., Li, X., Akhter, K., Hua, K., Faria, A. V., Mahmood, A., Woods, R., Toga, A. W., Pike, G. B., Neto, P. R., Evans, A., Zhang, J., Huang, H., Miller, M. I., van Zijl, P., & Mazziotta, J. (2008). Stereotaxic white matter atlas based on diffusion tensor imaging in an ICBM template. *NeuroImage*, 40(2), 570–582. <https://doi.org/10.1016/j.neuroimage.2007.12.035>
- Mouzon, B. C., Bachmeier, C., Ferro, A., Ojo, J. O., Crynen, G., Acker, C. M., Davies, P., Mullan, M., Stewart, W., & Crawford, F. (2014). Chronic neuropathological and neurobehavioral changes in a repetitive mild traumatic brain injury model. *Annals of Neurology*, 75(2), 241–254. <https://doi.org/10.1002/ana.24064>
- Munce, T. A., Dorman, J. C., Odney, T. O., Thompson, P. A., Valentine, V. D., & Bergeron, M. F. (2014). Effects of youth football on selected clinical measures of neurologic function: A pilot study. *Journal of Child Neurology*, 29(12), 1601–1607. <https://doi.org/10.1177/0883073813509887>
- Murphy, K., & Fox, M. D. (2017). Towards a consensus regarding global signal regression for resting state functional connectivity MRI. *NeuroImage*, 154, 169–173. <https://doi.org/10.1016/j.neuroimage.2016.11.052>
- Nakamura, K., Guizard, N., Fonov, V. S., Narayanan, S., Collins, D. L., & Arnold, D. L. (2014). Jacobian integration method increases the statistical power to measure gray matter atrophy in multiple sclerosis. *NeuroImage: Clinical*, 4, 10–17. <https://doi.org/10.1016/j.nicl.2013.10.015>
- Narayana, P. A., Yu, X., Hasan, K. M., Wilde, E. A., Levin, H. S., Hunter, J. v., Miller, E. R., Patel, V. K. S., Robertson, C. S., & McCarthy, J. J. (2015). Multi-modal MRI of mild traumatic brain injury. *NeuroImage: Clinical*, 7, 87–97. <https://doi.org/10.1016/j.nicl.2014.07.010>
- Narayanan, S., Nakamura, K., Fonov, V. S., Maranzano, J., Caramanos, Z., Giacomini, P. S., Collins, D. L., & Arnold, D. L. (2020). Brain volume loss in individuals over time: Source of variance and limits of detectability. *NeuroImage*, 214. <https://doi.org/10.1016/j.neuroimage.2020.116737>
- Nauman, E. A., & Talavage, T. M. (2018). Subconcussive trauma. *Handbook of Clinical Neurology*, 158, 245–255. <https://doi.org/10.1016/B978-0-444-63954-7.00024-0>
- Nauman, E. A., Breedlove, K. M., Breedlove, E. L., Talavage, T. M., Robinson, M. E., & Leverenz, L. J. (2015). Post-season neurophysiological deficits assessed by ImPACT and fMRI in athletes competing in American football. *Developmental Neuropsychology*, 40(2), 85–91. <https://doi.org/10.1080/87565641.2015.1016161>
- Nauman, E. A., Talavage, T. M., & Auerbach, P. S. (2020). Mitigating the Consequences of Subconcussive Head Injuries. *Annual review of biomedical engineering*, 22, 387–407. <https://doi.org/10.1146/annurev-bioeng-091219-053447>
- Neselius, S., Brisby, H., Theodorsson, A., Blennow, K., Zetterberg, H., & Marcusson, J. (2012). Csf-biomarkers in olympic boxing: Diagnosis and effects of repetitive head trauma. *Plos one*, 7(4). <https://doi.org/10.1371/journal.pone.0033606>

- Nishida, M., Makris, N., Kennedy, D. N., Vangel, M., Fischl, B., Krishnamoorthy, K. S., Caviness, V. S., & Grant, P. E. (2006). Detailed semiautomated MRI based morphometry of the neonatal brain: preliminary results. *NeuroImage*, 32(3), 1041–1049. <https://doi.org/10.1016/j.neuroimage.2006.05.020>
- Nordin, L. E., Möller, M. C., Julin, P., Bartfai, A., Hashim, F., & Li, T. Q. (2016). Post mTBI fatigue is associated with abnormal brain functional connectivity. *Scientific Reports*, 6. <https://doi.org/10.1038/srep21183>
- O'Connor, K. L., Rowson, S., Duma, S. M., & Broglio, S. P. (2017). Head-impact-measurement devices: A systematic review. *Journal of Athletic Training*, 52(3), 206–227. <https://doi.org/10.4085/1062-6050.52.2.05>
- Papa, L., Brophy, G. M., Welch, R. D., Lewis, L. M., Braga, C. F., Tan, C. N., Ameli, N. J., Lopez, M. A., Haeussler, C. A., Mendez Giordano, D. I., Silvestri, S., Giordano, P., Weber, K. D., Hill-Pryor, C., & Hack, D. C. (2016). Time Course and Diagnostic Accuracy of Glial and Neuronal Blood Biomarkers GFAP and UCH-L1 in a Large Cohort of Trauma Patients With and Without Mild Traumatic Brain Injury. *Jama neurology*, 73(5), 551–560. <https://doi.org/10.1001/jamaneurol.2016.0039>
- Papa, L., Ramia, M. M., Edwards, D., Johnson, B. D., & Slobounov, S. M. (2015). Systematic review of clinical studies examining biomarkers of brain injury in athletes after sports-related concussion. *Journal of Neurotrauma*, 32(10), 661–673. <https://doi.org/10.1089/neu.2014.3655>
- Papa, L., Slobounov, S. M., Breiter, H. C., Walter, A., Bream, T., Seidenberg, P., Bailes, J. E., Bravo, S., Johnson, B., Kaufman, D., Molfese, D. L., Talavage, T. M., Zhu, D. C., Knollmann-Ritschel, B., & Bhomia, M. (2019). Elevations in MicroRNA Biomarkers in Serum Are Associated with Measures of Concussion, Neurocognitive Function, and Subconcussive Trauma over a Single National Collegiate Athletic Association Division I Season in Collegiate Football Players. *Journal of Neurotrauma*, 36(8), 1343–1351. <https://doi.org/10.1089/neu.2018.6072>
- Patel, J. B., Wilson, S. H., Oakes, T. R., Santhanam, P., & Weaver, L. K. (2020). Structural and volumetric brain MRI findings in mild traumatic brain injury. *American Journal of Neuroradiology*, 41(1), 92–99. <https://doi.org/10.3174/ajnr.A6346>
- Patenaude, B., Smith, S. M., Kennedy, D. N., & Jenkinson, M. (2011). A Bayesian model of shape and appearance for subcortical brain segmentation. *NeuroImage*, 56(3), 907–922. <https://doi.org/10.1016/j.neuroimage.2011.02.046>
- Pekny, M., & Pekna, M. (2014). Astrocyte reactivity and reactive astrogliosis: costs and benefits. *Physiological reviews*, 94(4), 1077–1098. <https://doi.org/10.1152/physrev.00041.2013>

- Plog, B. A., Dashnaw, M. L., Hitomi, E., Peng, W., Liao, Y., Lou, N., Deane, R., & Nedergaard, M. (2015). Biomarkers of traumatic injury are transported from brain to blood via the glymphatic system. *Journal of Neuroscience*, 35(2), 518–526. <https://doi.org/10.1523/JNEUROSCI.3742-14.2015>
- Poole, V. N., Abbas, K., Shenk, T. E., Breedlove, E. L., Breedlove, K. M., Robinson, M. E., Leverenz, L. J., Nauman, E. A., Talavage, T. M., & Dydak, U. (2014). MR spectroscopic evidence of brain injury in the non-diagnosed collision sport athlete. *Developmental Neuropsychology*, 39(6), 459–473. <https://doi.org/10.1080/87565641.2014.940619>
- Poole, V. N., Breedlove, E. L., Shenk, T. E., Abbas, K., Robinson, M. E., Leverenz, L. J., Nauman, E. A., Dydak, U., & Talavage, T. M. (2015). Sub-concussive hit characteristics predict deviant brain metabolism in football athletes. *Developmental Neuropsychology*, 40(1), 12–17. <https://doi.org/10.1080/87565641.2014.984810>
- Prince, C., & Bruhns, M. E. (2017). Evaluation and Treatment of Mild Traumatic Brain Injury: The Role of Neuropsychology. *Brain sciences*, 7(8), 105. <https://doi.org/10.3390/brainsci7080105>
- Raji, C. A., Merrill, D. A., Barrio, J. R., Omalu, B., & Small, G. W. (2016). Progressive Focal Gray Matter Volume Loss in a Former High School Football Player: A Possible Magnetic Resonance Imaging Volumetric Signature for Chronic Traumatic Encephalopathy. *American Journal of Geriatric Psychiatry*, 24(10), 784–790. <https://doi.org/10.1016/j.jagp.2016.07.018>
- Ramirez, J., Berezuk, C., McNeely, A. A., Gao, F., McLaurin, J., & Black, S. E. (2016). Imaging the Perivascular Space as a Potential Biomarker of Neurovascular and Neurodegenerative Diseases. *Cellular and molecular neurobiology*, 36(2), 289–299. <https://doi.org/10.1007/s10571-016-0343-6>
- Rapp, P. E., & Curley, K. C. (2012). Is a diagnosis of mild traumatic brain injury a category mistake? *Journal of Trauma and Acute Care Surgery*, 73(2). <https://doi.org/10.1097/TA.0b013e318260604b>
- Redell, J. B., Maynard, M. E., Underwood, E. L., Vita, S. M., Dash, P. K., & Kobori, N. (2020). Traumatic brain injury and hippocampal neurogenesis: Functional implications. *Experimental neurology*, 331, 113372. <https://doi.org/10.1016/j.expneurol.2020.113372>
- Register-Mihalik, J. K., Guskiewicz, K. M., McLeod, T. C. V., Linnan, L. A., Mueller, F. O., & Marshall, S. W. (2013). Knowledge, attitude, and concussion-reporting behaviors among high school athletes: A preliminary study. *Journal of Athletic Training*, 48(5), 645–653. <https://doi.org/10.4085/1062-6050-48.3.20>
- Reyes-Haro, D., Labrada-Moncada, F. E., Miledi, R., & Martínez-Torres, A. (2015). Dehydration-induced anorexia reduces astrocyte density in the rat corpus callosum. *Neural Plasticity*, 2015(3), 1-8. <https://doi.org/10.1155/2015/474917>

- Rinholm, J. E., Vervaeke, K., Tadross, M. R., Tkachuk, A. N., Kopek, B. G., Brown, T. A., Bergersen, L. H., & Clayton, D. A. (2016). Movement and structure of mitochondria in oligodendrocytes and their myelin sheaths. *Glia*, 64(5), 810–825. <https://doi.org/10.1002/glia.22965>
- Robinson, M. E., Shenk, T. E., Breedlove, E. L., Leverenz, L. J., Nauman, E. A., & Talavage, T. M. (2015). The role of location of subconcussive head impacts in fMRI brain activation change. *Developmental Neuropsychology*, 40(2), 74–79. <https://doi.org/10.1080/87565641.2015.1012204>
- Ross, D. E., Seabaugh, J. D., Seabaugh, J. M., Plumley, J., Ha, J., Burton, J. A., Vandervaart, A., Mischel, R., Blount, A., Seabaugh, D., Shepherd, K., Barcelona, J., & Ochs, A. L. (2021). Patients with chronic mild or moderate traumatic brain injury have abnormal longitudinal brain volume enlargement more than atrophy. *Journal of Concussion*, 2021(1). <https://doi.org/10.1177/20597002211018049>
- Rubenstein, R., Sharma, D. R., Chang, B., Oumata, N., Cam, M., Vaucelle, L., Lindberg, M. F., Chiu, A., Wisniewski, T., Wang, K. K. W., & Meijer, L. (2019). Novel Mouse Tauopathy Model for Repetitive Mild Traumatic Brain Injury: Evaluation of Long-Term Effects on Cognition and Biomarker Levels After Therapeutic Inhibition of Tau Phosphorylation. *Frontiers in Neurology*, 10. <https://doi.org/10.3389/fneur.2019.00124>
- Rudick, R. A., Fisher, E., Lee, J. C., Simon, J., & Jacobs, L. (1999). Use of the brain parenchymal fraction to measure whole brain atrophy in relapsing-remitting MS. *Multiple Sclerosis Collaborative Research Group. Neurology*, 53(8), 1698–1704. <https://doi.org/10.1212/wnl.53.8.1698>
- Sa, T., & Syed, N. (2014). Traumatic Brain Injury: The Neglected Epidemic of Modern Society. *International Journal of Science and Research*, 3(12), 2319-7064. www.ijsr.net
- Savica, R., Parisi, J. E., Wold, L. E., Josephs, K. A., & Ahlskog, J. E. (2012). High school football and risk of neurodegeneration: a community-based study. *Mayo Clinic proceedings*, 87(4), 335–340. <https://doi.org/10.1016/j.mayocp.2011.12.016>
- Schneider, D. K., Galloway, R., Bazarian, J. J., Diekfuss, J. A., Dudley, J., Leach, J. L., Mannix, R., Talavage, T. M., Yuan, W., & Myer, G. D. (2019). Diffusion tensor imaging in athletes sustaining repetitive head impacts: A systematic review of prospective studies. *Journal of Neurotrauma*, 36(20), 2831–2849. <https://doi.org/10.1089/neu.2019.6398>
- Seitz, J., Walter, M., Mainz, V., Herpertz-Dahlmann, B., Konrad, K., & von Polier, G. (2015). Brain volume reduction predicts weight development in adolescent patients with anorexia nervosa. *Journal of Psychiatric Research*, 68, 228–237. <https://doi.org/10.1016/j.jpsychires.2015.06.019>

- Semple, B. D., Lee, S., Sadjadi, R., Fritz, N., Carlson, J., Griep, C., Ho, V., Jang, P., Lamb, A., Popolizio, B., Saini, S., Bazarian, J. J., Prins, M. L., Ferriero, D. M., Basso, D. M., & Noble-Haeusslein, L. J. (2015). Repetitive concussions in adolescent athletes - translating clinical and experimental research into perspectives on rehabilitation strategies. *Frontiers in neurology*, 6, 69. <https://doi.org/10.3389/fneur.2015.00069>
- Sharma, N., Ray, A. K., Shukla, K. K., Sharma, S., Pradhan, S., Srivastva, A., & Aggarwal, L. (2010). Automated medical image segmentation techniques. *Journal of Medical Physics*, 35(1), 3–14. <https://doi.org/10.4103/0971-6203.58777>
- Sharp, D. J., & Ham, T. E. (2011). Investigating white matter injury after mild traumatic brain injury. *Current Opinion in Neurology*, 24(6), 558–563. <https://doi.org/10.1097/WCO.0b013e32834cd523>
- Shen, X., Tokoglu, F., Papademetris, X., & Constable, R. T. (2013). Groupwise whole-brain parcellation from resting-state fMRI data for network node identification. *NeuroImage*, 82, 403–415. <https://doi.org/10.1016/j.neuroimage.2013.05.081>
- Shenk, T. E., Robinson, M. E., Svaldi, D. O., Abbas, K., Breedlove, K. M., Leverenz, L. J., Nauman, E. A., & Talavage, T. M. (2015). FMRI of visual working memory in high school football players. *Developmental Neuropsychology*, 40(2), 63–68. <https://doi.org/10.1080/87565641.2015.1014088>
- Shrey, D. W., Griesbach, G. S., & Giza, C. C. (2011). The Pathophysiology of Concussions in Youth. *Physical Medicine and Rehabilitation Clinics of North America*, 22(4), 577–602. <https://doi.org/10.1016/j.pmr.2011.08.002>
- Signoretti, S., Lazzarino, G., Tavazzi, B., & Vagnozzi, R. (2011). The pathophysiology of concussion. *PM & R : the journal of injury, function, and rehabilitation*, 3(10 Suppl 2), S359–S368. <https://doi.org/10.1016/j.pmrj.2011.07.018>
- Siman, R., Giovannone, N., Hanten, G., Wilde, E. A., McCauley, S. R., Hunter, J. v., Li, X., Levin, H. S., & Smith, D. H. (2013). Evidence that the blood biomarker SNTF predicts brain imaging changes and persistent cognitive dysfunction in mild TBI patients. *Frontiers in Neurology*, 4(11). <https://doi.org/10.3389/fneur.2013.00190>
- Sinopoli, K. J., Chen, J. K., Wells, G., Fait, P., Ptito, A., Taha, T., & Keightley, M. (2014). Imaging “brain strain” in youth athletes with mild traumatic brain injury during dual-task performance. *Journal of Neurotrauma*, 31(22), 1843–1859. <https://doi.org/10.1089/neu.2014.3326>
- Slobounov, S. M., Walter, A., Breiter, H. C., Zhu, D. C., Bai, X., Bream, T., Seidenberg, P., Mao, X., Johnson, B., & Talavage, T. M. (2017). The effect of repetitive subconcussive collisions on brain integrity in collegiate football players over a single football seasonA multi-modal neuroimaging study. *NeuroImage: Clinical*, 14, 708–718. <https://doi.org/10.1016/j.nicl.2017.03.006>

- Slobounov, S. M., Zhang, K., Pennell, D., Ray, W., Johnson, B., & Sebastianelli, W. (2010). Functional abnormalities in normally appearing athletes following mild traumatic brain injury: A functional MRI study. *Experimental Brain Research*, 202(2), 341–354. <https://doi.org/10.1007/s00221-009-2141-6>
- Smith, S. M., Jenkinson, M., Woolrich, M. W., Beckmann, C. F., Behrens, T. E., Johansen-Berg, H., Bannister, P. R., De Luca, M., Drobnjak, I., Flitney, D. E., Niazy, R. K., Saunders, J., Vickers, J., Zhang, Y., De Stefano, N., Brady, J. M., & Matthews, P. M. (2004). Advances in functional and structural MR image analysis and implementation as FSL. *NeuroImage*, 23 Suppl 1, S208–S219. <https://doi.org/10.1016/j.neuroimage.2004.07.051>
- Smith, S. M., Zhang, Y., Jenkinson, M., Chen, J., Matthews, P. M., Federico, A., & de Stefano, N. (2002). Accurate, robust, and automated longitudinal and cross-sectional brain change analysis. *NeuroImage*, 17(1), 479–489. <https://doi.org/10.1006/nimg.2002.1040>
- Smits, M., Houston, G. C., Dippel, D. W. J., Wielopolski, P. A., Vernooij, M. W., Koudstaal, P. J., Hunink, M. G. M., & van der Lugt, A. (2011). Microstructural brain injury in post-concussion syndrome after minor head injury. *Neuroradiology*, 53(8), 553–563. <https://doi.org/10.1007/s00234-010-0774-6>
- Sofroniew M. V. (2014). Astrogliosis. *Cold Spring Harbor perspectives in biology*, 7(2), a020420. <https://doi.org/10.1101/cshperspect.a020420>
- Sollmann, N., Echlin, P. S., Schultz, V., Viher, P. v., Lyall, A. E., Tripodis, Y., Kaufmann, D., Hartl, E., Kinzel, P., Forwell, L. A., Johnson, A. M., Skopelja, E. N., Lepage, C., Bouix, S., Pasternak, O., Lin, A. P., Shenton, M. E., & Koerte, I. K. (2018). Sex differences in white matter alterations following repetitive subconcussive head impacts in collegiate ice hockey players. *NeuroImage: Clinical*, 17, 642–649. <https://doi.org/10.1016/j.nicl.2017.11.020>
- Sours, C., Chen, H., Roys, S., Zhuo, J., Varshney, A., & Gullapalli, R. P. (2015). Investigation of multiple frequency ranges using discrete wavelet decomposition of resting-state functional connectivity in mild traumatic brain injury patients. *Brain Connectivity*, 5(7), 442–450. <https://doi.org/10.1089/brain.2014.0333>
- Spitz, G., Bigler, E. D., Abildskov, T., Maller, J. J., O’Sullivan, R., & Ponsford, J. L. (2013). Regional cortical volume and cognitive functioning following traumatic brain injury. *Brain and Cognition*, 83(1), 34–44. <https://doi.org/10.1016/j.bandc.2013.06.007>
- Stein, M. B., & McAllister, T. W. (2009). Exploring the convergence of posttraumatic stress disorder and mild traumatic brain injury. *The American journal of psychiatry*, 166(7), 768–776. <https://doi.org/10.1176/appi.ajp.2009.08101604>
- Strauss, S. B., Fleysher, R., Ifrah, C., Hunter, L. E., Ye, K., Lipton, R. B., Zimmerman, M. E., Kim, M., Stewart, W. F., & Lipton, M. L. (2021). Framing potential for adverse effects of repetitive subconcussive impacts in soccer in the context of athlete and non-athlete controls. *Brain Imaging and Behavior*, 15(2), 882–895. <https://doi.org/10.1007/s11682-020-00297-4>

- Sussman, D., da Costa, L., Chakravarty, M. M., Pang, E. W., Taylor, M. J., & Dunkley, B. T. (2017). Concussion induces focal and widespread neuromorphological changes. *Neuroscience Letters*, 650, 52–59. <https://doi.org/10.1016/j.neulet.2017.04.026>
- Svaldi, D. O., Joshi, C., McCuen, E. C., Music, J. P., Hannemann, R., Leverenz, L. J., Nauman, E. A., & Talavage, T. M. (2020). Accumulation of high magnitude acceleration events predicts cerebrovascular reactivity changes in female high school soccer athletes. *Brain Imaging and Behavior*, 14(1), 164–174. <https://doi.org/10.1007/s11682-018-9983-0>
- Svaldi, D. O., Joshi, C., Robinson, M. E., Shenk, T. E., Abbas, K., Nauman, E. A., Leverenz, L. J., & Talavage, T. M. (2015). Cerebrovascular reactivity alterations in asymptomatic high school football players. *Developmental Neuropsychology*, 40(2), 80–84. <https://doi.org/10.1080/87565641.2014.973959>
- Svaldi, D. O., McCuen, E. C., Joshi, C., Robinson, M. E., Nho, Y., Hannemann, R., Nauman, E. A., Leverenz, L. J., & Talavage, T. M. (2017). Cerebrovascular reactivity changes in asymptomatic female athletes attributable to high school soccer participation. *Brain Imaging and Behavior*, 11(1), 98–112. <https://doi.org/10.1007/s11682-016-9509-6>
- Tagge, C. A., Fisher, A. M., Minaeva, O. v., Gaudreau-Balderrama, A., Moncaster, J. A., Zhang, X. L., Wojnarowicz, M. W., Casey, N., Lu, H., Kokiko-Cochran, O. N., Saman, S., Ericsson, M., Onos, K. D., Veksler, R., Senatorov, V. v., Kondo, A., Zhou, X. Z., Miry, O., Vose, L. R., ... Goldstein, L. E. (2018). Concussion, microvascular injury, and early tauopathy in young athletes after impact head injury and an impact concussion mouse model. *Brain*, 141(2), 422–458. <https://doi.org/10.1093/brain/awx350>
- Takizawa, K., Matsumae, M., Sunohara, S., Yatsushiro, S., & Kuroda, K. (2017). Characterization of cardiac and respiratory-driven cerebrospinal fluid motion based on asynchronous phase-contrast magnetic resonance imaging in volunteers. *Fluids and Barriers of the CNS*, 14(1). <https://doi.org/10.1186/s12987-017-0074-1>
- Talavage, T. M., Nauman, E. A., & Leverenz, L. J. (2016). The role of medical imaging in the recharacterization of mild traumatic brain injury using youth sports as a laboratory. *Frontiers in Neurology*, 6(1). <https://doi.org/10.3389/fneur.2015.00273>
- Talavage, T. M., Nauman, E. A., Breedlove, E. L., Yoruk, U., Dye, A. E., Morigaki, K. E., Feuer, H., & Leverenz, L. J. (2014a). Functionally-detected cognitive impairment in high school football players without clinically-diagnosed concussion. *Journal of Neurotrauma*, 31(4), 327–338. <https://doi.org/10.1089/neu.2010.1512>
- Tang, C. Y., Eaves, E., Dams-O'Connor, K., Ho, L., Leung, E., Wong, E., Carpenter, D., Ng, J., Gordon, W., & Pasinetti, G. (2012). Diffuse disconnectivity in Traumatic Brain Injury: A resting state fMRI and DTI study. *Translational Neuroscience*, 3(1), 9–14. <https://doi.org/10.2478/s13380-012-0003-3>
- Tang, L., Ge, Y., Sodickson, D. K., Miles, L., Zhou, Y., Reaume, J., & Grossman, R. I. (2011). Thalamic resting-state functional networks: Disruption in patients with mild traumatic brain injury. *Radiology*, 260(3), 831–840. <https://doi.org/10.1148/radiol.11110014>

- Taoka, T., & Naganawa, S. (2020). Glymphatic imaging using MRI. *Journal of Magnetic Resonance Imaging*, 51(1), 11–24. <https://doi.org/10.1002/jmri.26892>
- Tarasoff-Conway, J. M., Carare, R. O., Osorio, R. S., Glodzik, L., Butler, T., Fieremans, E., Axel, L., Rusinek, H., Nicholson, C., Zlokovic, B. v., Frangione, B., Blennow, K., Ménard, J., Zetterberg, H., Wisniewski, T., & de Leon, M. J. (2015). Clearance systems in the brain - Implications for Alzheimer disease. *Nature Reviews Neurology*, 11(8) 457–470. <https://doi.org/10.1038/nrneuro.2015.119>
- Thomas Yeo, B. T., Krienen, F. M., Sepulcre, J., Sabuncu, M. R., Lashkari, D., Hollinshead, M., Roffman, J. L., Smoller, J. W., Zöllei, L., Polimeni, J. R., Fisch, B., Liu, H., & Buckner, R. L. (2011). The organization of the human cerebral cortex estimated by intrinsic functional connectivity. *Journal of Neurophysiology*, 106(3), 1125–1165. <https://doi.org/10.1152/jn.00338.2011>
- Tiernan, S., Byrne, G., & O'Sullivan, D. M. (2019). Evaluation of skin-mounted sensor for head impact measurement. *Proceedings of the Institution of Mechanical Engineers. Journal of engineering in medicine*, 233(7), 735–744. <https://doi.org/10.1177/0954411919850961>
- Tohka, J. (2014). Partial volume effect modeling for segmentation and tissue classification of brain magnetic resonance images: A review. *World Journal of Radiology*, 6(11), 855. <https://doi.org/10.4329/wjr.v6.i11.855>
- Tong, Y., & Frederick, B. de B. (2010). Time lag dependent multimodal processing of concurrent fMRI and near-infrared spectroscopy (NIRS) data suggests a global circulatory origin for low-frequency oscillation signals in human brain. *NeuroImage*, 53(2), 553–564. <https://doi.org/10.1016/j.neuroimage.2010.06.049>
- Tong, Y., & Frederick, B. de B. (2012). Concurrent fNIRS and fMRI processing allows independent visualization of the propagation of pressure waves and bulk blood flow in the cerebral vasculature. *NeuroImage*, 61(4), 1419–1427. <https://doi.org/10.1016/j.neuroimage.2012.03.009>
- Tremblay, S., de Beaumont, L., Henry, L. C., Boulanger, Y., Evans, A. C., Bourgouin, P., Poirier, J., Théoret, H., & Lassonde, M. (2013). Sports concussions and aging: A neuroimaging investigation. *Cerebral Cortex*, 23(5), 1159–1166. <https://doi.org/10.1093/cercor/bhs102>
- Tremblay, S., Desjardins, M., Bermudez, P., Iturria-Medina, Y., Evans, A. C., Jolicœur, P., & de Beaumont, L. (2019). Mild traumatic brain injury: The effect of age at trauma onset on brain structure integrity. *NeuroImage: Clinical*, 23. <https://doi.org/10.1016/j.nicl.2019.101907>
- Trivedi, M. A., Ward, M. A., Hess, T. M., Gale, S. D., Dempsey, R. J., Rowley, H. A., & Johnson, S. C. (2007). Longitudinal changes in global brain volume between 79 and 409 days after traumatic brain injury: Relationship with duration of coma. *Journal of Neurotrauma*, 24(5), 766–771. <https://doi.org/10.1089/neu.2006.0205>

- Turner, R. C., Lucke-Wold, B. P., Logsdon, A. F., Robson, M. J., Dashnaw, M. L., Huang, J. H., Smith, K. E., Huber, J. D., Rosen, C. L., & Petraglia, A. L. (2015). The quest to model chronic traumatic encephalopathy: A multiple model and injury paradigm experience. *Frontiers in Neurology*, 6(10). <https://doi.org/10.3389/fneur.2015.00222>
- Tzourio-Mazoyer, N., Landeau, B., Papathanassiou, D., Crivello, F., Etard, O., Delcroix, N., Mazoyer, B., & Joliot, M. (2002). Automated anatomical labeling of activations in SPM using a macroscopic anatomical parcellation of the MNI MRI single-subject brain. *NeuroImage*, 15(1), 273–289. <https://doi.org/10.1006/nimg.2001.0978>
- Unterberg, A. W., Stover, J., Kress, B., & Kiening, K. L. (2004). Edema and brain trauma. *Neuroscience*, 129(4), 1019–1027. <https://doi.org/10.1016/j.neuroscience.2004.06.046>
- Veeramuthu, V., Narayanan, V., Kuo, T. L., Delano-Wood, L., Chinna, K., Bondi, M. W., Waran, V., Ganesan, D., & Ramli, N. (2015). Diffusion tensor imaging parameters in mild traumatic brain injury and its correlation with early neuropsychological impairment: A longitudinal study. *Journal of Neurotrauma*, 32(19), 1497–1509. <https://doi.org/10.1089/neu.2014.3750>
- Vijayakrishnan Nair, V., Kish, B. R., Inglis, B., Yang, H.-C., Wu, Y.-C., Zhou, X., Schwichtenberg, A. J., & Tong, Y. (2021). Human CSF Movement Influenced by Vascular Low Frequency Oscillations and Respiration. *Biorxiv*, <https://doi.org/10.21203/rs.3.rs-1190237/v1>
- Viviani, R. (2016). A digital atlas of middle to large brain vessels and their relation to cortical and subcortical structures. *Frontiers in Neuroanatomy*, 10(2). <https://doi.org/10.3389/fnana.2016.00012>
- Vrenken, H., Vos, E. K., van der Flier, W. M., Sluimer, I. C., Cover, K. S., Knol, D. L., & Barkhof, F. (2014). Validation of the automated method VIENA: an accurate, precise, and robust measure of ventricular enlargement. *Human brain mapping*, 35(4), 1101–1110. <https://doi.org/10.1002/hbm.22237>
- Fonov, V.S., Evans, A.C., McKinstry, R.C., Almli, C.R., & Collins, D.L. (2009) Unbiased nonlinear average age-appropriate brain templates from birth to adulthood, *NeuroImage*, 47(Suppl 1). [http://dx.doi.org/10.1016/S1053-8119\(09\)70884-5](http://dx.doi.org/10.1016/S1053-8119(09)70884-5)
- Washington, P. M., Villapol, S., & Burns, M. P. (2016). Polypathology and dementia after brain trauma: Does brain injury trigger distinct neurodegenerative diseases, or should they be classified together as traumatic encephalopathy? *Experimental Neurology*, 275, 381–388. <https://doi.org/10.1016/j.expneurol.2015.06.015>
- Whitwell, J. L., Crum, W. R., Watt, H. C., & Fox, N. C. (2001). Normalization of cerebral volumes by use of intracranial volume: implications for longitudinal quantitative MR imaging. *AJNR. American journal of neuroradiology*, 22(8), 1483–1489.

- Wintermark, M., Sanelli, P. C., Anzai, Y., Tsiouris, A. J., Whitlow, C. T., Druzgal, T. J., Gean, A. D., Lui, Y. W., Norbash, A. M., Raji, C., Wright, D. W., & Zeineh, M. (2015). Imaging evidence and recommendations for traumatic brain injury: Advanced neuro- and neurovascular imaging techniques. *American Journal of Neuroradiology*, 36(2), E1–E11. <https://doi.org/10.3174/ajnr.A4181>
- Wylie, G. R., Freeman, K., Thomas, A., Shpaner, M., OKeefe, M., Watts, R., & Naylor, M. R. (2015). Cognitive improvement after mild traumatic brain injury measured with functional neuroimaging during the acute period. *Plos one*, 10(5). <https://doi.org/10.1371/journal.pone.0126110>
- Yaakub, S. N., Heckemann, R. A., Keller, S. S., McGinnity, C. J., Weber, B., & Hammers, A. (2020). On brain atlas choice and automatic segmentation methods: a comparison of MAPER & FreeSurfer using three atlas databases. *Scientific Reports*, 10(1). <https://doi.org/10.1038/s41598-020-57951-6>
- Yan, S., Qian, T., Maréchal, B., Kober, T., Zhang, X., Zhu, J., Lei, J., Li, M., & Jin, Z. (2020). Test-retest variability of brain morphometry analysis: an investigation of sequence and coil effects. *Annals of Translational Medicine*, 8(1), 12–12. <https://doi.org/10.21037/atm.2019.11.149>
- Yang, H.-C., Inglis, B., Talavage, T., Vijayakrishnan Nair, V., Fitzgerald, B., Schwichtenberg, A. J., & Tong, Y. (2021). Coupling brain cerebrovascular oscillations and CSF flow during wakefulness: An fMRI study. *Biorxiv*, <https://doi.org/10.1101/2021.03.29.437406>
- Yang, J., Fan, J., Ai, D., Zhou, S., Tang, S., & Wang, Y. (2015). Brain MR image denoising for Rician noise using pre-smooth non-local means filter. *BioMedical Engineering Online*, 14(1). <https://doi.org/10.1186/1475-925X-14-2>
- Yang, Z., Wang, P., Morgan, D., Lin, D., Pan, J., Lin, F., Strang, K. H., Selig, T. M., Perez, P. D., Febo, M., Chang, B., Rubenstein, R., & Wang, K. K. W. (2015). Temporal MRI characterization, neurobiochemical and neurobehavioral changes in a mouse repetitive concussive head injury model. *Scientific Reports*, 5. <https://doi.org/10.1038/srep11178>
- Yatsushiro, S., Sunohara, S., Hayashi, N., Hirayama, A., Matsumae, M., Atsumi, H., & Kuroda, K. (2018). Cardiac-driven pulsatile motion of intracranial cerebrospinal fluid visualized based on a correlation mapping technique. *Magnetic Resonance in Medical Sciences*, 17(2), 151–160. <https://doi.org/10.2463/mrms.mp.2017-0014>
- Zeng, Y., Zhang, B., Zhao, W., Xiao, S., Zhang, G., Ren, H., Zhao, W., Peng, Y., Xiao, Y., Lu, Y., Zong, Y., & Ding, Y. (2020). Magnetic Resonance Image Denoising Algorithm Based on Cartoon, Texture, and Residual Parts. *Computational and Mathematical Methods in Medicine*, 2020. <https://doi.org/10.1155/2020/1405647>
- Zhang, Y., Brady, M., & Smith, S. (2001). Segmentation of brain MR images through a hidden Markov random field model and the expectation-maximization algorithm. *IEEE transactions on medical imaging*, 20(1), 45–57. <https://doi.org/10.1109/42.906424>

- Zhou, Y., Kierans, A., Kenul, D., Ge, Y., Rath, J., Reaume, J., Grossman, R. I., & Lui, Y. W. (2013). Mild traumatic brain injury: Longitudinal regional brain volume changes. *Radiology*, 267(3), 880–890. <https://doi.org/10.1148/radiol.13122542>
- Zhou, Y., Milham, M. P., Lui, Y. W., Miles, L., Reaume, J., Sodickson, D. K., Grossman, R. I., & Ge, Y. (2012). Default-mode network disruption in mild traumatic brain injury. *Radiology*, 265(3), 882–892. <https://doi.org/10.1148/radiol.12120748>
- Zhu, Y., Li, Z., Bai, L., Tao, Y., Sun, C., Li, M., Zheng, L., Zhu, B., Yao, J., Zhou, H., & Zhang, M. (2014). Loss of microstructural integrity in the limbic-subcortical networks for acute symptomatic traumatic brain injury. *BioMed Research International*, 2014. <https://doi.org/10.1155/2014/548392>

APPENDIX

Functional Connectivity Alteration in Male Middle School Football Athletes

Introduction: Previous research has shown that asymptomatic high school (HS) athletes exposed to RHI (e.g., blows to the head, whiplash due to strikes to the body) had changes in their default mode network (DMN) (Abbas, Shenk, Poole, Robinson, et al., 2015). Resting-state fMRI (rs-fMRI) data from male middle school (MS) football athletes was evaluated for changes in connectivity before and after the competitive season in this study. Both a whole brain parcellation and a DMN sub-network mask revealed changes. The pattern of alterations is like what has been seen in cases of sports-related concussion (Papa et al., 2015). This finding supports the need for ongoing monitoring of youth athletes to avoid the long-term effects of RHT.

Resting state fMRI scans are based on the theory that neurons that require energy for firing, which will cause a transient change in cerebral blood flow through neurovascular coupling which gives rise to the blood-oxygen-level dependent T2*-weighted signal. Initially, fMRI was used to quantify different brain regions activated by different tasks performed by the subjects. The discovery of a task negative fMRI by Biswal et al. (1992) led to the development of resting state fMRI and studying the brain's circuits in the absence of any task.

Materials and Procedures:

Participants: A total of 32 male athletes, including 16 MS (years 12-13) football athletes and a control group of 16 non-collision sport athletes, participated on a voluntary basis at both the MS (n=3, ages 12-13; baseball, track and cross-country) and HS (n=13, ages 14-17) levels.

All athletes had two MRI sessions, spaced out according to the length of their competition seasons (football athletes: 10-12 weeks apart; MS controls: 4-5 months; HS controls: 4-6 weeks). Data was collected using a General Electric 3T Signa HDx MRI for all images. Each MRI session included an 8-minute rs-fMRI scan with eyes open (TR=2sec; 240 volumes) and high-resolution anatomical imaging (1mm isotropic T1-weighted).

Pre-processing of resting state scans (Figure A.1) includes slice-timing correction, despiking, motion correction, co-registration with corresponding anatomical scans, picture normalization, segmentation, and spatiotemporal smoothing (0.01-0.1 Hz passband). The number of connections surpassing a specific threshold ($r=0.4$) in the correlation network matrix obtained

using the average time series from each of the 278 ROIs was computed as a whole-brain metric after parcellation (Shen et al., 2013). The number of connections surpassing the stated correlation threshold with the average time series of a 12mm radius seed region was used to calculate the DMN measure (Posterior Cingulate Cortex seed region).

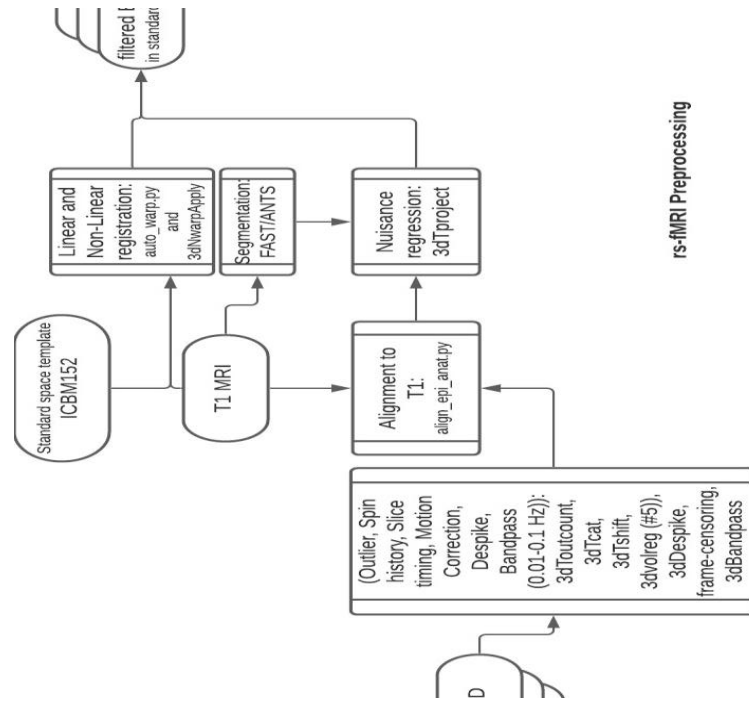


Figure A.1. rs-fMRI pre-processing pipeline.

Results and Discussion: Changes in DMN and whole-brain connectivity for MS football athletes and controls are shown in Figure A.2 (note that the three MS controls are denoted by a '*').

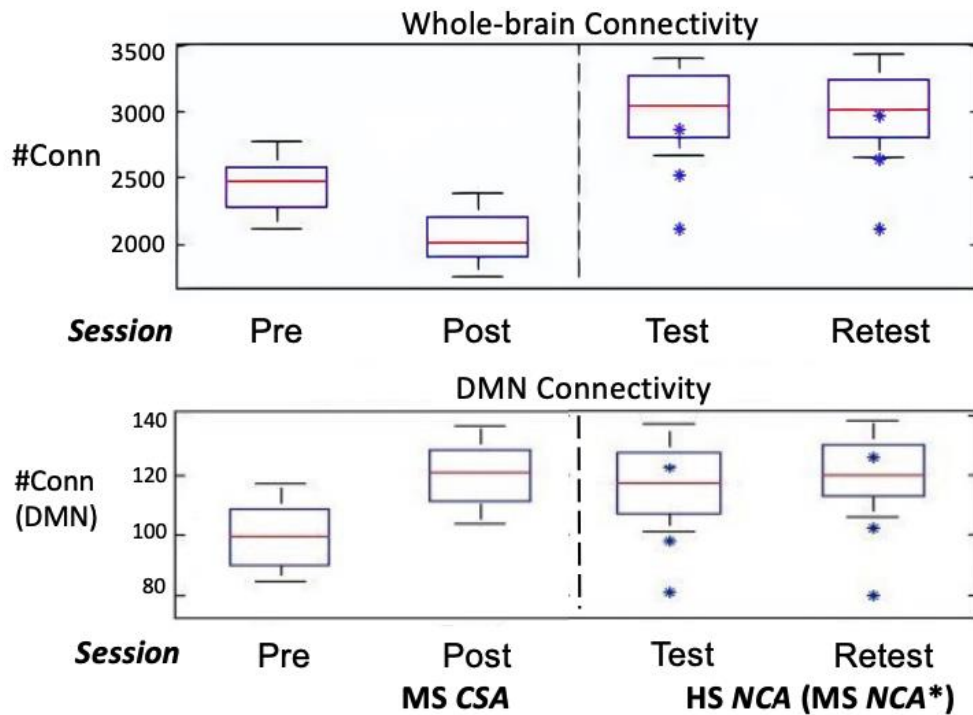


Figure A.2. Boxplot of connectivity values for DMN and whole-brain metric for MS athletes and controls

MS football athletes exhibited statistically significant ($p < 0.05$; paired t-test) increases in connectivity to the DMN seed (i.e., more of the brain involved in the DMN), and decreases in whole-brain connectivity (i.e., less coordination across the brain) after exposure to repeated head trauma. After the season, MS football athletes' DMN values were more like those of HS controls (i.e., the brain appeared "older"), although whole-brain connectivity measures fell significantly below those of either control group.

Conclusions: Changes in connection are likely a result of repeated head acceleration events associated with collision sports participation. It is worth noting that the DMN changes in MS football athletes differ in direction from previous findings in HS football athletes (Papa et al., 2015), but that they eventually return to "normal" HS control measures following exposure, implying neuroprotective responses. The decrease in whole-brain connection, on the other hand, is more symptomatic of injury and a decline in the brain's effective maturity. MS football athletes and similar-aged controls may have similar connection at the start, but changes in the football athletes signal that this is a population that should be monitored and perhaps intervened in to prevent or minimize repeated head trauma occurrences.

Functional Connectivity Alteration in Female Soccer Athletes

Introduction: Previous research work has found changes in the DMN in asymptomatic athletes who have been subjected to RHI (e.g., hits to the head, whiplash from blows to the body) (Abbas, Shenk, Poole, Robinson, et al., 2015). Data from female high school soccer athletes is analyzed over an eight-month period, encompassing activities prior to, during, and after the competition season. A whole brain parcellation map (Shen et al., 2013) is used to quantify changes in network connection, providing a comprehensive picture of connectivity changes. The findings have consequences for athletic trainers and players who are trying to avoid the long-term effects of concussion and other mild traumatic brain injuries.

Methods:

Participants and data acquisition: On a voluntary basis, 31 female high school athletes (17 soccer, 14 non-collision sport; ages 14-17) took part in the study. Around the time of their season, soccer players had 5 MRI sessions (Pre=before the start of the season; In1=1-4 weeks after the start of the season; In2=4-9 weeks after the start of the season; Post1=15-20 weeks after the start of the season; Post2=26-29 weeks after the start of the season). Non-collision athletes were imaged twice, 4-6 weeks apart, before (Test) and after (ReTest) the start of activity.

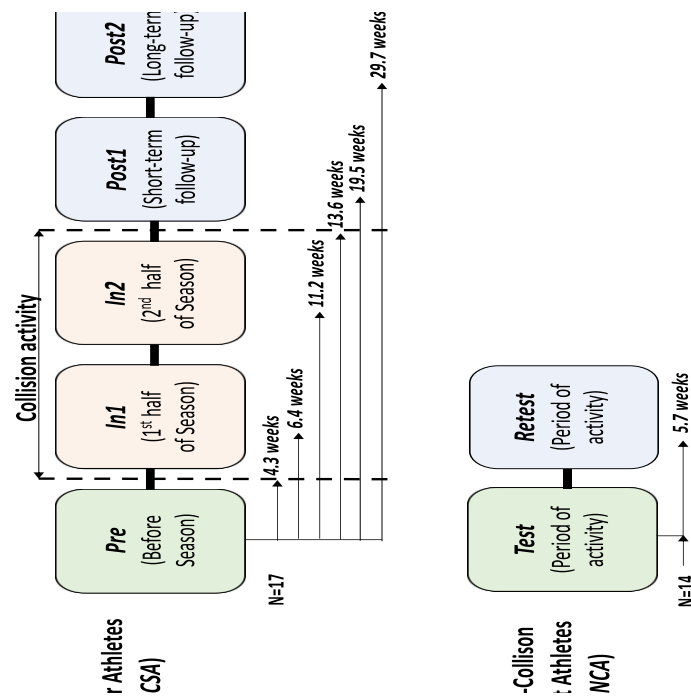


Figure A.3. Imaging schedule for the athlete populations representing median time-intervals.

Data was collected using a General Electric 3T Signa HDx MRI for all images. Athletes performed one 9min 48sec eyes-open resting state fMRI scan (TR=2s) and high-quality anatomical imaging during each MRI session (1mm isotropic T1-weighted).

Data processing and analysis: Slice timing correction, despiking, motion correction, co-registration with its corresponding anatomical scan, image normalization, segmentation, spatio-temporal smoothing (0.01-0.1 Hz passband), and removal of physiological Neuroimaging Informatics Tools and Resources Clearinghouse (NITRC) v2.1.31-0 and local white matter noise were all used in the pre-processing of resting-state scans. Following parcellation (Shen et al., 2013) the average time series from each of the 278 ROIs were used to create a correlation network matrix. The 278-node network matrix was evaluated for each subject over correlation thresholds ranging from 0.30 to 0.80, with the count of supra-threshold connections (#Conn) used as the metric of resting state functional connectivity (noting that $r=0.15$ corresponds to $p_{uncorrected} < 0.01$ for 290 measurements). Using a paired t-test, #Conn values at In1, In2, Post1, and Post2 were compared to Pre for soccer- and ReTest to Test for non-collision-athletes at each threshold.

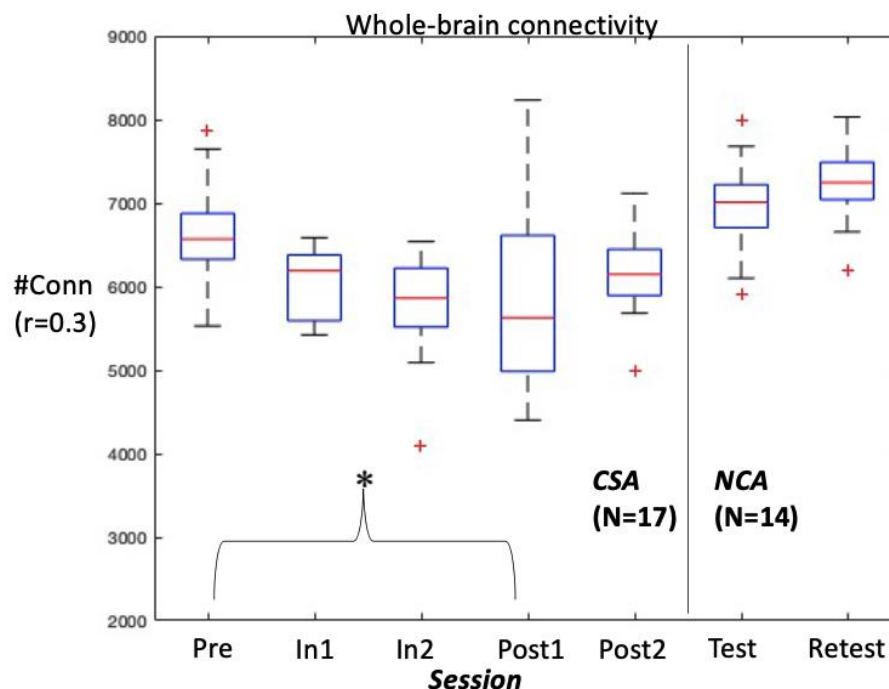


Figure A.4. Longitudinal variation of #Conn (at $r=0.3$)

Results: Figure A.4 depicts the network connectivity differences across CSA and NCA for #Conn threshold at $r=0.3$. Corresponding average #Conn values are shown in Table A.1, in which statistically significant differences ($p_{Bonferroni} < 0.05$) from Pre are indicated by asterisks.

Trends of longitudinal decrease in #Conn for In1, In2 and Post1 are apparent in Table A.1, with corrected statistical significance observed at Post1, shortly after the end of their 9-10 week competition season. For soccer athletes, #Conn levels return approximately to Pre levels at Post2, following several months of rest after the competition season. These changes are consistent with prior work in high school football athletes (Poole et al., 2014) (Talavage et al., 2014b) and are posited to arise from accumulation of head trauma by the athletes during practices and games. Unlike the work in football athletes, like-aged non-collision athletes had higher #Conn values than for soccer but were consistent in showing no significant change over time. Unlike football players, non-collision athletes of similar ages had higher #Conn values than soccer players but showed no significant change over time.

Table A.1. Subject average supra-threshold connection count (#Conn) by imaging session across correlation thresholds, for high school female soccer and non-collision athletes. (Corrected for MCP=4)

	Supra-Threshold Connection Count (#Conn) by Imaging Session						
	Soccer Athletes (N=17)					Non-Collision Athletes (N=14)	
$r_{\text{threshold}}$	Pre	In1	In2	Post1	Post2	Test	ReTest
0.3	6432	5916 [†]	5876 [†]	5611*	6222	7032	7212
0.4	2649	2274 [†]	2198 [†]	2011*	2423	3037	3143
0.5	1187	1007 [†]	977 [†]	897*	1048	1463	1572
0.6	567	508	493	449*	515	743	829
0.7	343	311	314	303	324	425	476
0.8	266	253	258	253	271	302	337

* Statistically-significantly different from Pre ($p_{Bonferroni} < 0.05$; paired t-test)

[†] Different from Pre at $p_{uncorrected} < 0.05$ (paired t-test)

Conclusions: The modifications in brain connections are most likely the result of the athletes' repeated RHI during the season. Given that these alterations predominantly influence broader networks with lower correlations, immediate obvious cognitive repercussions are unlikely, which is consistent with these athletes' asymptomatic nature.

VITA

<https://www.linkedin.com/in/pratik-kashyap/>

EDUCATION

Purdue University, Electrical and Computer Engineering

West Lafayette, IN

Ph.D. in Biomedical Image and Sensing (POS GPA: 3.5/4.0)

May 2022

Purdue University, Electrical and Computer Engineering

West Lafayette, IN

M.S. in Electrical and Computer Engineering (GPA: 3.6/4.0)

December 2019

PESIT, Electrical and Communications Engineering

Bangalore, India

B.Tech. in Electrical and Communications Engineering (WES GPA: 3.9/4.0)

August 2014

PROFESSIONAL EXPERIENCE

Database analyst II for **Duke University** (Department of child, family health & community Psychiatry)

Durham, NC

September 2021-January 2021

- Managing diffusion tensor imaging pipelines primarily focused on infant tractography
- Statistical analysis of post-processed open-source (ABCD, BCP, HBN, dHCP) imaging data investigating aging, traumatic brain injury and ADHD
- Interfacing with principal investigators and directors of NIH funded research
- Apply machine learning/deep learning methodologies to improve and streamline the quality assurance of imaging data
- Volunteer at NYSPI RFMH to manage local biomedical databases

Research support assistant/ Biomedical imaging analytic intern for **Nathan Kline Institute**

Orangeburg, NY

May 2019-August 2019

- Working on Nipype/ CPAC pipelines for BIDS of the Rockland study
- Creating pipelines on Nipype Porcupine GUI, ETL of BIDS
- Writing functions, wrappers, and creating workflows to execute the pre-processing pipelines efficiently in amortized time
- Editing and fine-tuning individual sub-routines for data dependent (MRI, rs-fMRI and ECoG) parameters

- Conducting cognitive testing (ImPACT, SAC, Brainscope EEG)
- Operating (MRI pulse sequence protocol development and execution) a GE 3T MRI (250+ hours)
- Bruker 7T MRI operating and systems knowledge (20+ hours)

RESEARCH EXPERIENCE

Published research

- **Pratik Kashyap**, Ikbeom Jang, Kausar Abbas, Diana Svaldi and Thomas Talavage, “*Resting state functional connectivity alteration in asymptomatic high-school female soccer athletes*”, Presented at CSESC 2017 and OHBM 2017
- **Pratik Kashyap**, Kausar Abbas, Sharlene Newman and Thomas Talavage, “*Functional connectivity alteration in middle school male football athletes with controls*”, Oral presentation at BMES 2017, CSESC 2018
- **Pratik Kashyap**, Trey Shenk, Diana Svaldi and Thomas Talavage, “*Region-based T1-weighted MRI morphometric changes in high school collision sport athletes*”, Presented at Neurotrauma 2018, IU/PU Symposium 2018, Annual conference on Brain Imaging 2020 & published in Journal of head trauma rehabilitation 2020
- **Pratik Kashyap**, Trey Shenk, Diana Svaldi, Roy Lycke, Taylor Lee, Eric Nauman and Thomas Talavage, “*Relative regional anatomical volumetric alterations of youth athletes participating in contact sports*”, Poster presentation at BMES 2021
- **Pratik Kashyap**, Trey Shenk, Diana Svaldi, Greg Tamer, Eric Nauman and Thomas Talavage, “*Normalized brain tissue-level evaluation of volumetric changes of youth athletes participating in collision sports*”, published in Journal of Neurotrauma Reports 2022
- Joseph Beckman, Melissa Dark, **Pratik Kashyap**, Sumra Bari, Samuel Wagstaff, Yingjie Chen and Baijan Yang, “*Cognitive processing of cryptography concepts: An fMRI study*”, Presented at ASEE 2017
- Sumra Bari, **Pratik Kashyap**, Kausar Abbas, Brenna McDonald and Thomas Talavage, “*Multi-site reliability of Default Mode Network and graph theoretical measures in rs-fMRI*”, Presented at ISMRM 2018
- Ikbeom Jang, **Pratik Kashyap**, Sumra Bari and Thomas Talavage, “*Test-Retest and between-site reliability in a multisite Diffusion Tensor Imaging study*”, Presented at ISMRM 2018
- Sumra Bari, Kausar Abbas, **Pratik Kashyap** and Thomas Talavage, “*Multisite reliability of Default Mode Network in resting state fMRI*”, Presented at BMES 2017
- Ho-Ching Yang, Jinxia Yao, James Wang, Nicole Vike, **Pratik Kashyap**, Sumra Bari, Yukai Zou, Ikbeom Jang, Taylor Lee, Gregory Tamer, Eric Nauman, Thomas Talavage and Yunjie Tong, “*Characterizing physiological components of near-infrared spectroscopy signal under hypercapnia*”, Presented at OHBM 2019, Presented at BMES 2019
- Yukai Zou, Wenbin Zhu, Ho-Ching Yang, **Pratik Kashyap**, Apekshya Chhetri, Thomas M Talavage, Joseph V Rispoli, “*Population-specific brain atlases for early-to-middle adolescent collision-sport athletes*”, Archived in Purdue university research repository 2020

TEACHING EXPERIENCE

- **Graduate Course Instructor** at Purdue University
Course: ECE255 – Electronic circuit analysis and design Spring 2015
Course: ECE302 – Probabilistic methods in EE Summer 2015
Course: ECE302 – EE fundamentals 2 Summer 2021

- Graduate Teaching Assistant** at Purdue University

Course: ECE600 – Random variables and signals	Fall 2017
Course: ECE255 – Electronic circuit analysis and design	Fall 2014
Course: MA162 – Program writer for LON-CAPA	Fall 2015
Course: ECE201 – Linear circuit analysis	Spring 2016
Course: ECE302 – Probabilistic methods in EE	
Fall 2016, Fall 2020, Spring 2017, Spring 2021 (head TA), Summer 2018, Summer 2020	
Course: ECE208 – Electrical circuit design and analysis lab	Fall 2017, 2018, Spring 2018, Spring 2020
Course: ECE362 – Microprocessor systems and interfacing	Fall 2019
Course: ECE490 – Senior design in Electrical Engineering	Spring 2019, Spring 2020